AD-A058 338 DAVID W TAYLOR NAVAL SHIP RESEARCH AND DEVELOPMENT CE--ETC F/G 20/4
AUTOROTATION OF PLATES.(U)
AUG 78 H J LUGT
UNCLASSIFIED DTNSRDC-78/058 NL

1 OF 2
AD
A058 338

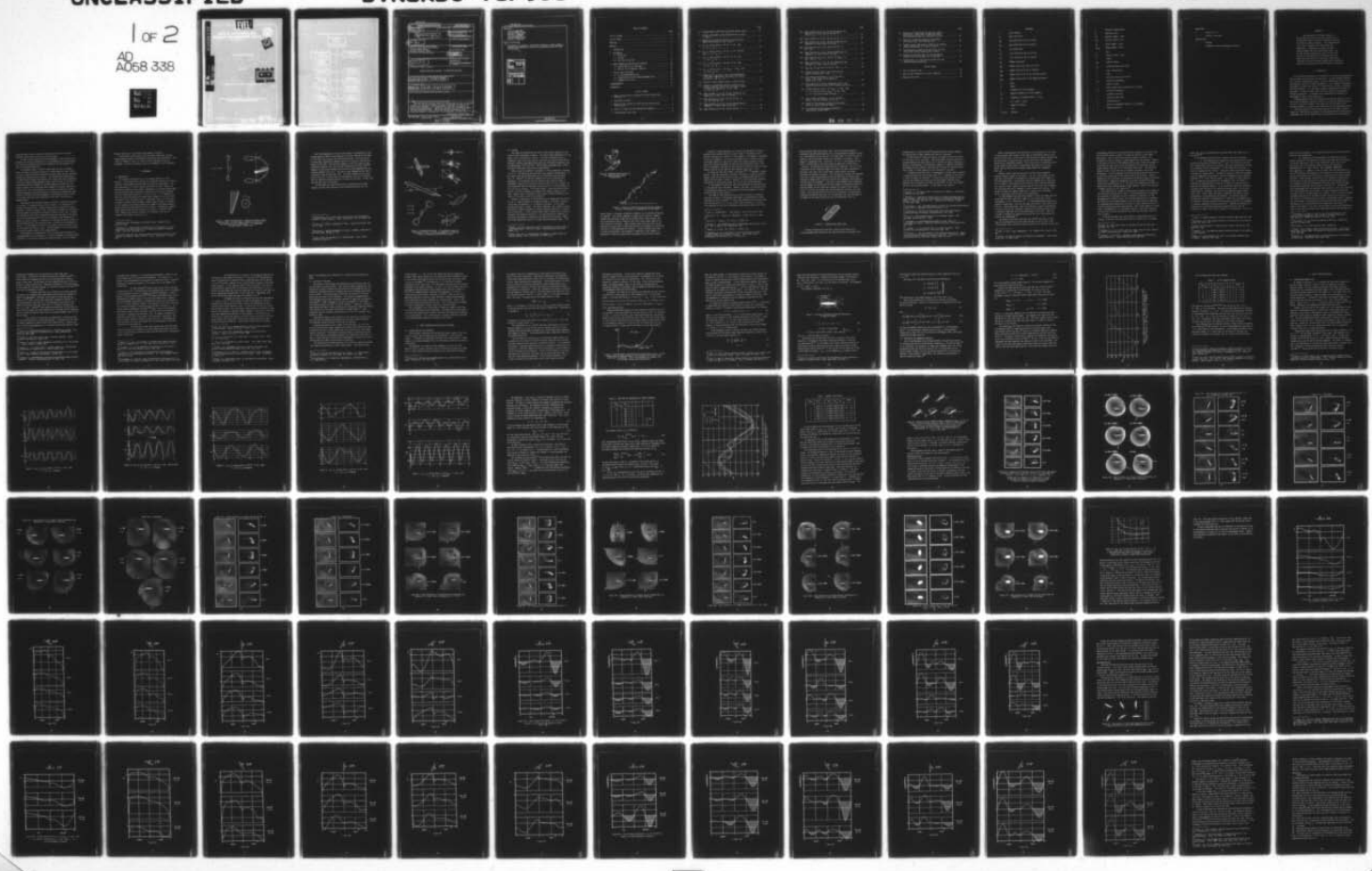

LEVEL II

(12)

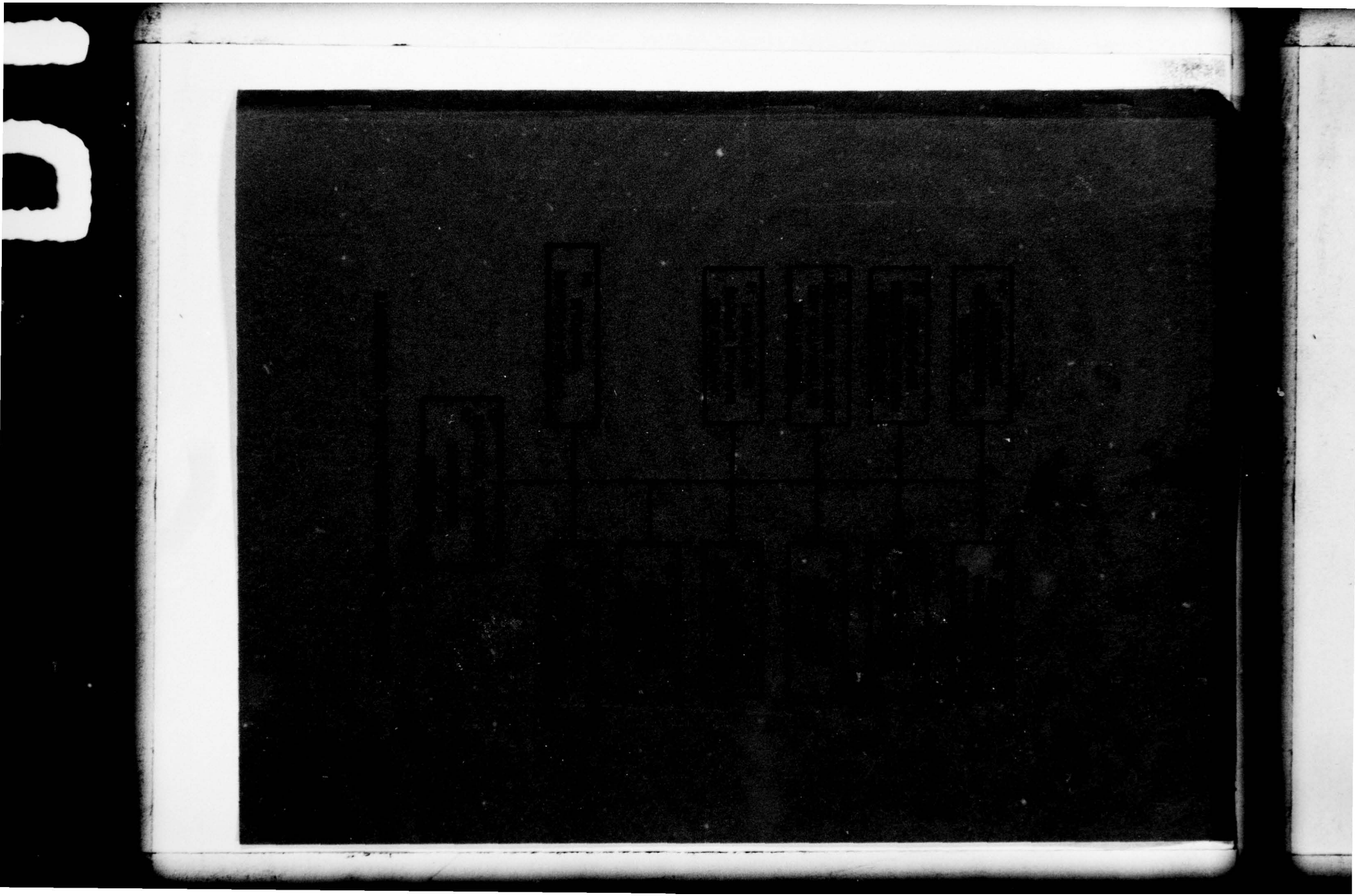

UNCLASSIFIED

SECURITY CLASSIFICATION OF THIS PAGE (When Data Entered)

REPORT DOCUMENTATION PAGE

READ INSTRUCTIONS BEFORE COMPLETING FORM

(14) 1. REPORT NUMBER: DTNSRDC-78/058

2. GOVT ACCESSION NO.

3. RECIPIENT'S CATALOG NUMBER

4. TITLE (and Subtitle)

(6) AUTOROTATION OF PLATES.

(9) 5. TYPE OF REPORT & PERIOD COVERED: Final rept.,

6. PERFORMING ORG. REPORT NUMBER

7. AUTHOR(s)

(10) Hans J. Lugt

8. CONTRACT OR GRANT NUMBER(s)

9. PERFORMING ORGANIZATION NAME AND ADDRESS
David W. Taylor Naval Ship Research
and Development Center
Bethesda, Maryland 20084

10. PROGRAM ELEMENT, PROJECT, TASK AREA & WORK UNIT NUMBERS
(See reverse side)

11. CONTROLLING OFFICE NAME AND ADDRESS

(11) 12. REPORT DATE: August 1978

13. NUMBER OF PAGES: 113

14. MONITORING AGENCY NAME & ADDRESS (if different from Controlling Office)

(12) 112 p.

15. SECURITY CLASS. (of this report): UNCLASSIFIED

15a. DECLASSIFICATION/DOWNGRADING SCHEDULE

16. DISTRIBUTION STATEMENT (of this Report)

APPROVED FOR PUBLIC RELEASE: DISTRIBUTION UNLIMITED.

17. DISTRIBUTION STATEMENT (of the abstract entered in Block 20, if different from Report)

(16) WR02302, SR01403

18. SUPPLEMENTARY NOTES

(17) WR02302,03, SR0140301

19. KEY WORDS (Continue on reverse side if necessary and identify by block number)

20. ABSTRACT (Continue on reverse side if necessary and identify by block number)

The autorotation of plates normal to a uniform parallel flow is explained in detail for low Reynolds numbers by means of numerical solutions of the Navier-Stokes equations. The incompressible fluid flow is assumed to be laminar and two-dimensional. Comparisons are made with high Reynolds number and three-dimensional flows. The article defines autorotation, gives an historical account of investigations into autorotation, and shows that →

(Continued on reverse side)

DD FORM 1 JAN 73 1473 EDITION OF 1 NOV 65 IS OBSOLETE
S/N 0102-014-6601

UNCLASSIFIED

SECURITY CLASSIFICATION OF THIS PAGE (When Data Entered)

387 682

(Block 10)

Task Area WR0230203
Program Element 61153N
Work Unit 1-1840-002
Task Area SR0140301
Program Element 61153N
Work Unit 1-1808-010

(Block 20 continued)

autorotation is caused by a complicated interplay of vortex shedding, boundary-layer hysteresis, and vorticity generation around the edges of the plate.

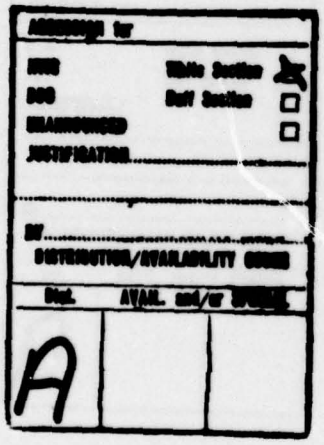

TABLE OF CONTENTS

LIST OF FIGURES

LIST OF TABLES

NOTATION

a	Focal distance
C_D	Drag coefficient
C_{DF}	Drag coefficient due to friction
C_{DP}	Drag coefficient due to pressure
C_L	Lift coefficient
C_{LF}	Lift coefficient due to friction
C_{LP}	Lift coefficient due to pressure
C_M	Moment coefficient
C_{MF}	Moment coefficient due to friction
C_{MP}	Moment coefficient due to pressure
C_{MR}	Moment coefficient in the retarding period
C_{MS}	Moment coefficient in the supporting period
D	Drag
d	Chord
f	Frequency of vortex shedding
f_N	Natural frequency of vortex shedding
f_p	Frequency of rotating plate, $\Omega = 2\pi f_p$
h	$h^2 = \cosh^2\eta - \cos^2\theta$
I	Moment of inertia
L	Lift
i,j,k,n	Integers

p	Pressure, dimensionless
R	Resultant force
Re	Reynolds number = $2aU/\nu$
Re_d	Reynolds number = dU/ν
Ro	Rossby number = $U/a\,\Omega$
$Ro_{d/2}$	Rossby number = $2U/d\,\Omega$
s	Span
St	Strouhal number = fd/U
T	Torque
T_{EX}	External torque
T_{FL}	Torque exerted by the fluid
t	Time, dimensionless
t'	Time
U	Constant velocity at infinity
x,y	Cartesian coordinates
α	Angle of attack
β	Angle between free stream and axis of body
η,θ	Elliptic coordinates
ν	Kinematic viscosity
ρ	Density of the fluid
ψ	Stream function
ω	Vorticity (component normal to (η,θ)-plane)
Ω	Angular velocity

Subscripts:

0	Value at t = 0
1	Surface of the body

Superscripts:

$\bar{}$	Average
*	Related to flow not rotating at infinity

ABSTRACT

The autorotation of plates normal to a uniform parallel flow is explained in detail for low Reynolds numbers by means of numerical solutions of the Navier-Stokes equations. The incompressible fluid flow is assumed to be laminar and two-dimensional. Comparisons are made with high Reynolds-number and three-dimensional flows. The article defines autorotation, gives an historical account of investigations into autorotation, and shows that autorotation is caused by a complicated interplay of vortex shedding, boundary-layer hysteresis, and vorticity generation around the edges of the plate.

1. INTRODUCTION

The aerodynamic phenomenon of autorotation has puzzled aerodynamicists, ballisticians, and biologists for many years. In most technical applications in which autorotation occurs, it has an undesirable effect on the performance of the device under consideration. For instance, autorotation can greatly influence the control of finned missiles, rockets, airplanes, and reentry bodies. In a few areas, however, autorotation of bodies is exploited. In nature certain tree fruits and seeds are disseminated through autorotation. In aeroballistics autorotation of bomblets is encouraged to cover a wide target area.

Although special cases of autorotation and partial aspects of it are fairly well understood, the basic reason for it and the detailed explanation of it are still lacking. This paper will clarify some of the unsolved problems, at least for the simple case of an autorotating plate.

The brief account of the 125-year history of the study of autorotation will familiarize the reader with the motivations for studying this phenomenon, give him an appreciation of the difficulties by describing

successes and failures, and explain why only the advent of powerful computers could give the solutions to the problem.

In order to follow the historical development of the study of autorotation, the essential mechanism of this phenomenon must be anticipated. The following paragraphs outline this mechanism for the simplest case, that of an autorotating plate.

A rectangular plate is free to rotate about an axis of symmetry which is fixed in a position normal to a uniform parallel flow. After an initial impulse the plate continues to rotate under certain conditions without any external source of power. The spinning plate then obtains its whole kinetic energy from the parallel stream; the plate autorotates. Flow visualization and measurements reveal that the rate of rotation is synchronous with the frequency of vortex shedding, and that this frequency is equal to or larger than the frequency of vortices shed from a fixed plate. This synchronization is an essential condition to understanding autorotation because without it previously or prematurely shed vortices interfere with the development of the boundary layer in front of the plate and with vortex separation in the rear, thus causing a damping effect.

During each half-revolution there is a period in which the rotation of the plate is supported and a period in which it is retarded by the action of the fluid flow. Surplus torque, which is required for autorotation, is mainly obtained in the retarding period when the plate moves from the normal to the parallel position relative to the flow. Location and strength of the vortices generated behind the two edges of the plate as well as the deceleration of the front boundary layer determine the amount of surplus torque. In addition, to overcome the braking effect of the retarding period, the plate must have a sufficiently large moment of inertia. If this moment of inertia is too small the plate cannot rotate. It will wobble and slow to a stop. The same happens if the concentration of vorticity near the edge is not strong enough.

The mechanism of autorotation is thus a complicated interplay and synchronization of four processes: (1) vortex shedding, (2) boundary-layer hysteresis, (3) vorticity generation around the edges, and (4) flywheel

behavior requiring a sufficiently large moment of inertia.

A plate with a freely moving axis may obtain additional rotation energy through rhythmic translational acceleration and deceleration. The classical example is that of a freely falling rectangular piece of cardboard. Lift due to rotation causes the cardboard to fall obliquely.

2. BACKGROUND

2.1 DEFINITION

The concept of autorotation is not uniquely defined in fluid dynamics. A few researchers consider any continuous rotation of a body in a parallel flow without external source of power as autorotation. The body then derives its kinetic energy from the fluid flow. Under this definition, windmills, water wheels, anemometers, helicopter blades (when rotating without power during fall), and certain tree fruits and seeds are such "autorotating" devices [1,2] (Fig. 1a, b). It is important to point out that these bodies are geometrically shaped in such a way that even under static conditions, that is, when kept fixed in a fluid flow, a torque is present which initiates rotation when the body is released. In this category also belong symmetrically shaped bodies whose geometric centers do not coincide with the centers of mass. Furthermore, symmetric bodies with uniform mass distribution can rotate in a parallel shear flow. Spheres and circular cylinders, for instance, spin due to asymmetric wall-shear stress[3] (Fig. 1c).

---

[1] McCormick, B.W., Aerodynamics of V/STOL flight. Academic Press. New York, 1967.

[2] Norberg, R.A., Autorotation, Self-Stability, and Structure of Single-Winged Fruits and Seeds (Samaras) with Comparative Remarks on Animal Flight. Biol. Rev. 48 (1973), 561.

[3] Poe, G.G. and A. Acrivos, Closed-streamline flows past rotating single cylinders and spheres: inertia effects. Journ. Fluid Mech. 72 (1975), 605.

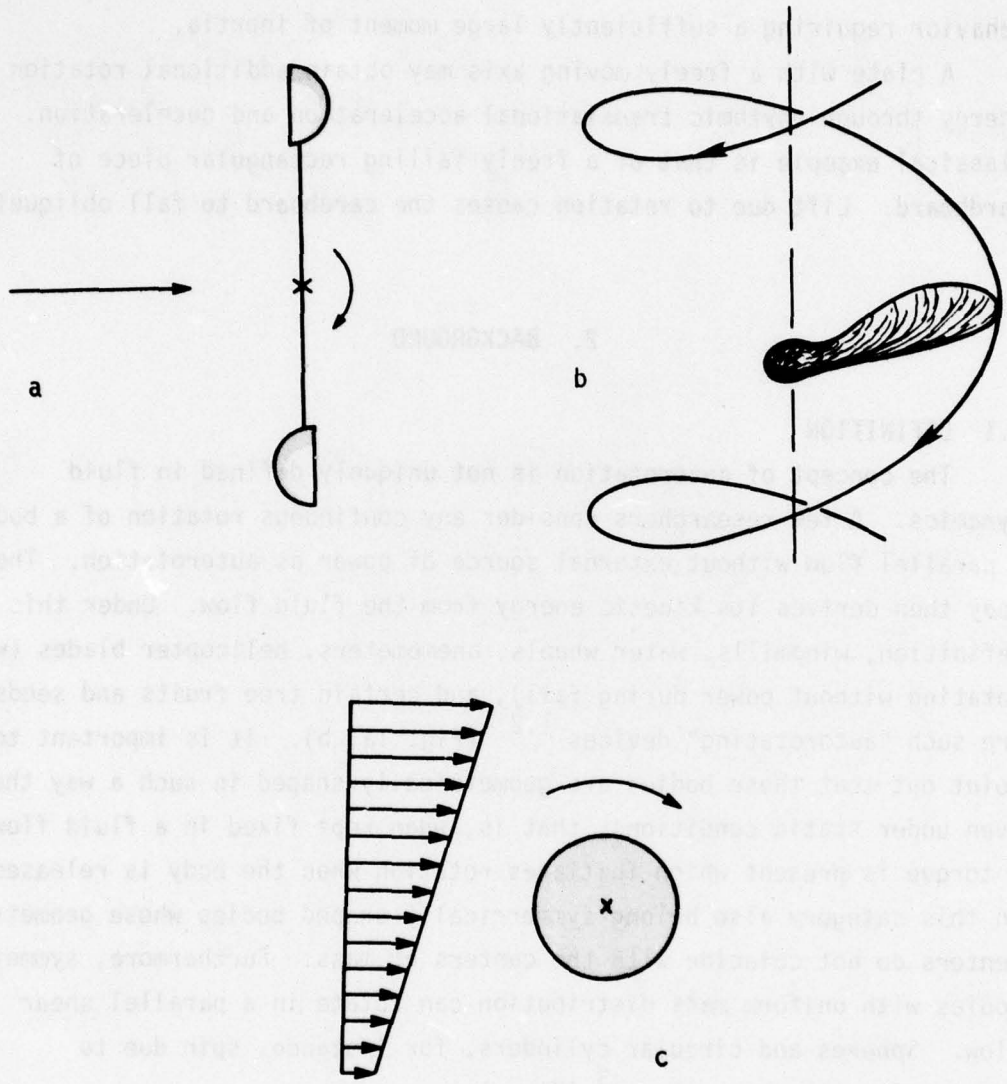

Figure 1 - Bodies Spinning Due to Transfer of Kinetic Energy from the Flow. (In this paper, spinning of this type is not considered to be autorotation.) a) Anemometer; b) Maple Seed; c) Shear Flow

Most fluid dynamicists restrict the concept of autorotation to the induced motion of bodies which requires an initial rotation of the body in the fluid flow to cause self-sustained spinning. Two cases may be distinguished, depending on whether the axis of rotation is parallel or normal to the flow. The classical examples of the first case are the Lanchester propeller (Fig. 2a) and the spinning airfoil (Fig. 2b).[4,5,6] Examples of the second (normal) case are the falling cardboard and the rotating dumbbell (Fig. 2c).[7] The axis of the cardboard may be free to translate or may be fixed (Fig. 2d). Cruciform systems can also autorotate (Fig. 2e). In both cases of autorotation, the axis of rotation does not need to be exactly parallel or normal to the flow. In fact, one case may pass over to the other.

In this paper the latter definition for autorotation has been adopted, and the study focusses on the autorotating plate, Fig. 2d.

---

[4] Riabouchinsky, D.P., Thirty years of theoretical and experimental research in fluid mechanics. Journ. Royal Aeron. Soc. 39 (1935), 282.

[5] Durand, W.F. (editor), Aerodynamic Theory. Dover Publications 1963. Vol. V , 208.

[6] Bairstow, L., Applied Aerodynamics. 2nd ed. Longmans, Green and Co., New York, 1939. Chapter V, 212.

[7] Smith, A.M.O., On the Motion of a Tumbling Body. Journ. Aeron. Sciences 20 (1953), 73.

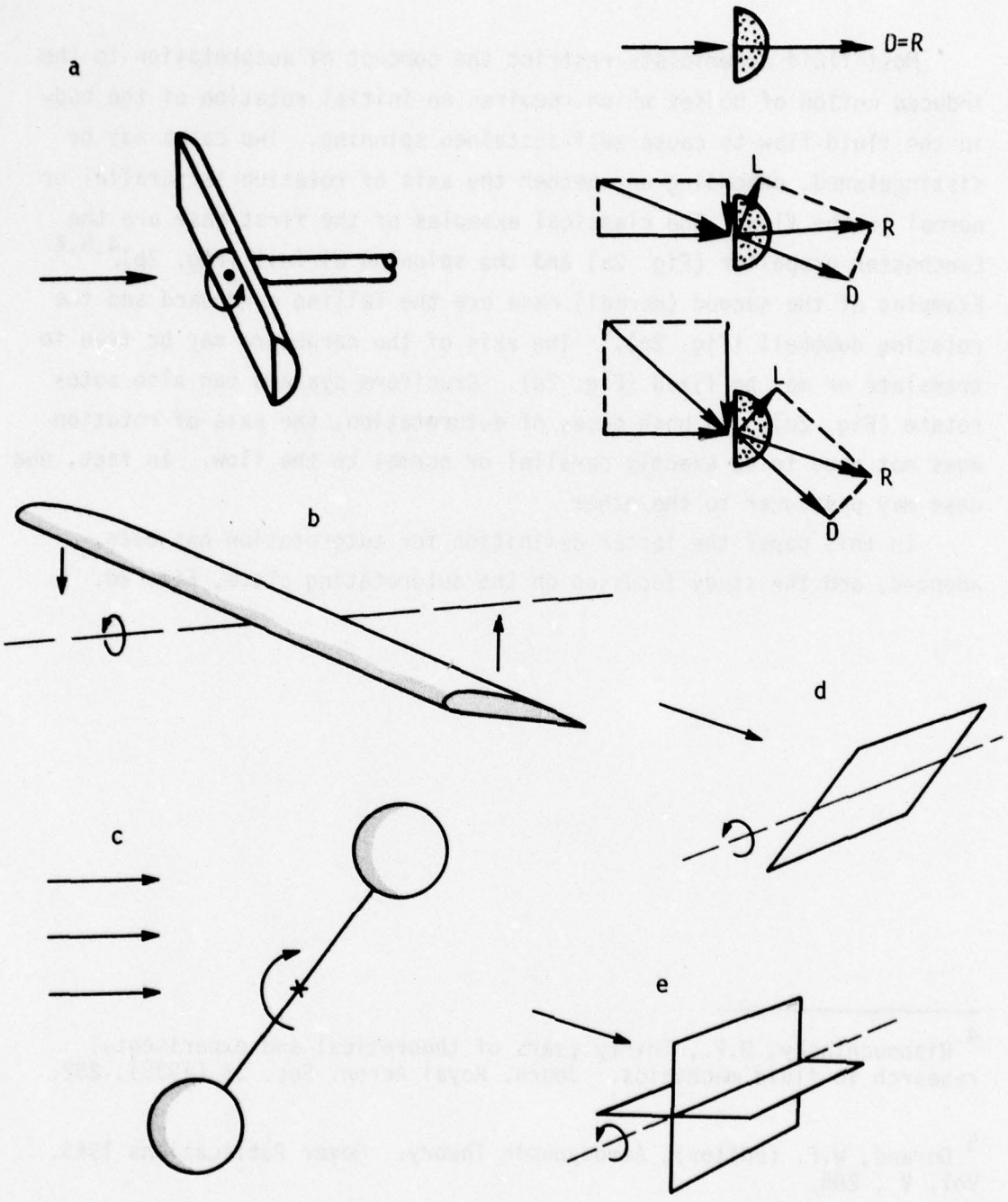

Figure 2 - Autorotating Bodies. a) Lanchester Propeller; b) Spinning Airfoil; c) Rotating Dumbbell; d) Rotating Plate; e) Rotating Cruciform Plate System

2.2 HISTORY

The study of autorotation has quite a long history compared to the study of other aerodynamic concepts. The oldest known explanation for the normal type of autorotation, that for a falling rectangular piece of cardboard, never really went beyond a qualitative or partial description, and until recently experiments gave data only for overall properties such as average drag, lift, and roll. The following paragraphs give a brief history of the study of this type of autorotation.

When a piece of cardboard is dropped, it starts wobbling as sketched in Fig. 3. This wobbling may continue or may change to autorotation. In the latter case the cardboard does not fall vertically but obliquely (Fig. 4). Maxwell[8] in 1853 was probably the first to describe this phenomenon. He recognized that the center of mass and the center of aerodynamic forces do not coincide, and this gives rise to a torque. He also recognized that the deviation from vertical fall is attributable to the lift due to rotation. This latter phenomenon was described slightly earlier (in 1851) by Magnus, but Maxwell was probably unaware of his work. Magnus' name is attached to this effect although recognition and study of it go back to the time of Newton.[9]

Maxwell's explanation of autorotation may be summarized with the aid of Fig. 4. Shortly before it assumes position 1, the plate is parallel to the path; at position 2 it is normal to the path. In the latter position the drag is larger. The plate, therefore, has a higher velocity at position 1 than at position 3, and the torque at position 1 is larger than at position 3. Since a plate always tends to place itself normal to the path, the torque at position 1 is in the direction of rotation; at position 3 the torque is opposite to the direction of rotation. Hence, the torque supporting rotation is larger than the adverse torque. This

---

[8] Maxwell, J.C., On a particular case of the descent of a heavy body in a resisting medium. Scientific Papers. Cambridge University Press (1890), 115.

[9] Barkla, H.M. and L.J. Auchterlonie, The Magnus or Robins effect on rotating spheres. Journ. Fluid Mech. 47 (1971), 437.

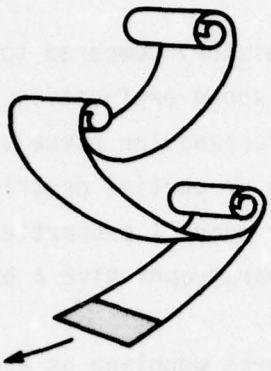

Figure 3 - Wobbling Plate During Fall with Vortices Shed at each Turning Point

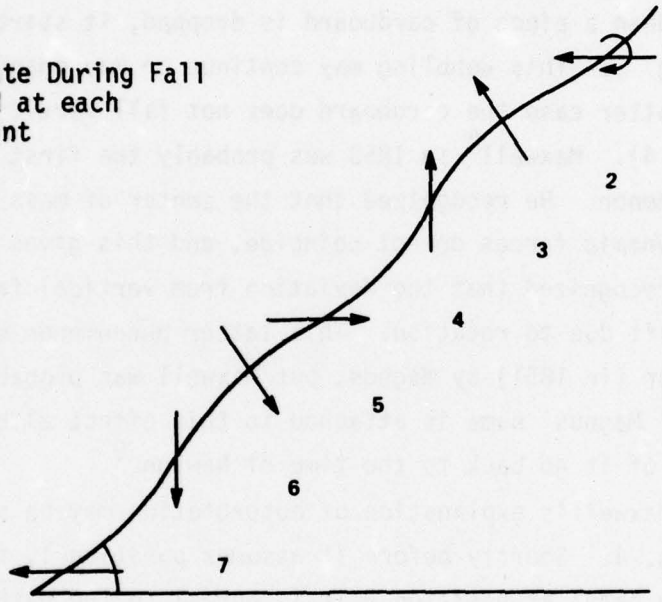

Figure 4 - Path of a Freely Falling Autorotating Cardboard The Axis of Rotation is Perpendicular to this Sheet

excess torque is balanced, according to Maxwell, by an opposing torque due to rotation. This latter statement is generally not correct. Maxwell assumed that the total torque can be divided into a "quasi-steady" part and a contribution due to rotation, the latter being always opposite to the direction of rotation. "Quasi-steady" means that the forces on the body vary so slowly with rotation that they can be computed at a particular instant as if the body were not rotating. It will be shown later that, to explain autorotation, the asymmetric (sometimes called "dynamic" or hysteresis") effect of rotation must contribute to the driving torque.

Greenhill in 1880 developed, on the basis of Kirchhoff's studies, a potential-flow solution which is cited in Lamb.[10] According to this solution the motion of a plate or a disk subject to an impulse is analogous to that of a pendulum. The oscillating phase (Fig. 3 without vortices) can become rotatory if the kinetic energy and certain constants (which implicitly contain the moment of inertia) are sufficiently large. The path is undulatory, with the vertical position of the plate and the lowest angular velocity at the peak of the trajectory (Ref. 10, p. 176).

At about the same time (1880) a few papers[11,12,13] appeared in which Maxwell's idea was essentially restated: the centers of gravity and aerodynamic forces do not coincide and, thus, a torque develops which is a function of the angle of attack. Ahlborn[13] in 1897 presented a detailed explanation of this process based only on the quasi-steady approach.

In 1901 Köppen[14] applied the idea of autorotation to construction of a flying machine and a parachute. However, the small lift-to-drag ratio of autorotating plates did not encourage further development of flying machines based on that principle.

From 1904 to 1918 Riabouchinsky's private institute in Koutchino performed a number of interesting experiments on autorotation in which Joukowsky was also involved.[4,15] About 1905 Riabouchinsky introduced the term "autorotation" as it is used in this paper (Section 2.1), and he distinguished for the first time between autorotating plates with fixed

---

[10] Lamb, H., Hydrodynamics. Sixth edition. Dover Publication, 1945.

[11] Mouillard, M., Théorie de l'Aéroplane. L'empire de l'air, 1881, 210.

[12] Gerlach, E., Zeitschr. für Luftsch. 5 (1886), 65.

[13] Ahlborn, F., Der Schwebflug und die Fallbewegung ebener Tafeln in der Luft. Abh. d. Naturw. Ver. Hamburg XV, 1897.

[14] Köppen, W., Illustr. aër. Mitteil. 5 (1901), 158.

[15] Joukowsky, N., De la chute dans l'air de corps légers de forme allongée, animés d'un mouvement rotatoire. Bulletin de l'Inst. aérodynamique de Koutchino, fasc. 1 (1912), 51.

axes and those with freely moving axes. He realized that Maxwell's explanation was deficient because, for a plate autorotating about a fixed axis, the velocity of the flow (or in a frame fixed in a fluid at rest at infinity, the translational velocity of the body) is constant. Thus, Maxwell's assumption that, in position 1 of Fig. 4, the movement of the plate is faster than in position 3 does not apply for a plate with a fixed axis. He offered the explanation that in position 1 of Fig. 4 the streamlines at the retreating edge of the plate are more curved than in position 3 and, thus, due to the higher suction effect the torque favorable to rotation is greater. This recognition includes the important facts that a quasi-steady theory cannot be sufficient to explain autorotation of plates with fixed axes and that the asymmetric flow effect of rotation must be considered. A few years later Riabouchinsky recognized that the moment of inertia must be large enough to overcome the period of adverse torque. He also found that systems with three or four plates (Fig. 2e), as well as projectiles and nonstabilized airships, can autorotate. He also observed that the ratio of rotational to translational speed must be smaller than unity for autorotation, and that the shape of the edges of the plate affects the rate of autorotation (Fig. 5).

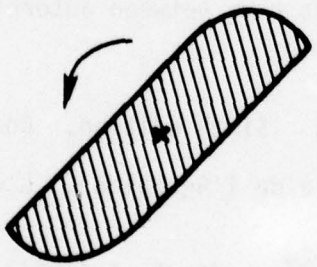

Figure 5 - "Riabouchinsky-type" Body

Although Riabouchinsky observed a strong vortex behind the rotating plate which revolved in the same direction as the plate,[4] and

although later, in 1929, Ahlborn[16] mentioned periodic vortex shedding, the significance of these observations was not recognized.

In 1941 Dupleich[17] published results of extensive work with freely falling plates in air and water. These experiments provide a wealth of valuable quantitative data which will be referred to again in Section 4.3. Dupleich's explanation of autorotation, however, is adopted from Maxwell, and depends on the incorrect idea that the influence of rotation on the total torque is always opposite to the direction of rotation.

In Germany during World War II autorotation of plates was of interest in producing high lift on aircraft wings.[18-21] A summary of this effort is given in English by Crabtree.[22] An auxiliary wing capable of autorotation was mounted just below the trailing edge of the main wing. Another study in Germany, described by Schneller[23] in 1941, was probably the first on rotating missiles. It described "lunar motion".

---

[16] Ahlborn, F., The Magnus Effect in Theory and in Reality. Translation in NACA TM 567, May 1930.

[17] Dupleich, P., Rotation par Chute Libre des Ailettes Rectangulaires de Forme Allongée. Publications Scientifiques et Techniques du Secretariat d'État a l'Aviation, 1941, No. 176. Translated into English in NACA TM 1201, April 1949.

[18] von Holst, E., Der rotierende Flügel als Mittel zur Hochauftriebserzeugung. Jahrbuch 1941 d. deutschen Luftfahrtforschung I, 372.

[19] Küchemann, D., Auftrieb und Widerstand eines rotierenden Flügels. Deutsche Luftfahrt forschung, Forschungsbericht 1651, 1942.

[20] Wiese, H., Drehleistungsmessungen an rotierenden Flügeln. AVA Göttingen, Bericht 42/A/14. 1942.

[21] Küchemann, D., Dreikomponentenmessungen an einem Flügel mit rotierendem Hilfsflügel. Deutsche Luftfahrtforschung, Forschungsbericht 1513, 1941.

[22] Crabtree, L.F., The rotating flap as a high-lift device. Royal Aircraft Est. Farnborough Tech. Note, Aero 2492, 1957.

[23] Schneller, E., The lunar motion of fin stabilized projectiles. Report from the Technische Hochschule Darmstadt 1940/1941. Translated by CADO, Wright-Patterson Air Force Base, Dayton, Ohio. ATI 3271.

Before investigations after World War II are discussed, it will help to review briefly the history of the study of autorotation about an axis parallel to the flow. At the turn of the century this type of autorotation was discovered in connection with a device now called the Lanchester tourbillon or Lanchester propeller. (The origin of this terminology could not be traced by the author.) Riabouchinsky mentioned in his survey paper[4] that in 1905 Patrick Alexander demonstrated this phenomenon (Fig. 2a).

Without initial rotation the force R acting on the Lanchester propeller blade is equal to the drag D. Fig. 2a. With a small initial spin the flow relative to the body has a nonzero angle with respect to the undisturbed flow. The resultant force R, composed now of drag D and lift L, causes a torque opposite to the initial spin, and the propeller will come to a stop. Above a certain value of the initial spin, however, the resulting force has a component in the direction of rotation. This torque increases the angular speed until a balance with the damping forces is achieved, and the device then autorotates.

In 1906 Riabouchinsky published a paper[4] in which he showed that the blade does not need a profile as shown in Fig. 2a but that it also autorotates if it is infinitely thin. In 1909 Riabouchinsky found that a propeller blade with a slot near one edge autorotates in the direction of the slot. During World War I and in the Twenties a type of autorotation similar to that of the Lanchester propeller was studied carefully since it played an important role in the performance of aircraft. Relf and Lavender in England are credited with being the first investigators to observe this phenomenon.[24]

According to Bairstow[6] and Bryant and Gates[25] the origin of this type of autorotation may be explained with the aid of Fig. 2b in the following way: Once an airfoil rotates around an axis parallel to the flow,

---

[24] Fuchs, R. and L. Hopf, Aerodynamik. R.C. Schmidt & Co., Berlin, 1922, 424.

[25] Bryant, L.W. and S.B. Gates, The spinning of aeroplanes. Journ. Royal Aeron. Soc. 31 (1927), 619.

the downward moving part of the wing usually encounters a relative flow velocity which causes a higher lift than the velocity on the upward moving part. This is due to the different angles of attack. The difference in the lift causes a torque opposite to the rotation. However, if the angle of attack of the downward moving part of the wing becomes so large that this part stalls, the corresponding lift decreases and may become smaller than the lift of the upward moving part. The resulting torque is then in the direction of rotation, and again, the airfoil autorotates. In this connection one distinguishes steep and flat spin of an aircraft on the basis of the spiral path of the aircraft. Overall summaries of the literature on autorotating airplanes are given by Durand[5] and Bairstow.[6] Additional references are given by Knight[26] and more recent ones by Neihouse et al.[27] The theory of autorotating airplanes is based on the quasi-steady approach (strip theory). Work on the spinning of modern aircraft is still going on.[28]

After World War II interest in autorotation around an axis normal to the flow arose in three basic areas: (1) the aerodynamics of releasable nose sections of fuselages for use in emergency situations; (2) the aerodynamics of finned missiles; and (3) the aeroballistics of bomblets. All three cases are highly complex, since the flow around the body must be considered three-dimensional, and since in many instances the axis of rotation performs precession and nutation. Most of the research in these areas is documented in U.S. Government reports, a fact which reflects not only their military application but also the preliminary nature of their contents.

It may be mentioned that some interest in autorotation exists in biology. There are tree seeds which not only rotate like a helicopter

---

[26] Knight, M., Wind tunnel tests on autorotation and the "Flat Spin". NACA Rep. 273, 1927.

[27] Neihouse, A.I., W.J. Klinar, and S.H. Scher, Status of spin research for recent airplane designs. NASA TR 57, 1960.

[28] Spangler, S.B. and M.F.E. Dillenius, Investigation of Aerodynamic Loads at Spin Entry. Report ONR-CR212-225-2, May 1976.

blade (Fig. 1b) but simultaneously autorotate about the longer axis of the seed.[29,30]

In the following the three basic research areas are discussed:

(1) The autorotation of projectiles and nonstabilized airships was earlier observed by Riabouchinsky.[4] Later, this effect was noticed with released nose sections of fuselages, and investigations were carried out at Douglas Aircraft Corporation. A 1953 summary of this effort is given in a paper by A.M.O. Smith.[7] Some years later autorotation became a problem for reentry bodies. The Mercury capsule of Glenn and Carpenter could be stabilized during reentry into the atmosphere only by opening a parachute.[31,32] A.M.O. Smith's paper[7] is of interest in other respects also. He mentions the autorotation of dumbbells (Fig. 2c) which is explained by the difference in drag of the spheres at subcritical and supercritical Reynolds numbers. In the transition range from laminar to turbulent flow the drag of the sphere drops drastically. This kind of autorotation is, therefore, restricted to the Reynolds-number range of about $4 \cdot 10^5$. A.M.O. Smith also made an important contribution to the understanding of the autorotating cardboard. He realized (what had already been indicated in Riabouchinsky's idea[4]) that the asymmetry due to rotation is the key to explaining autorotation and that this asymmetry is caused by hysteresis during acceleration. Although the importance of hysteresis for oscillating wings was recognized earlier (see the literature in [33]), A.M.O. Smith linked it to autorotation. It will be

---

[29] Paturi, F., Nature, Mother of Invention. Harper & Row, New York, 1976.

[30] McCutchen, C.W., The Spinning Rotation of Ash and Tulip Tree Samaras. Science 197 (1977), 691.

[31] Results of the Second U.S. Manned Orbital Space Flight May 24, 1962. NASA SP-6, 1962.

[32] Campbell, J.P., Low-Speed Aerodynamic Research Related to the Landing of Space Vehicles.

[33] More, F.K., Lift Hysteresis at Stall as an Unsteady Boundary-layer Phenomenon. NACA Rep. 1291, 1956.

seen later that hysteresis is an important necessary, but not sufficient condition for autorotation.

(2) Research on the autorotation of finned missiles and rockets, because of its importance in stabilizing rotating finned bodies, is the most extensive of that in the three basic areas, and is still continuing. The investigation probably started with Schneller's contribution[23] on "lunar motion" and expanded immediately after World War II. However, it was not until 1955 that Nicolaides and Griffin[34] described the problem of "roll speed-up" as the self-sustained spinning of missiles with cruciform fins at high angles of attack (larger than 36°). Oddly enough, the relation of this problem to autorotating plates normal to the flow was not recognized, and the explanation for roll speed-up rested on the hypothesis that the single vortex shed from the spinning cylindrical body interferes with the fins. Nicolaides[35] soon acknowledged that this hypothesis was incorrect, since fins themselves can rotate without the missile body. He proposed another approach by including stall in a quasi-steady strip theory. In this context Nicolaides mentioned autorotation of spinning aircraft (around an axis parallel to the flow), but he noticed that this kind of autorotation and roll speed-up are not the same. The work during the period from 1955 through 1958 with references to prior investigations was summarized by Nicolaides,[36] Brown,[37] and Greene.[38] At that time two movies of wind-tunnel experiments with a plate and a cruciform plate system were made at the Department of

---

[34] Nicolaides, J.D. and T.F. Griffin, On a Fluid Mechanism for Roll Lock-in and Rolling Speed-up Due to Angle of Attack of Cruciform Configurations. BUORD Tech. Note No. 16, Sept. 1955.

[35] Nicolaides, J.D., On the Rolling Motion of Missiles. BUORD Tech. Note No. 33, March 1957.

[36] Nicolaides, J.D., Final Technical Note. BUORD 1961.

[37] Brown, F.N.M., Summary report on cruciform fin study. University of Notre Dame, Indiana, Dept. of Aeronautical Engineering, Contract NORD 17702, May 1958.

[38] Greene, J.E., An Investigation of the Rolling Motion of Cruciform-fin Configurations. NAVORD Rep. 6262, March 1960.

Aeronautical Engineering of the University of Notre Dame under F.N.M. Brown. On the basis of these revealing flow pictures Lugt[39] in 1961 related roll speed-up explicitly to the autorotation of plates normal to the flow. In this paper he also suggested the use of slots to prevent or reduce autorotation. Subsequent experiments at the University of Notre Dame and the Naval Academy, as reported by Daniels and Clare,[40,41] verified the usefulness of slots.

In recent years work has continued to accurately analyze and predict roll speed-up from experimental data without any attempt to explain the phenomenon. Nonlinear least-square fitting was done by Cohen et al,[42] with a third order polynomial suggested by Daniels.[43] It may be pointed out that there is a close analogy of the curve for the moment coefficient versus roll with that for rotating airplanes [see Ref. 5, p. 209]. Fiechter[44] also observed autorotation in the region of "roll lock-in" (angles of attack between roll slow-down and roll speed-up) which is caused by vortices shed from the disturbed boundary layer of the missile body.

(3) Parallel to the study of autorotation of finned missiles was the investigation of autorotating bomblets. The purpose of this work is directly opposite to that of work with finned missiles. Whereas the goal of missile aerodynamicists is to prevent uncontrolled rotation, that

---

[39] Lugt, H.J., Self-Sustained Spinning of a Cruciform Fin System. Proc. Fifth U.S. Navy Symposium on Aeroballistics. Naval Ordnance Lab., White Oak, Md., 1961.

[40] Daniels P., Fin Slots vs Roll Lock-In and Roll Speed-Up. Journ. Spacecraft and Rockets 4 (1967), 410.

[41] Daniels, P. and T.A. Clare, Aerodynamic Characteristics of the Slotted Fin. Journ. Aircraft 9 (1972), 603.

[42] Cohen, C.J., T.A. Clare, and F.L. Stevens, Analysis of the Nonlinear Rolling Motion of Finned Missiles. AIAA 12 (1974), 303.

[43] Daniels, P., A Study of the Nonlinear Rolling Motion of a Four-Finned Missile. Journ. Spacecraft and Rockets 7 (1970), 510.

[44] Fiechter, M., Kegelpendelung, Autorotation und Wirbelsysteme schlanker Flugkorper. Zeitschr. Flugwissenschaften 20 (1972), 281.

of aeroballistic engineers is to encourage autorotation in order to cover a wide target area for self-dispersing bomblets. This process is similar to the dissemination of rotating tree seeds and fruits. Burgess[45] assembled a collection of papers on the subject and a few comments are offered here.

In 1948 Zaroodney[46] observed that mortar shells can have a high rate of spin. He postulated a new phenomenon due to the "instability of spin" without relating it to known autorotation phenomena. Flatau,[47] Gebman,[45] and Bustamante and Stone[45,48] obtained experimental data on the autorotation of plates normal to the flow with application to bomblets. Flatau and Gebman investigated a "Riabouchinsky-type" device sketched in Fig. 5. Strictly speaking, however, the rotation of this device does not fall under the concept of autorotation as defined in Section 2.1. For reentry studies Bustamante and Stone[45,48] made a series of experiments with plates, right circular cylinders, and disks with freely moving and fixed axes in subsonic and hypersonic flow. It appears, although not absolutely conclusively, that plates can autorotate in hypersonic flow. Right circular cylinders clearly are able to do this. Bustamante and Stone consider the vortex shed behind the retreating edge of the plate responsible for autorotation.

In recent years some investigations have been performed which are not directly related to the three application areas discussed so far, but which give valuable insight into the mechanism of autorotation normal to the flow.

---

[45] Burgess, F.F. (ed.), Proceedings of Conference on Dynamics and Aerodynamics of Bomblets. Vol. I. Tech. Rep. AFATL-TR-67-195, Oct. 1967.

[46] Zaroodney, S.J., On the Mechanism of Dispersion and Short Ranges of Motor Fire. Ballistic Research Lab. No. 668, 1948.

[47] Flatau, A., An Investigation of the Rotational and Aerodynamic Characteristics of High Aspect Ratio Rotors. U.S. Army Edgewood Arsenal CRDL TM 1-4, 1964.

[48] Bustamante, A.C. and G.W. Stone, The Autorotation Characteristics of Various Shapes for Subsonic and Hypersonic Flows. Journ. AIAA 69-132, 1969.

The characteristics of freely falling oblate spheroids are of interest in the study of hailstones.[49] Kry and List[50] determined the range of autorotation in which the quasi-steady technique can be applied. List et al[51] actually computed rates of autorotation by means of the quasi-steady approach. In the same way Soong[52] used experimental data for non-rotating bodies from Stilley[53] to determine the flight path of a discus. During a no-spin throw (no rotation around the axis normal to the disk) the discus autorotates perpendicular to the flight path. Experiments with freely falling disks have been made by Willmarth et al.[54]

An important paper on autorotating plates was published by E.H. Smith in 1971.[55] In this paper he reports and analyzes results of experiments on the hysteresis effect on which the explanation of auto-rotating plates with fixed axes rests. He also gives for the first time detailed data on drag, lift, and moment coefficients as a function of time. Data on the influence of Reynolds number, moment of inertia, etc. are also given and compared with sketches of flow patterns. E.H. Smith claims originality of these flow patterns, but this claim is not valid since the movies made at the University of Notre Dame a decade earlier are more detailed and more informative. Despite this slight criticism, Smith's

---

[49] Kry, P.R. and R. List, Angular motions of freely falling spheroidal hailstone models. Physics of Fluids 17 (1974), 1093.

[50] Kry, P.R. and R. List, Aerodynamic torques on rotating oblate spheroids. Physics of Fluids 17 (1974), 1087.

[51] List, R., U.W. Rentsch, A.C. Byram, and E.P. Lozowski, Journ. Atmos. Sci. 30 (1973), 653.

[52] Soong, T.C., The Dynamics of Discus Throw. Trans. ASME, Journ. Appl. Mech., Dec. 1976, 531.

[53] Stilley, G.D., Aerodynamic Analysis of the Self-Sustained Flare. AD-740117, Naval Ammunition Depot, Crane, Ind., Oct. 1972.

[54] Wilmarth, W.W., N.E. Hawk, A.J. Galloway, and F.W. Roos, Aerodynamics of oscillating disks and a right-circular cylinder. Journ. Fluid Mech. 27 (1967), 177.

[55] Smith, E.H., Autorotating wings: an experimental investigation. Journ. Fluid Mech. 50 (1971), 513.

paper is an important one, and more of its content will be referred to later.

2.3 THE STATE OF THE ART

The history of the concept and explanation of autorotation over the last 125 years is quite colorful. The various attempts, motivations, and experiences related to explaining and exploiting this phenomenon have an element of incoherence which is probably due to the different application areas involved. This may account for the lack of concern for previous work which one finds in the literature. For instance, Riabouchinsky's contributions seem entirely forgotten; Greenhill's paper was uncovered by the author[56] in 1965, although his results are contained in the widely used reference books of Lamb[10] and Milne-Thomson.[57] Dupleich's extensive experimental data were largely unnoticed, or were merely referenced despite the translation of his paper into English in a NACA report.[17] Some researchers do not reference previous work at all as, for instance, the authors of [48].

Autorotation about an axis parallel to the flow (Fig. 2a and b) can be explained and computed approximately by the quasi-steady technique. This approach neglects dynamic effects due to rotation.

Autorotation about an axis normal to the flow (Fig. 2c, d, e) can also be explained and crudely computed for bodies with freely moving axes by means of the quasi-steady method (see, e.g. [50, 52]), at least under certain conditions. The neglect of dynamic effects is here more serious than in the study of autorotation about an axis parallel to the flow. In fact, if the plate has a sufficiently large moment of inertia, the freely falling body will behave like one with a fixed axis.

The autorotation of plates about an axis fixed in a parallel constant flow cannot be explained by a quasi-steady theory. The average torque

---

[56] Lugt, H.J., On the autorotation of fin systems. U.S. Naval Weapons Laboratory, Dahlgren, Va., Tech. Memo. No. K-22/65, Jan. 1965.

[57] Milne-Thomson, L.M., Theoretical Hydrodynamics, The MacMillan Co., N.Y., 1968, 5th ed.

is here always zero. Nor can the flow around the body be computed by boundary layer theory (because of the complicated vortex-shedding process) or by discrete vortex models (which are inaccurate when the vortex sheet is close to the body).[56] Experimentally, it is difficult to obtain information on the local drag, lift, and moment coefficients which require knowledge of the surface pressure. In fact, it is only recently that such measurements have been made on the spinning right circular cylinder by Miller[58] at Edgewood Arsenal, Aberdeen Proving Ground. A fruitful investigation must be based, according to Lugt[56] in 1965, on the time-dependent equations of motion, whose solutions include delayed boundary-layer separation and vortex shedding of a rotating body. That is, the full Navier-Stokes equations must be used. This is why previous attempts to explain autorotation failed or gave only a partial answer.

Thus, autorotation of plates about a fixed axis normal to the flow is still not sufficiently well understood. The objective of this paper is to clarify the problem and to present a detailed and quantitative explanation of autorotation. This investigation is based on numerical solutions of the Navier-Stokes equations for laminar fluid motion.

3. MODEL FORMULATION AND SOLUTION TECHNIQUE

3.1 DESCRIPTION OF THE FLOW MODEL

The available information on autorotating plates normal to the flow clearly reveals that the mechanism of autorotation is intricate and complex. A theoretical study should be made with a model which is simple enough to be handled mathematically yet sufficiently realistic to explain autorotation.

The movement of a freely falling cardboard in air or of a thin metallic plate in water indicates that the autorotation around the longer axis is quite stable, and that the model can be simplified by assuming

---

[58] Miller, M.C., Surface Pressure Measurements on a Spinning Wind Tunnel Model. AIAA Journ. 14 (1976), 1669.

the laminar flow of an incompressible fluid around an infinitely long plate in two space dimensions. More careful experiments with endplates confirm that three-dimensional effects are not essential for autorotation. In fact, they interfere with autorotation. Since autorotation of a plate about a fixed axis cannot be explained by a quasi-steady theory, the assumption of a fixed axis focusses the study on the essential features which generate autorotation. Under this assumption the motion of the body has one degree of freedom, that is, the body rotates only about the fixed axis with the angular velocity $\Omega = d\alpha/dt'$, where α is the angle of attack and t' the time. The equation for the angular motion is then

$$I \frac{d\Omega}{dt'} = T_{FL} + T_{EX} \tag{1}$$

where I is the moment of inertia, and T_{FL} and T_{EX} are the torques exerted on the body by the fluid and from the outside, respectively. Autorotation is defined by

$$\bar{T}_{FL} = \frac{1}{2\pi} \int_0^{2\pi} T_{FL}\, d\alpha = 0, \quad T_{EX} \equiv 0 \tag{2}$$

In general, of course, the value of the integral $\int_0^{\alpha} T_{FL}\, d\tilde{\alpha}$ is not zero except for certain values of α.

The experiments of E.H. Smith[55] show that autorotation can occur at Reynolds numbers as low as 100 and that the angular velocity Ω of the rotating plate can be almost constant for a sufficiently large dimensionless moment of inertia.[7] These observations make a numerical analysis of the problem attractive.

The occurrence of autorotation at low Reynolds numbers permits the construction of solutions of the Navier-Stokes equations with presently available computers and experience in numerical analysis. The assumption of constant Ω overcomes another difficulty in numerical formulations and solutions: In order to induce the plate to autorotate a certain amount of initial rotation must be provided. If this initial impulse is too weak, the plate will oscillate a few times, and the motion may then come to a stop or it may become autorotation. If the initial rotation is too strong, the plate will rotate due to this initial impulse and may

subsequently autorotate. In both cases numerical computations would require a number of trials with excessively long computer runs to arrive at a solution for the state of autorotation. This situation can be avoided by assuming a constant Ω of the plate. Then, only the Reynolds number, the Rossby number (which is the ratio of translational to rotational velocity of the plate), and the geometric quantities occur as flow parameters after the initial phase.

In general, the condition of autorotation (Equation (2)) will not be satisfied for a prescribed set of flow parameters if Ω is a constant. Rather, it follows from Equation (1) that $T_{FL} = - T_{EX}$. If $\overline{T}_{FL}$ is positive, the plate must be driven by the external torque T_{EX}, for instance, by an electric motor. If $\overline{T}_{FL}$ is negative, T_{EX} will cause braking. If T_{EX} is zero, autorotation exists.

Riabouchinsky[4] experimented with the Lanchester propeller (Fig. 2a) and obtained a relation between the average torque $\overline{T}_{FL}$ and Ω as indicated in Fig. 6. (In this figure $\overline{T}_{FL}$ and Ω have been replaced by the average moment coefficient $\overline{C}_M$ (to be defined later) and by the ratio $\Omega d/2U$, where d is the chord of the wing and U the constant speed of the parallel flow.) If the propeller rotates in a fluid at rest at infinity (Ro = 0), $\overline{C}_M$ is always positive. Energy must be provided to rotate the propeller.

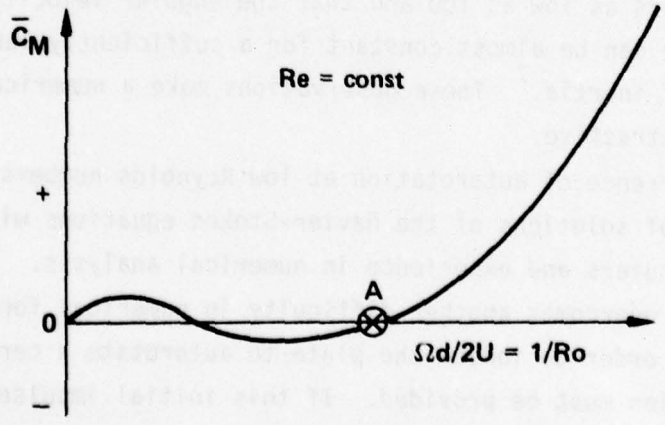

Figure 6 - Average Moment Coefficient $\overline{C}_M$ Plotted Against $\Omega d/2U$. In the Shaded Area the Body Autorotates but Increases its Rotation Until the Point A is Reached. This is the Condition for Stable, (in the average) Steady-State Autorotation

Near the other extreme, if the propeller rotates very slowly relative to the parallel flow ($Ro \to \infty$), the torque is also positive. In between, a region of negative torque exists, which Riabouchinsky called "autorotative". Here, T_{EX} has a braking effect. If this effect were removed, the propeller would increase its rotation until the point A in Fig. 6. This is the state of stable, steady autorotation.[11] For this, Definition (2) must be augmented by the stability criterion $\partial \bar{C}_M/\partial \Omega > 0$ or $\partial \bar{C}_M/\partial Ro < 0$. The same situation, observed by Riabouchinsky for the Lanchester propeller, holds also for the plate rotating about a fixed axis normal to the flow. Thus, the phenomenon of autorotation can be studied by examining the flow behavior for various values of Ro.

For numerical reasons, as given by Lugt and Ohring,[59] it is convenient to approximate the plate by a thin elliptic cylinder in a coordinate system (η,θ) which is related to the Cartesian coordinates (x,y) through

$$x + iy = a \cosh(\eta + i\theta),\ a > 0 \tag{3}$$

where a is the focal distance. $\eta = \eta_1$ is the elliptic body contour. Its value is also a measure of the relative thickness of the "plate". Again for numerical reasons, $\eta_1 = 0.1$ was chosen (except for one case with $\eta_1 = 0.6$) instead of $\eta_1 = 0$, which is the infinitely thin plate.[60] However, it may be mentioned that the difference in the results between $\eta_1 = 0$ and $\eta_1 = 0.1$ is insignificant.

If the reference frame is fixed to the body, the initial/boundary value problem for the Navier-Stokes equations expressed in terms of the vorticity ω and the stream function ψ is

$$\frac{\partial \omega}{\partial t} + \frac{1}{h^2} \frac{\partial(\psi,\omega)}{\partial(\eta,\theta)} = \frac{2}{Re} \nabla^2 \omega \tag{4}$$

$$\nabla^2 \psi = \omega \tag{5}$$

---

[59] Lugt, H.J. and S. Ohring, Rotating elliptic cylinders in a viscous fluid at rest or in a parallel stream. Journ. Fluid Mech. 79 (1977), 127.

[60] Lugt, H.J and H.J. Haussling, Laminar flow past an abruptly accelerated elliptic cylinder at 45° incidence. Journ. Fluid Mech. 65 (1974), 711.

where the flow quantities are made dimensionless by the constant velocity U and the focal distance a. Reynolds and Rossby numbers are defined by $Re = 2aU/\nu$, $Ro = U/a\Omega$. It is practical also to introduce $Re_d = dU/\nu$, $Ro_{d/2} = 2U/d\Omega$ with $d = 2a \cosh \eta_1$ as the chord of the plate. The parameter h is $h^2 = \cosh^2 \eta - \cos^2 \theta$.

The boundary conditions are (Fig. 7):

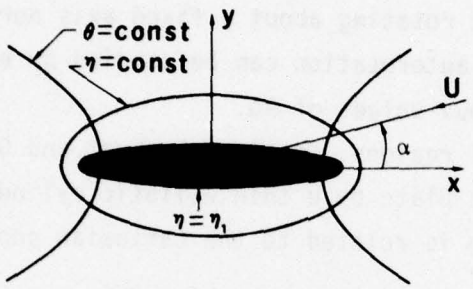

Figure 7 - Elliptic Coordinate System and Definition of Angle of Attack

$$\psi = 0, \quad \partial\psi/\partial\eta = 0 \quad \text{at} \quad \eta = \eta_1 \tag{6}$$

$$\left.\begin{aligned} h^{-1}\partial\psi/\partial\theta &= \cos(\theta - t/Ro) \\ h^{-1}\partial\psi/\partial\eta &= \sin(\theta - t/Ro) + (h\,Ro)^{-1} \cosh\eta \sinh\eta \end{aligned}\right\} \text{at } \eta = \infty \tag{7}$$

with $\alpha(t) \equiv t/Ro$ the angle of attack.

The abrupt start of the body from rest is chosen as the initial condition. A comparison with other acceleration models is given by Lugt and Haussling.[61] In this paper, the initial condition consists of the potential-flow solution and a vorticity sheet at the body surface enforcing the nonslip condition.[59] Part of the initial condition is the initial angle of attack $\alpha = \alpha_0$. In all examples α_0 is chosen to be 0°

---

[61] Lugt, H.J. and H.J. Haussling, The Acceleration of Thin Cylindrical Bodies in a Viscous Fluid. Journ. Appl. Mech. 45 (1978), 1.

since for this angle the transient period is short compared to that for $\alpha = \pi/2$.[59]

The drag, lift, and moment coefficients are defined by

$$\left.\begin{aligned} C_D &= \text{drag}/\tfrac{1}{2}\rho U^2 \tfrac{d}{2} \\ C_L &= \text{lift}/\tfrac{1}{2}\rho U^2 \tfrac{d}{2} \\ C_M &= \text{torque}/\tfrac{1}{2}\rho U^2 (\tfrac{d}{2})^2 \end{aligned}\right\} \qquad (8)$$

The torque here is the torque caused by the fluid, that is T_{FL}.

Each of the coefficients in Equation (8) consists of two parts. The drag coefficient is the sum of the drag due to pressure and the drag due to friction

$$C_D = C_{DP} + C_{DF} \qquad (9)$$

with

$$C_{DP} = \frac{4}{Re}\left[\tanh \eta_1 \cos\alpha \int_0^{2\pi} \left(\frac{\partial\omega}{\partial\eta}\right)_1 \sin\theta d\theta - \sin\alpha \int_0^{2\pi} \left(\frac{\partial\omega}{\partial\eta}\right)_1 \cos\theta d\theta\right] \qquad (10)$$

$$C_{DF} = \frac{4}{Re}\left[-\cos\alpha \int_0^{2\pi} \omega_1 \sin\theta d\theta + \tanh\eta_1 \sin\alpha \int_0^{2\pi} \omega_1 \cos\theta d\theta\right] \qquad (11)$$

The lift and moment coefficients may be expressed in a corresponding way.[60] In this notation, negative values of C_D, C_L, and C_M denote, respectively, drag, lift in the direction of the Magnus force, and torque supporting the body rotation.

3.2 OUTLINE OF THE NUMERICAL ANALYSIS

The initial/boundary-value problem defined in the previous section is solved by the same finite-difference scheme used in an earlier paper.[59] It is, therefore, not necessary to repeat the procedure here, but it may be mentioned that the vorticity equation (4) is discretized with the DuFort-Frankel scheme, and that the Poisson equation (5) is solved with Hockney's direct method. Furthermore, the following transformation is made for numerical reasons:[59]

$$\psi = \psi^* + 2/Ro(\cosh^2 \eta - \sin^2 \theta) \tag{12}$$

$$\omega = \omega^* + 2/Ro \tag{13}$$

This transformation avoids large values of ψ at the outer boundary but leaves the grid fixed to the body.

The grid has been chosen in such a way that the infinite region of integration is replaced by a finite network of points $\eta_1+(i-1)\Delta\eta$, $(j-\frac{1}{2})\Delta\theta$ with $i = 1,\ldots,97$ and $j = 1,\ldots,96$; $\Delta\eta = 0.04$. The time increments, except in the brief initial phase where they are very small, are

$Ro_{d/2} = 1, 2, 4,$ $\eta_1 = 0.1$ $\Delta t = 0.0025$

$Ro_{d/2} = 6$ $\Delta t = 0.003$

$Ro_{d/2} = 2,$ $\eta_1 = 0.6$ $\Delta t = 0.005$

Since $\Delta\alpha = \Delta t/Ro$, more computer time is required to calculate one plate revolution at higher Rossby number. The computer time required on the IBM 360-91 for each time step is 0.7 sec. One cycle, equal to half a plate revolution, requires then 1250 time steps times 0.7 times Ro, which is 870·Ro sec or 14.5·Ro min.

The accuracy of the numerical scheme was previously checked for the nonrotating plate[60] by comparing results with varying grids, with experimental results by Honji,[60] and with a different numerical scheme by Mehta of Stanford University (private communication) and by Collins and Dennis.[61] The general rotating plate program was checked for the special case of the rotating circular cylinder.[59] For Ro = 4 and 6 a new numerical phenomenon has been observed, the reason for which is not yet known. The curves for the force and moment coefficients show oscillations from time step to time step which may cease for a while and then resume (Figure 8).

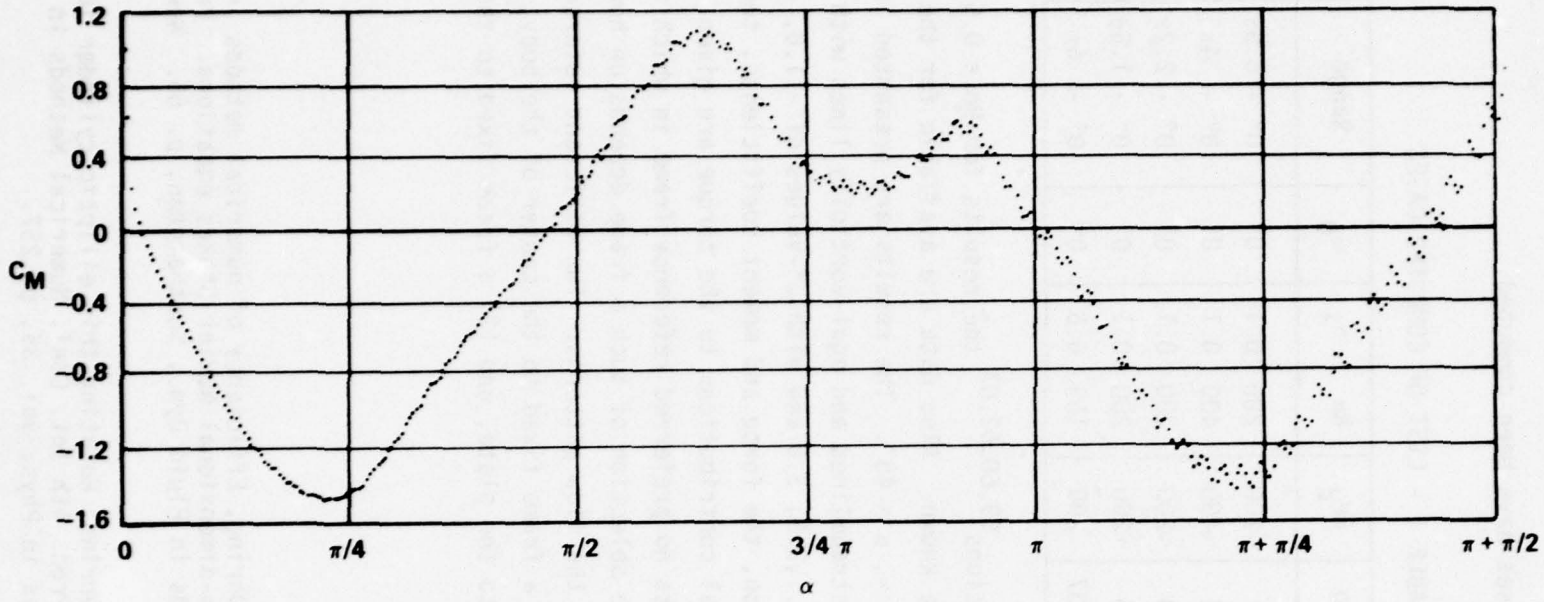

Figure 8 - Numerical Oscillations Observed in the Force and Moment Coefficients for Ro = 4 and 6. The Above Curve Represents C_M versus α for Ro = 6, Re = 200, $\eta_1 \approx 0.1$, $\alpha_0 = 0$ Degrees

The following cases have been computed.

TABLE 1 - LIST OF COMPUTED CASES

$Ro_{d/2}$	Ro	Re_d	Re	η_1	α_0	Range
$\sim$1	1	$\sim$200	200	0.1	0°	0° - 5.5π
$\sim$2	2	$\sim$400	400	0.1	0°	0° - 4π
$\sim$4	4	$\sim$200	200	0.1	0°	0° - 2.2π
$\sim$6	6	$\sim$200	200	0.1	0°	0° - 1.5π
2	2.37	200	169	0.6	0°	0° - 6π

From previous calculations[59,60,62,63] the results for Ro = 0.5, 2, Re = 200, η_1 = 0.1 are known. Also data are available for the limiting cases Ro = 0 and Ro = ∞, α = 45°. The results are presented in the form of flow patterns for streamlines and equi-vorticity lines with ψ*-values of -3.0, -2.8,...,0,...,2.8, 3.0 and with ω*-values of -11.0, -9.0,..., 9.0, 11.0. In addition, the force and moment coefficients, the surface pressure, and the local contributions to the torque are given.

Since there exists no preferred reference frame in which to present the streamlines,[59] the selection of such a frame depends on how useful it is for discussions of the flow patterns. Two different reference frames have been chosen: (1) a frame fixed to the center of the body, but rotating in relation to the plate, and (2) a frame fixed to the body.

---

[62] Lugt, H.J. and S. Ohring, Efficiency of numerical methods in solving the time-dependent two-dimensional Navier-Stokes equations. Proc. Int. Conf. Numerical Methods in Fluid Dyn., Southampton, p. 65. New York: Crane, Russak & Co.

[63] Lugt, H.J. and S. Ohring, Rotating thin elliptic cylinder in a parallel viscous fluid flow. Proc. 4th Int. Conf. Numerical Methods in Fluid Dyn., Boulder. Lecture Notes in Phys. vol. 35, p. 257.

4. RESULTS AND DISCUSSIONS

4.1 LOW REYNOLDS-NUMBER FLOW

As stated in Section 3.1 it is assumed that the plate rotates with constant angular velocity Ω about a fixed axis normal to a uniform parallel stream. For this situation potential-flow theory (discrete vortices are not considered) and quasi-steady viscous flow models predict a vanishing average torque for all Ro: $\bar{C}_M(Ro) \equiv 0$. This means that, once the plate starts rotating, it does not need a driving torque T_{EX}; it always autorotates. In potential-flow theory the average torque is even zero for periodic motions but arbitrary $\Omega(t)$. Here, "periodic" means $C_M(0°) = C_M(\pi n)$ with n = 1,2,3... Circulation does not contribute to the torque. Obviously, such mathematical models are unrealistic.

However, the variation of the torque with -sin 2α predicted in those theories is remarkably accurate. Except for a slight phase shift this relation is also found in experimental results of autorotation[55] and in numerical results based on the Navier-Stokes equations (Figures 9 through 13). The fixed (nonrotating plate) always tends to position itself normal to the parallel flow. Rotating plates behave in most cases in the same way. Except for the small phase shift the torque supports rotation when α changes from 0° to $\pi/2$ (supporting period), but it counteracts rotation from $\pi/2$ to π (retarding period).

The transient phase after the abrupt start is short, especially for $\alpha_0 = 0°$.[59] For the cases considered in this paper, the transient time interval is approximately $t = \alpha Ro = \pi$ with $t_0=0$, $\alpha_0=0°$. In some cases (Figures 9 and 13) the average C_D- and C_L-values increase and decrease, respectively, over the whole time span computed. This effect is probably due to the development of the wake and would vanish after a certain time. This conclusion is based on experience with flows past circular cylinders.[64] The C_M-curves do not show this "transient" effect.

---

[64] Dawson, C.W. and M. Marcus, DMC - A Computer Code to Simulate Viscous Flow About Arbitrarily Shaped Bodies. Proc. 1970 Heat Transfer and Fluid Mechanics Institute, Stanford University Press, 1970.

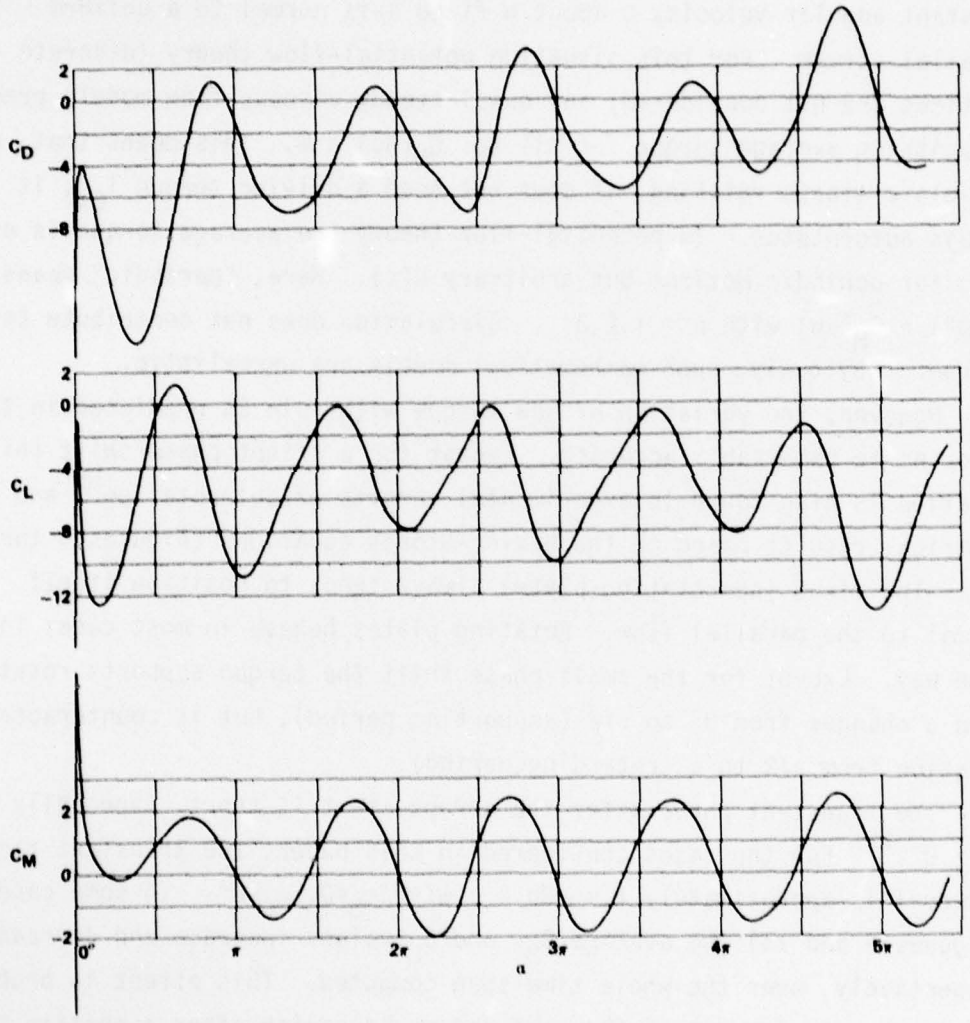

Figure 9 - C_D, C_L, and C_M versus α for Ro = 1, Re = 200, η_1 = 0.1, α_0 = 0 Degrees

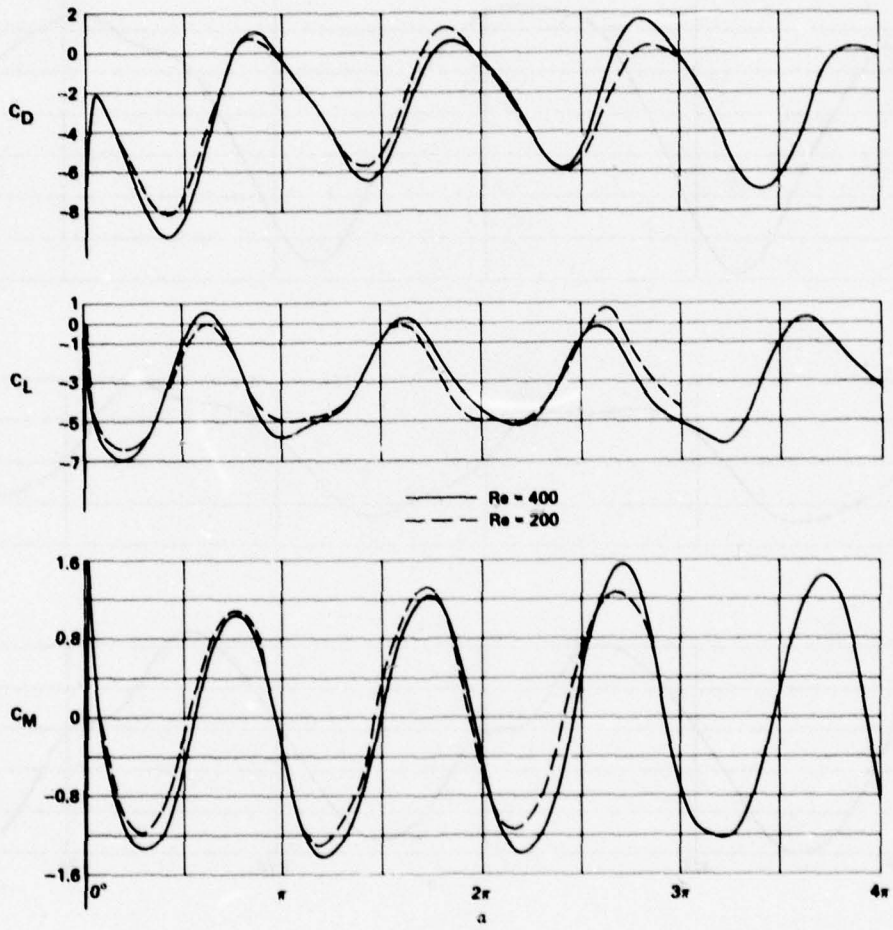

Figure 10 - C_D, C_L, and C_M versus α for Ro = 2, Re = 200 and 400, $\eta_1 = 0.1$, $\alpha_0 = 0$ Degrees

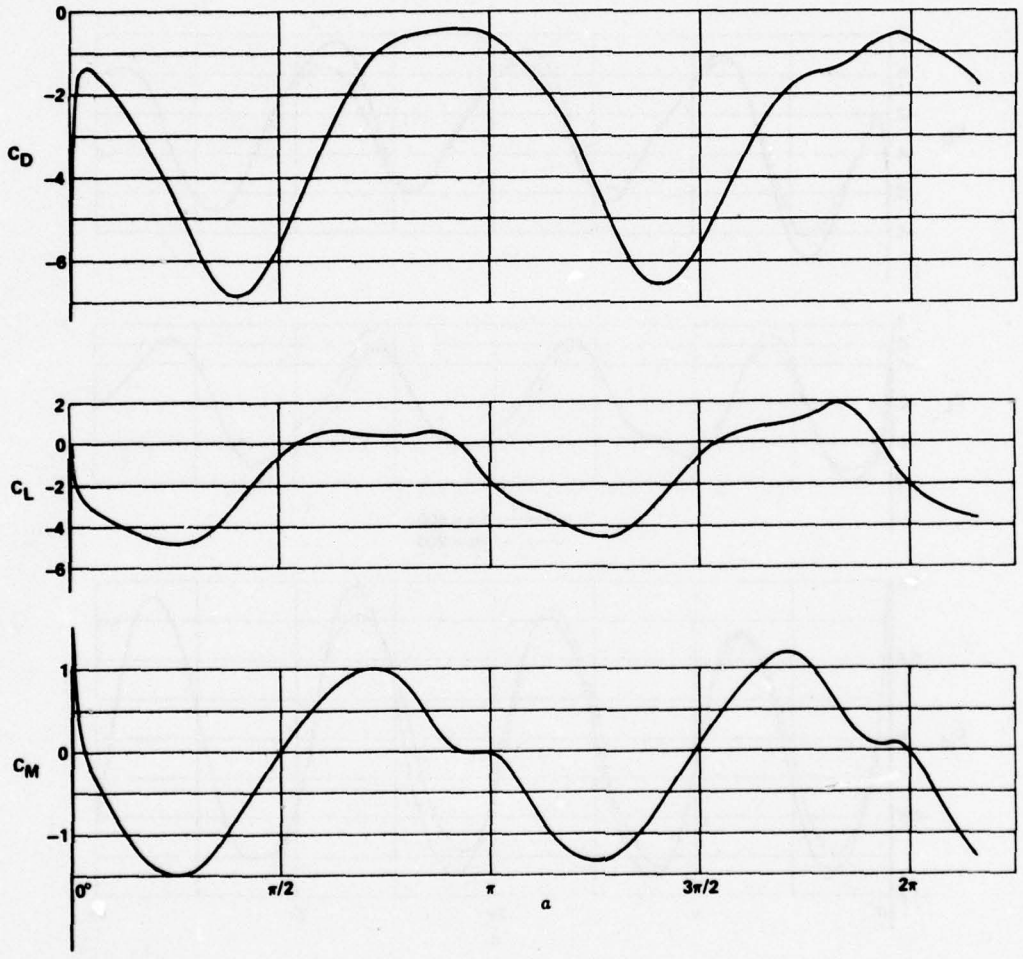

Figure 11 - C_D, C_L, and C_M versus α for Ro = 4, Re = 200, η_1 = 0.1, α_0 = 0 Degrees

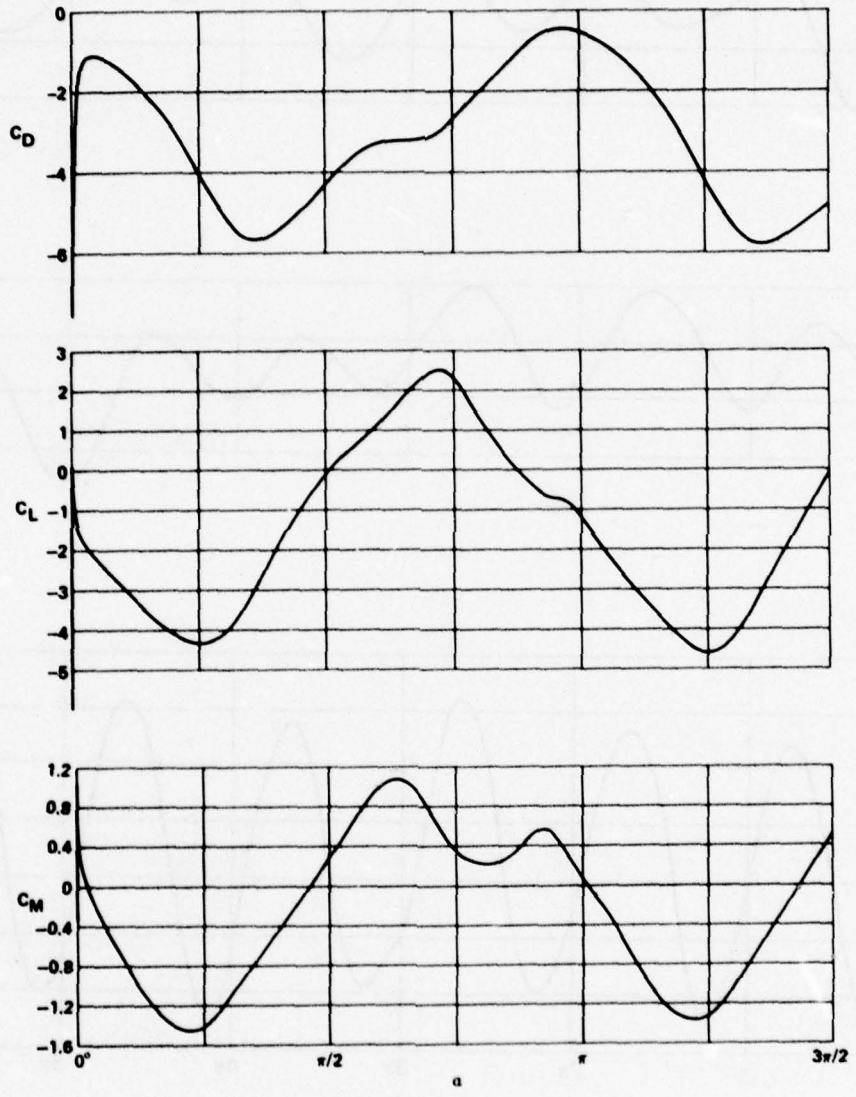

Figure 12 - C_D, C_L, and C_M versus α for Ro = 6, Re = 200
η_1 = 0.1, α_0 = 0 Degrees

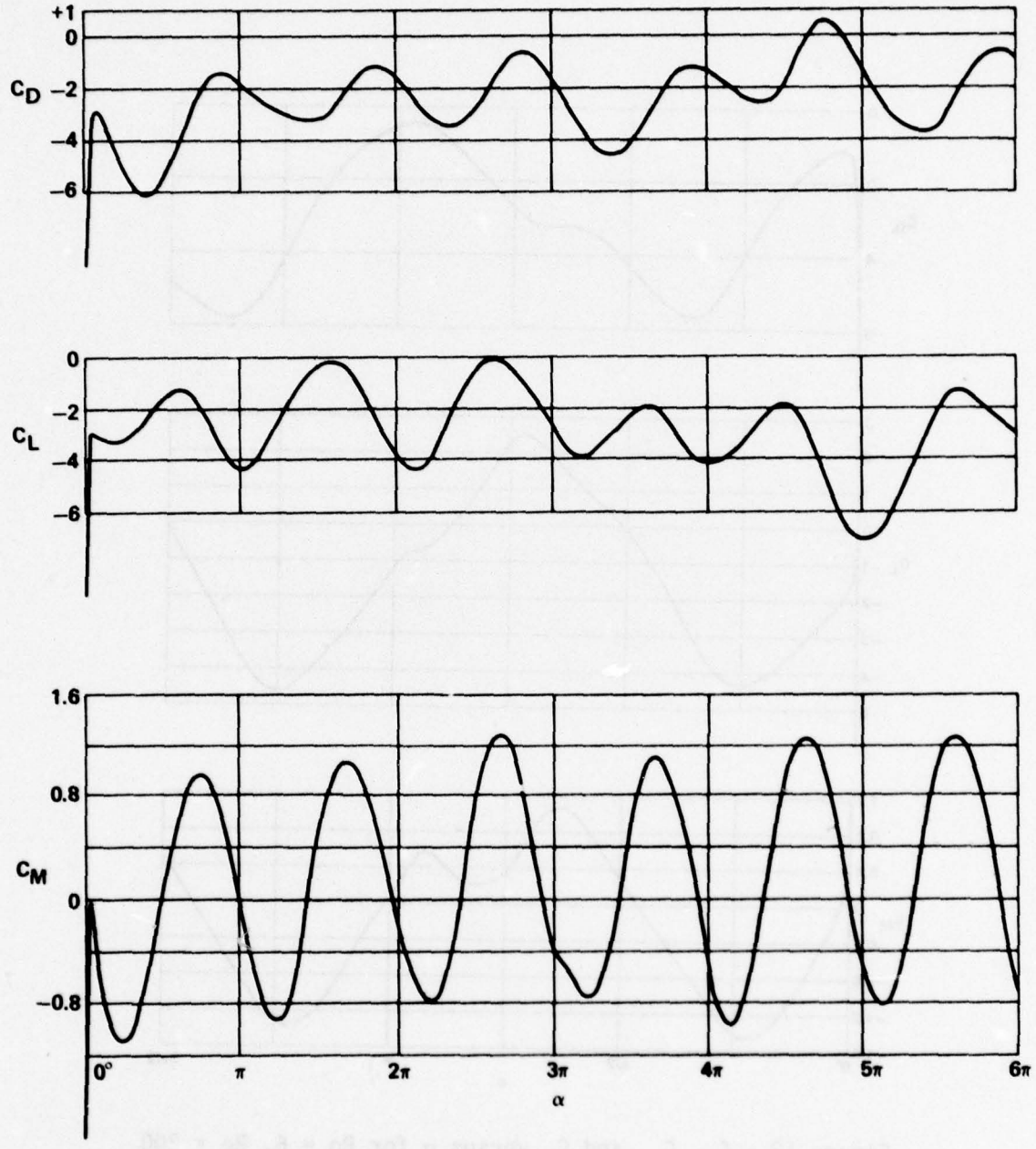

Figure 13 - C_D, C_L, and C_M versus α for $Ro_{d/2} = 2$, $Re_d = 200$, $\eta_1 = 0.6$, $\alpha_0 = 0$ Degrees

The amplitudes of the curves in Figures 9 through 13 may also change when the frequency of vortex shedding is different from the rate of body rotation. In order to further discuss the change in frequency the following notations are introduced. The frequency of vortex shedding behind a nonrotating body is called the "natural" frequency f_N, whereas the frequency of vortex shedding from a rotating body is designated by f. The frequency f_p of the rotating plate is $\Omega/2\pi$. Behind a flat plate a vortex at each tip may be washed downstream every half revolution. Then, vortex shedding and plate rotation are synchronous if

$$\Omega = \pi f \quad \text{or} \quad f_p = f/2 \tag{14}$$

If one introduces the dimensonless form of the frequency f, the Strouhal number $St = fd/U$, Equation (14) can be written in the dimensionless form

$$Ro_{d/2} = 2/\pi\, St \tag{15}$$

For the fixed plate with $Re = 200$, $\eta_1 = 0.1$, and $\alpha = 45°$, $St_N = fd \sin\alpha/U$ is, according to Lugt and Haussling,[60] about 0.18. Thus, for the synchronous situation one expects $Ro_{d/2} \approx 3.6$, provided $f = f_N$, which need not be the case.

In fact, condition (15) is usually not fulfilled. Two kinds of deviations may be distinguished: (1) $\Omega/f \approx \pi n$ with $n = 2,3,\ldots$, and (2) $\Omega/f = \pi + \delta\alpha$, where $|\delta\alpha| << \pi$. The magnitude of $\delta\alpha$ can be determined from Figures 9 through 13, whereas the integer n is best obtained from patterns of equi-vorticity lines.

By including previous results[59] the following data (which exclude the initial phase) are given in Table 2. According to this list only the cases $Ro_{d/2} = 2$ and 4, $Re_d = 200$, $\eta_1 = 0.1$ have synchronized frequencies. (The value for $Ro_{d/2} = 2$, $Re_d = 200$, $\eta_1 = 0.1$ has been taken from longer computer runs.) A comparison with the predicted synchronous value $Ro_{d/2} \approx 3.6$ for $f = f_N$ reveals that synchronization occurs at f_N and values of f above.

TABLE 2 - DATA FOR THE FREQUENCIES OF VORTEX SHEDDING

$Ro_{d/2}$	Re_d	η_1	n	$\delta\alpha$
0.5	200	0.1	3	
1	200	0.1	2	
2	200	0.1	1	
4	200	0.1	1	
6	200	0.1		-6° 45'
2	400	0.1		-3°
2	200	0.6		-4°

The average value of C_D is defined by

$$\overline{C}_D = \frac{1}{2\pi} \int_{2\pi n}^{2\pi(n+1)} C_D \, d\alpha \ , \ n = 0,1,... \qquad (16)$$

with corresponding definitions for $\overline{C}_L$ and $\overline{C}_M$. Negative values for these coefficients indicate real drag, lift in the direction of the Magnus force, and torque supporting rotation, respectively. It is also useful to distinguish between the retarding and supporting periods for C_M:

$$\left.\begin{matrix}\overline{C}_{MR} \\ \overline{C}_{MS}\end{matrix}\right\} = \int_{2\pi n}^{2\pi(n+1)} \overline{C}_M \, d\alpha \quad \text{for} \quad \left\{\begin{matrix}C_M > 0 \\ C_M < 0\end{matrix}\right. \quad \text{only} \qquad (17)$$

The data are given in Table 3. According to this table and Fig. 6 autorotation and rotation with braking ($\overline{C}_M < 0$) occur in the range $2 < Ro_{d/2} \leq 6$, $Re_d = 200$, $\eta_1 = 0.1$. The minimum of $\overline{C}_M$ is at $Ro_{d/2} = 4$, $Re_d = 200$.

In Fig. 14 a representative cycle of C_M (half revolution) for Ro = 1, 2, 4, 6, Re = 200, $\eta_1 = 0.1$ is plotted. As can be seen immediately the retarding period is crucial for explaining autorotation.

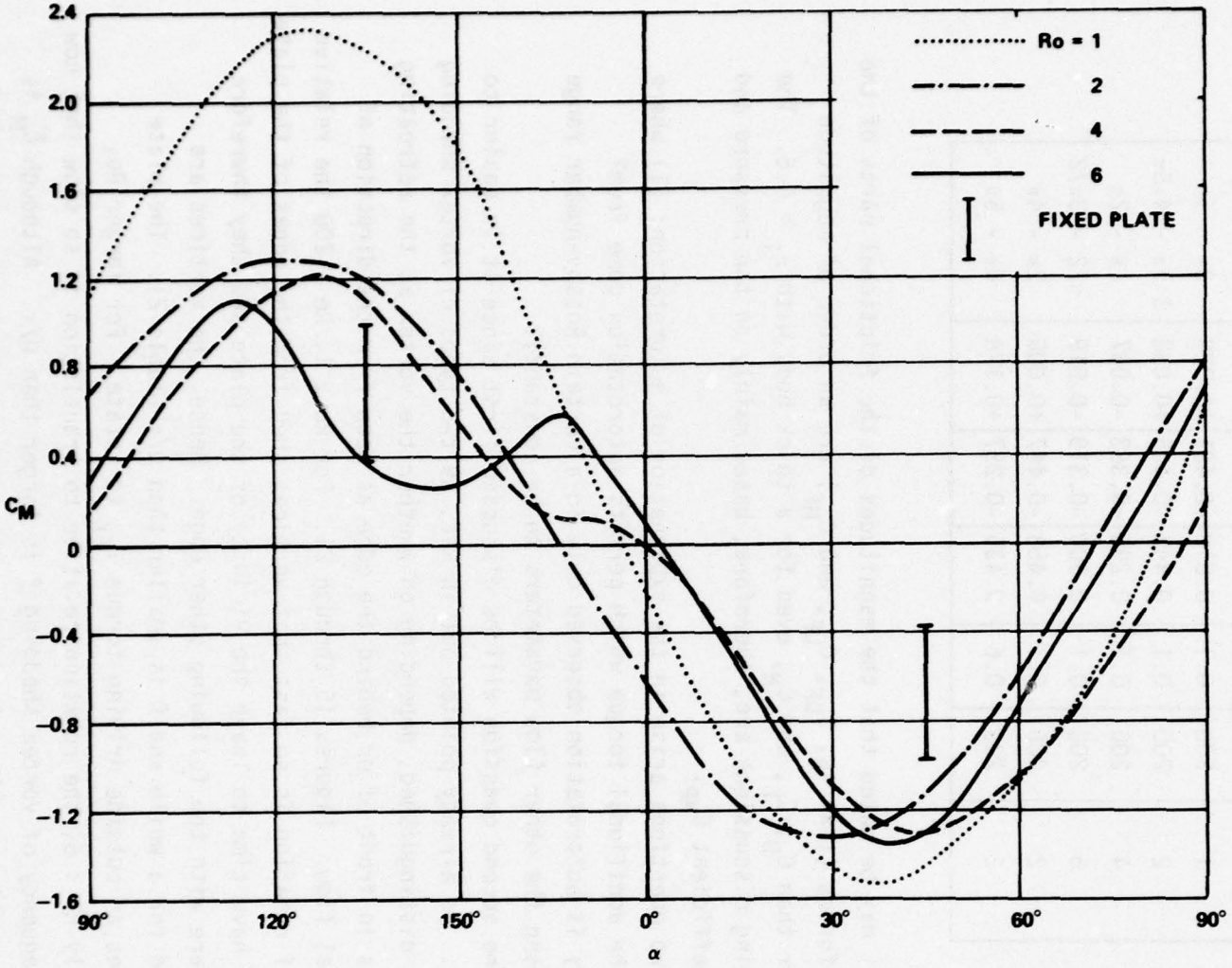

Figure 14 - Comparison of C_M versus α Over One Representative Cycle (half revolution of the plate) for Various Ro with Re 200, η_1 = 0.1

TABLE 3 - MOMENT COEFFICIENTS

$Ro_{d/2}$	Re_d	η_1	$\overline{C}_{MR}$	$\overline{C}_{MS}$	$\overline{C}_M$	Range
1	200	0.1	0.810	-0.481	+0.329	3π - 5π
2	200	0.1	0.443	-0.405	+0.038	3.5π - 4.5π
4	200	0.1	0.296	-0.383	-0.087	π - 2π
6	200	0.1	0.300	-0.319	-0.019	$\pi/2$ - $3\pi/2$
2	400	0.1	0.453	-0.447	+0.006	2π - 4π
2	200	0.6	0.435	-0.257	+0.178	4π - 5π

It may be noted that the magnitudes of the frictional parts of the total forces (that is, C_{DF}, C_{LF}, and C_{MF}) are an order of magnitude smaller than C_D, C_L, and C_M, even for a thick body with $\eta_1 = 0.6$. The following discussions are, therefore, based mainly on the pressure and the coefficient C_{MP}.

Two questions arise in the explanation of autorotation: (1) Where does the additional torque which permits autorotation come from? (2) Why is autorotation observed only in a certain Rossby-number range (assuming the other flow parameters to be constant)?

The second question will be discussed first since it is easier to answer. As already pointed out in Ref. 59 two types of vortex shedding can be distinguished, depending on whether the vortex at the retreating edge is in front of or behind the edge as seen from the direction of parallel flow. Figures 15 through 21. For $Ro \leq 1$, $Re = 200$ the relative rate of rotation is so fast that vortices shed from the edges of the plate do not have time to leave the vicinity of the plate and they therefore interfere with the following other edge. Hence, the vortices are trapped for a while and f is smaller than Ω/π (Table 2). The plate requires an outside driving torque T_{EX} to rotate. For larger Ro, probably $Ro \geq 6$, the rotation relative to translation is so slow that now the frequency of vortex shedding f is larger than Ω/π. Although $\overline{C}_M$ is still negative for $Ro = 6$, the fact that its absolute value is smaller than that for $Ro = 4$ indicates the trend toward positive values. The

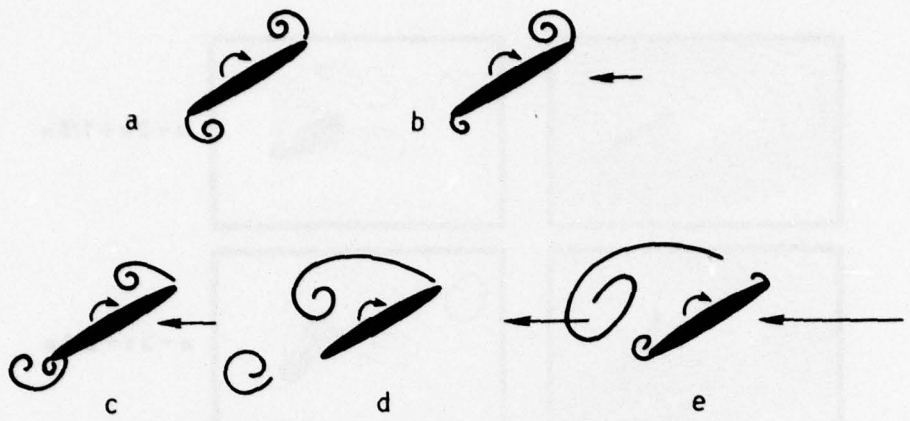

Figure 15 - Sketch of Vortex Shedding About a Rotating Plate. a) Initial Phase for Pure Rotation (Ro=0), b) Initial Phase for Small Rossby number (Ro<1), c) Vortex Pattern for $1 \leq Ro \leq 2$, Re = 200 at a Later Stage, d) Vortex Pattern for Maximum Support of Autorotation, $Ro \approx 4$, Re = 200, e) Vortex Pattern for $Ro \geq 6$, Re = 200

region $2 < Ro \leq 6$ or $0.167 \leq 1/Ro < 0.5$, Re = 200, $\eta_1 = 0.1$ corresponds roughly with the shaded area in Fig. 6 (see also Fig. 22). Since a freely rotating plate with $\bar{C}_M < 0$ increases its angular velocity, autorotation occurs a little above Ro = 2 for Re = 200, $\eta_1 = 0.1$. The motion is synchronous.

What mechanism provides excess torque in the shaded region of Figures 6 and 22 and damping in the other regions?

Supporting Period

In potential flow the moment coefficient is $C_M = -\pi \sin 2\alpha$ for a fixed plate, or for a rotating plate with constant Ω. The minimum value in the supporting period from $\alpha = 0°$ to π is $C_M \approx -\pi$ for $\eta_1 = 0.1$ at $\alpha = 45°$. This torque is generated through the asymmetric displacement of the stagnation points if the plate is neither parallel nor normal to the flow. In viscous fluid flows the torque is reduced considerably since the center of pressure in the rear of the body is generally much closer to the body center than it is in potential flow. Viscosity modifies the flow characteristics in the following way:

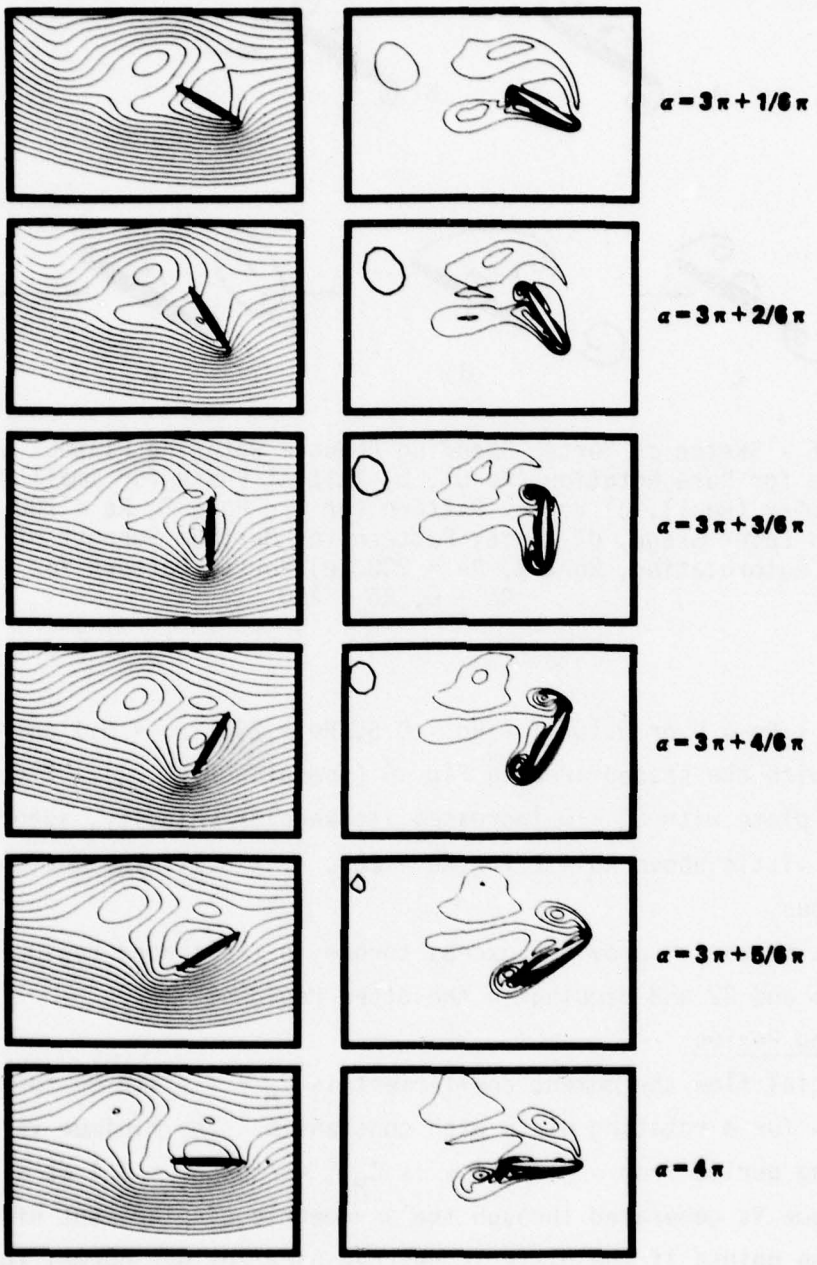

Figure 16a - Sequence of Streamlines and Equi-vorticity Lines Around a Rotating Thin Elliptic Cylinder ("plate") in a Parallel Flow for Ro = 1, Re = 200, η_1 = 0.1, α_0 = 0 Degrees. The Streamlines are Computed in a Frame Which is Fixed to the Body With Regard to Translation but Which is Fixed in Space with Regard to Rotation

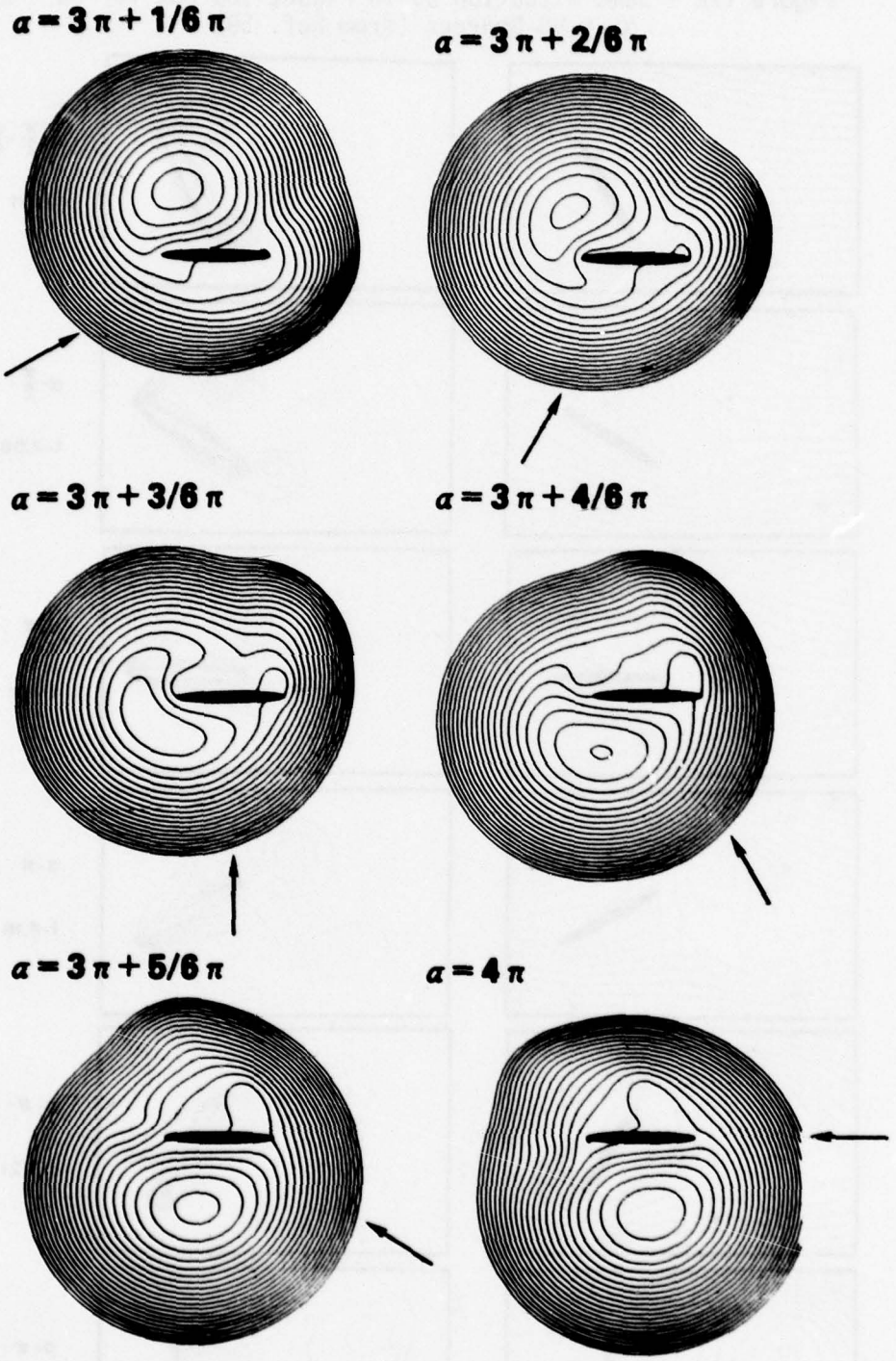

Figure 16b - Same Situation as in Figure 16a but Streamlines are Computed in a Frame Fixed to the Body

Figure 17a - Same Situation as in Figure 16a but for Ro = 2, α_0 = 90 Degrees (from Ref. 59)

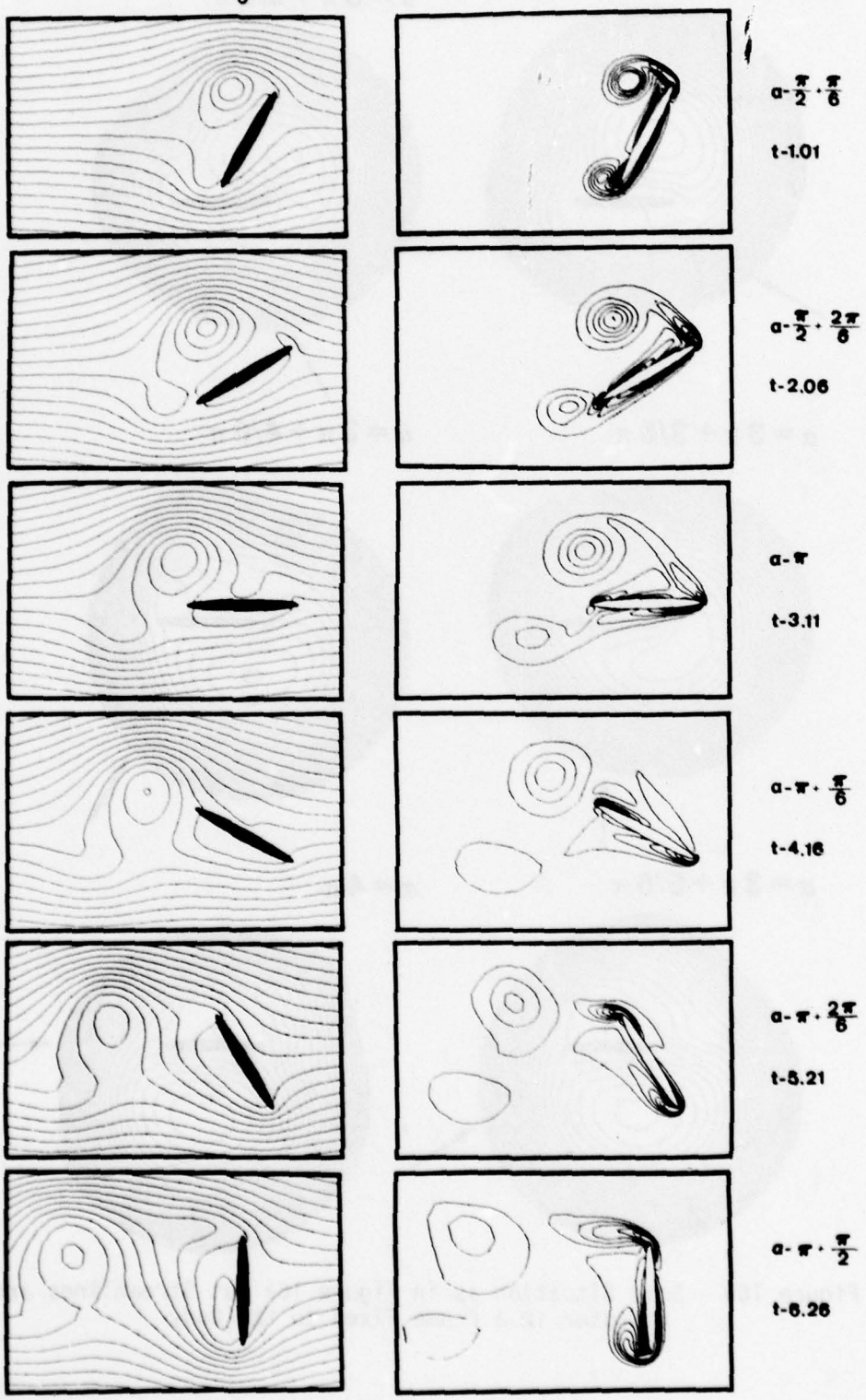

Figure 17a - (continued)

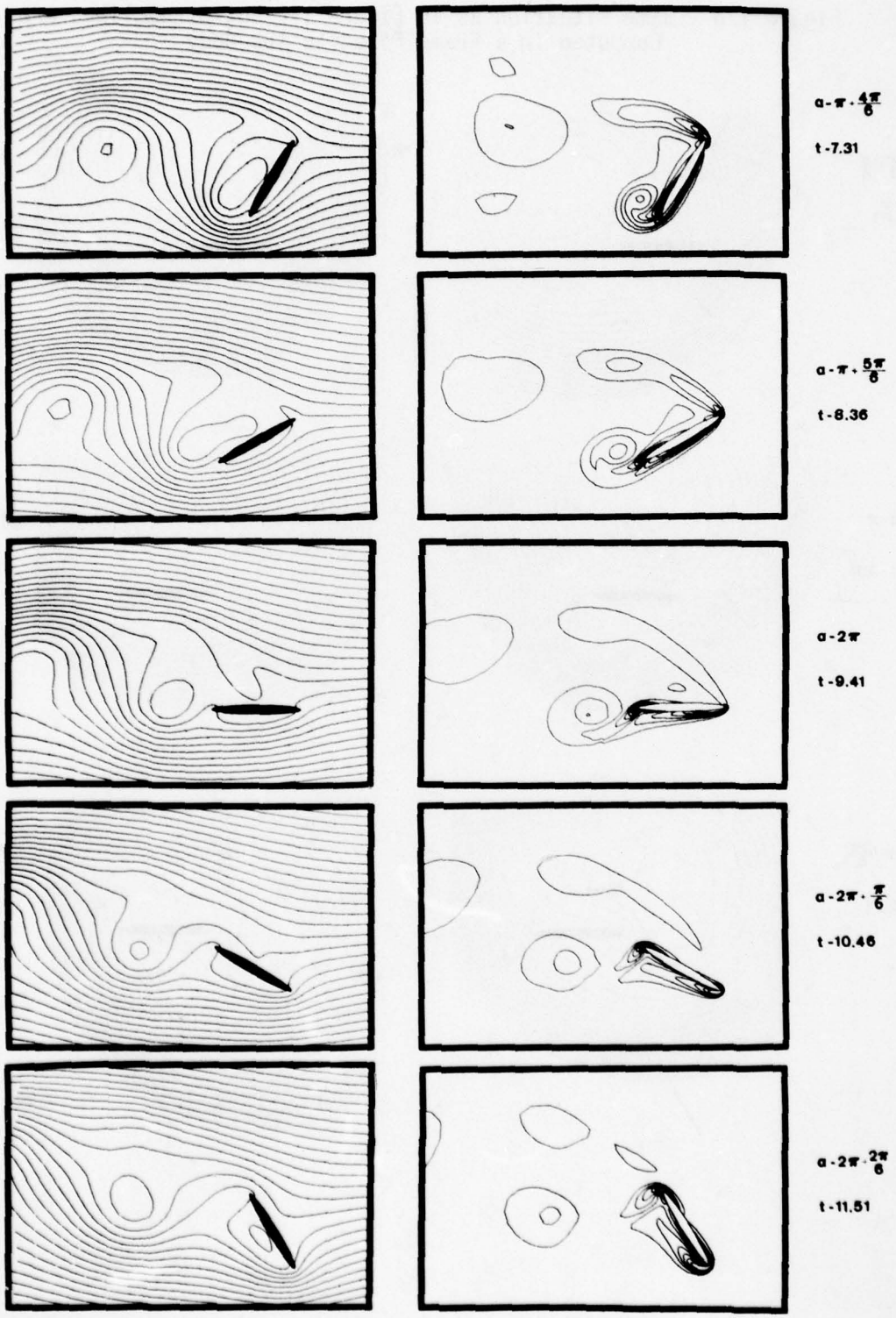

Figure 17b - Same Situation as in Figure 17a but Streamlines are Computed in a Frame Fixed to the Body

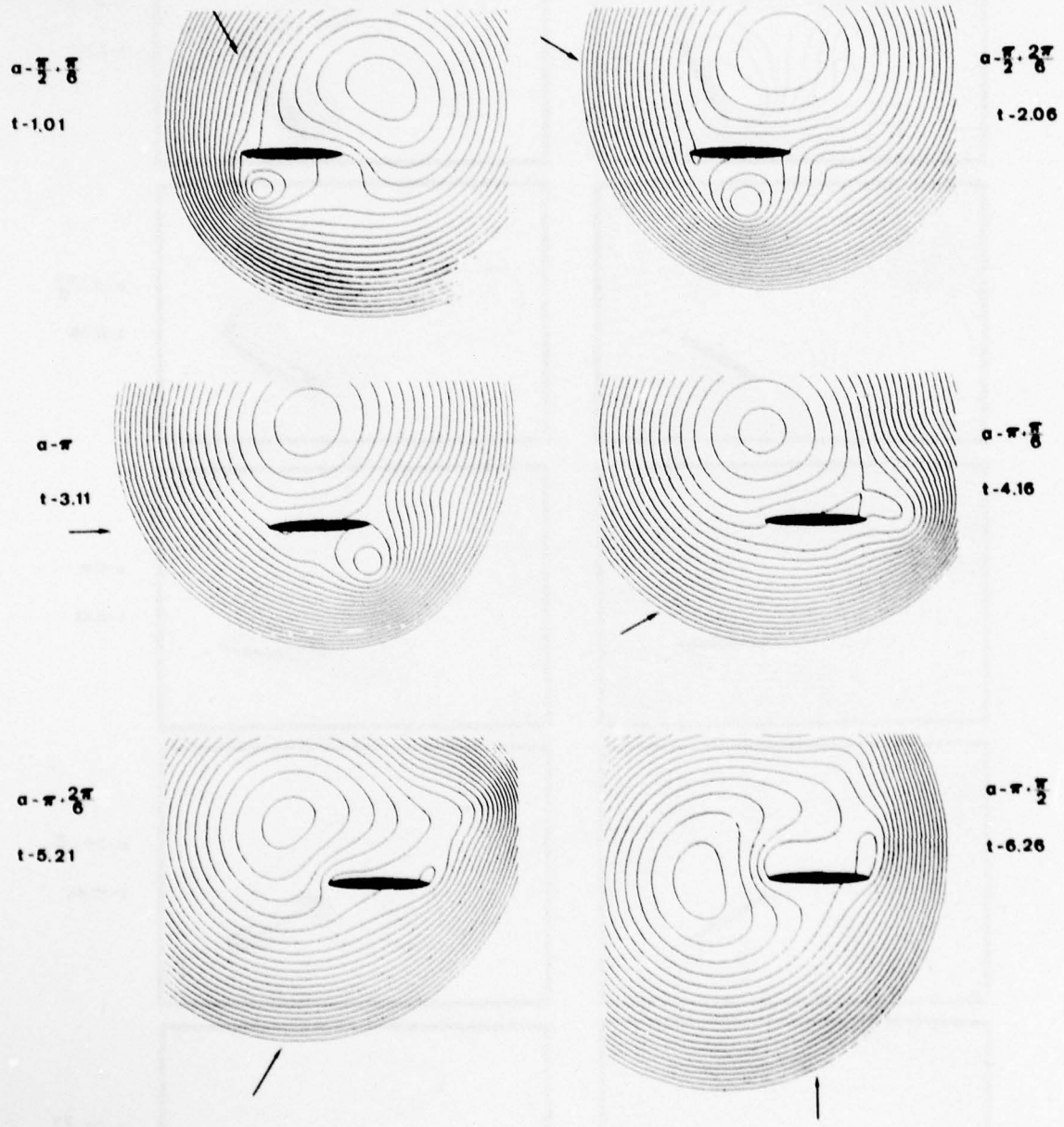

Figure 17b - (continued)

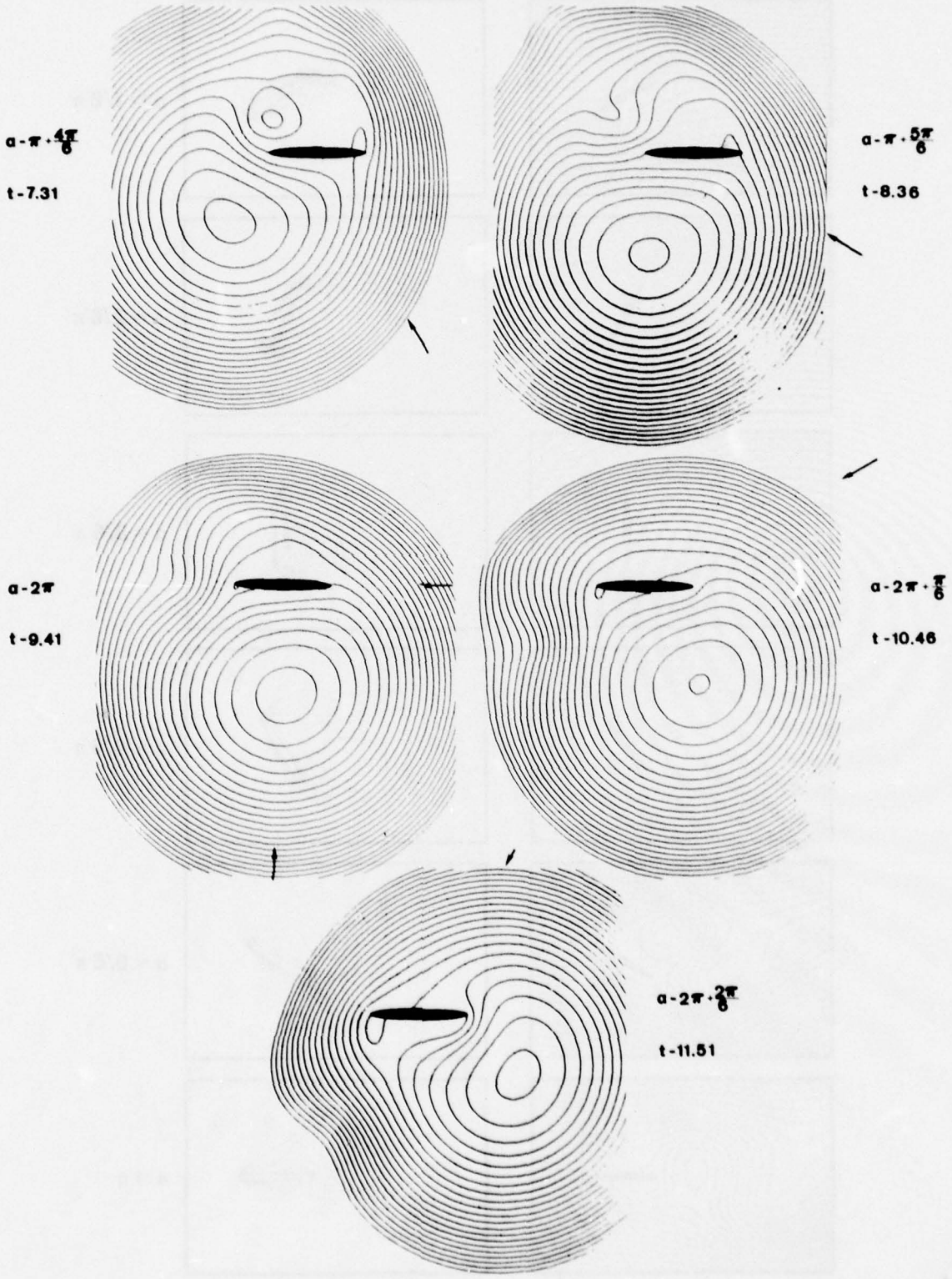

Figure 18a - Same Situation as in Figure 16a but for Ro = 4

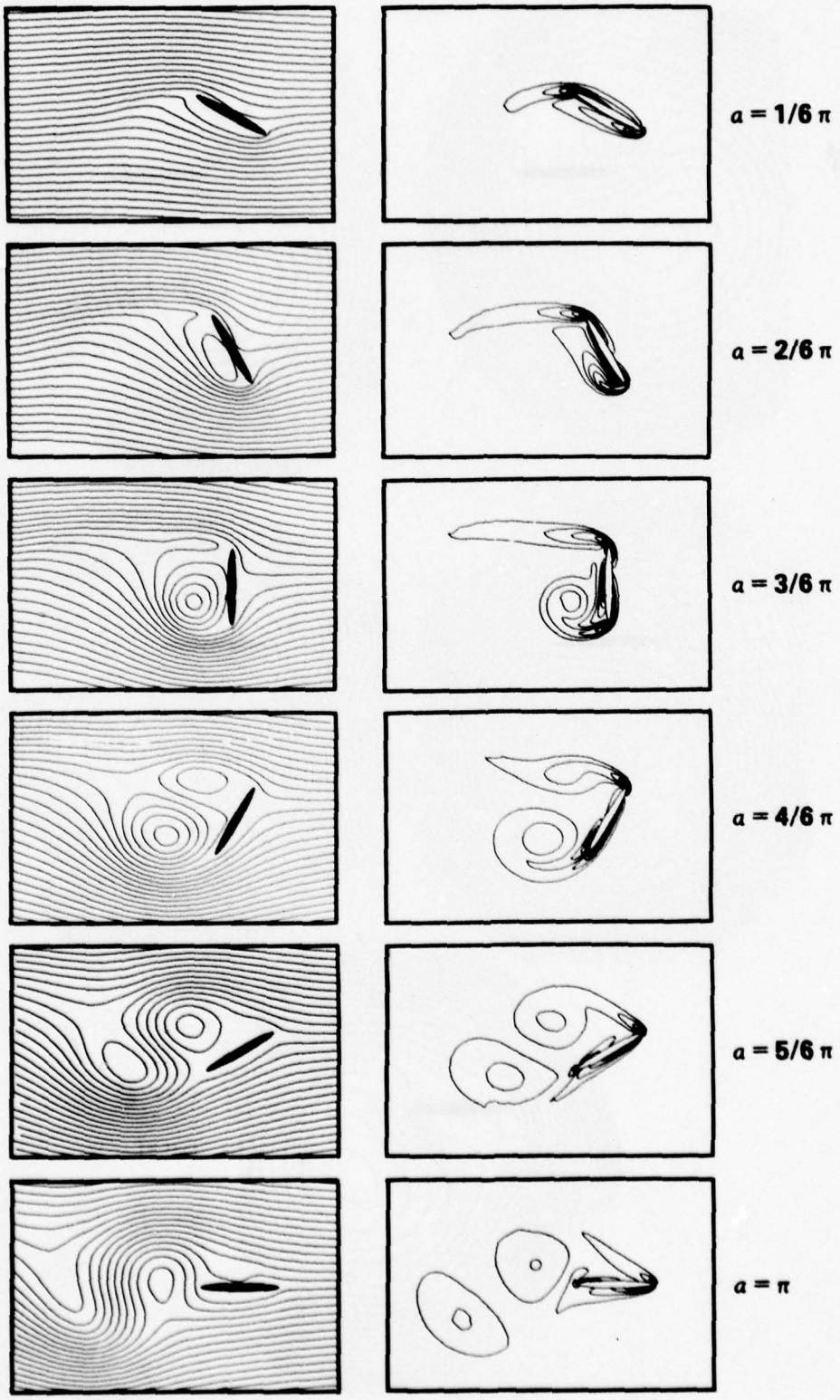

Figure 18a - (continued)

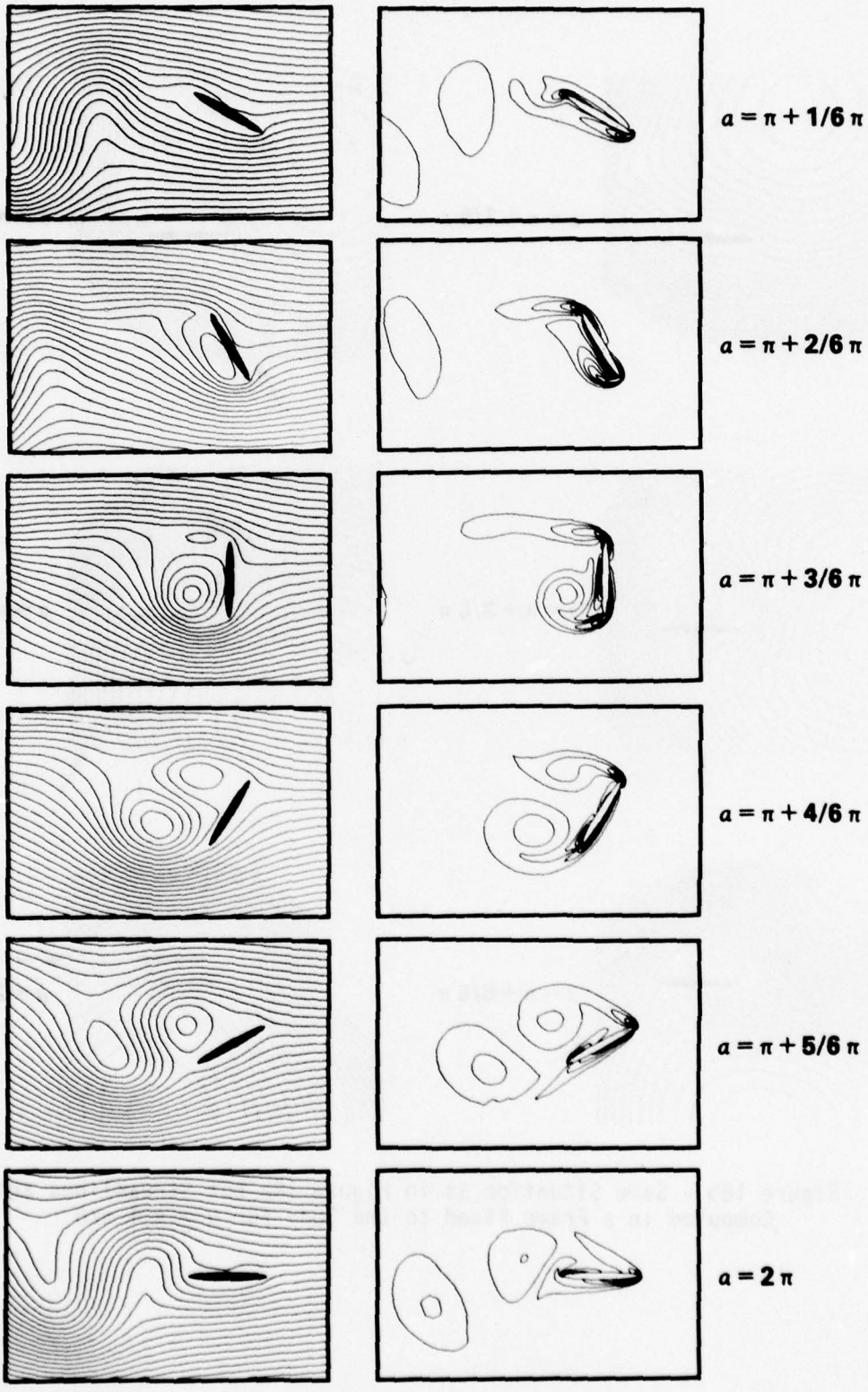

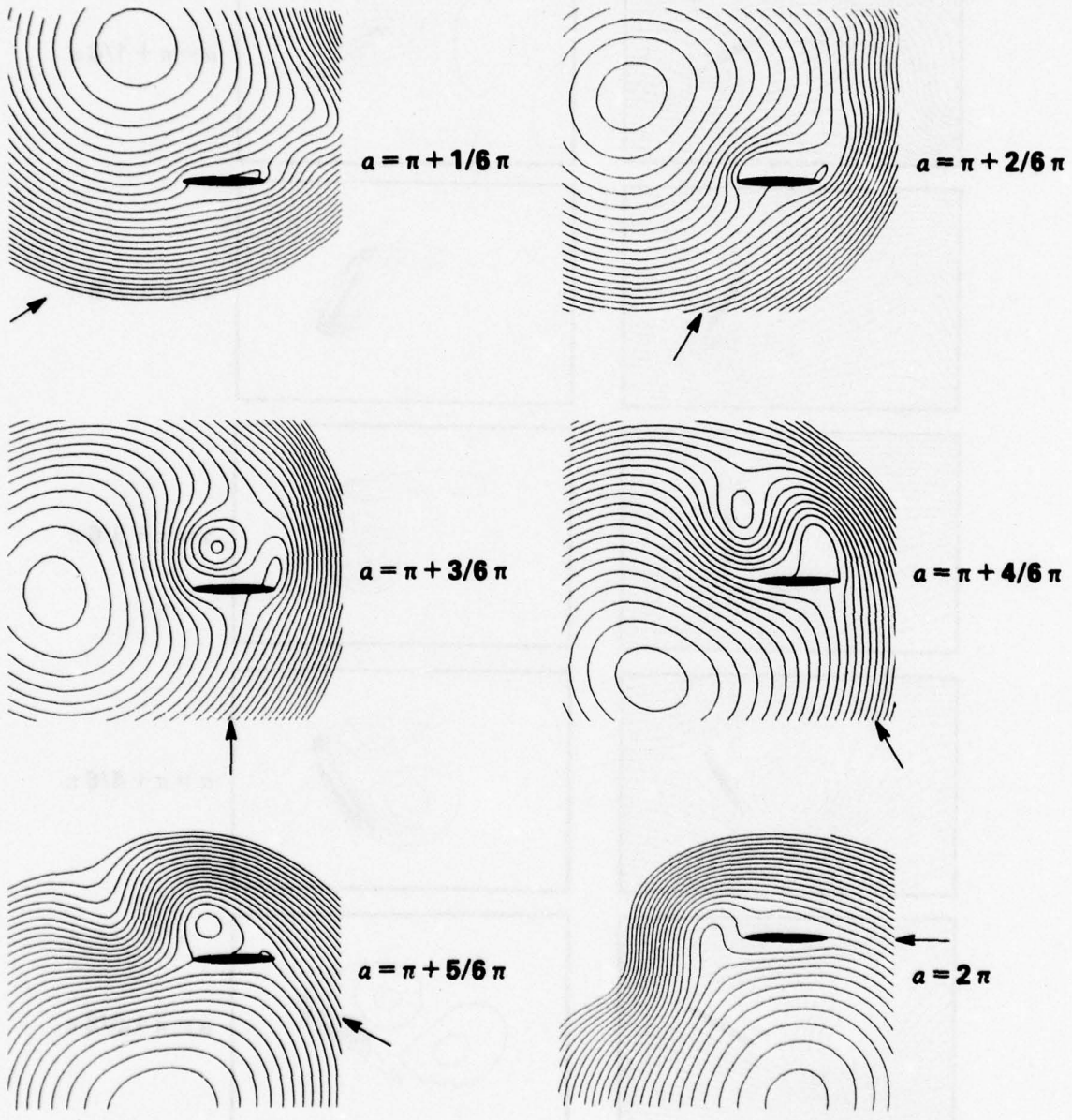

Figure 18b - Same Situation as in Figure 18a but Streamlines are Computed in a Frame Fixed to the Body for $\alpha \geq \pi + \pi/6$

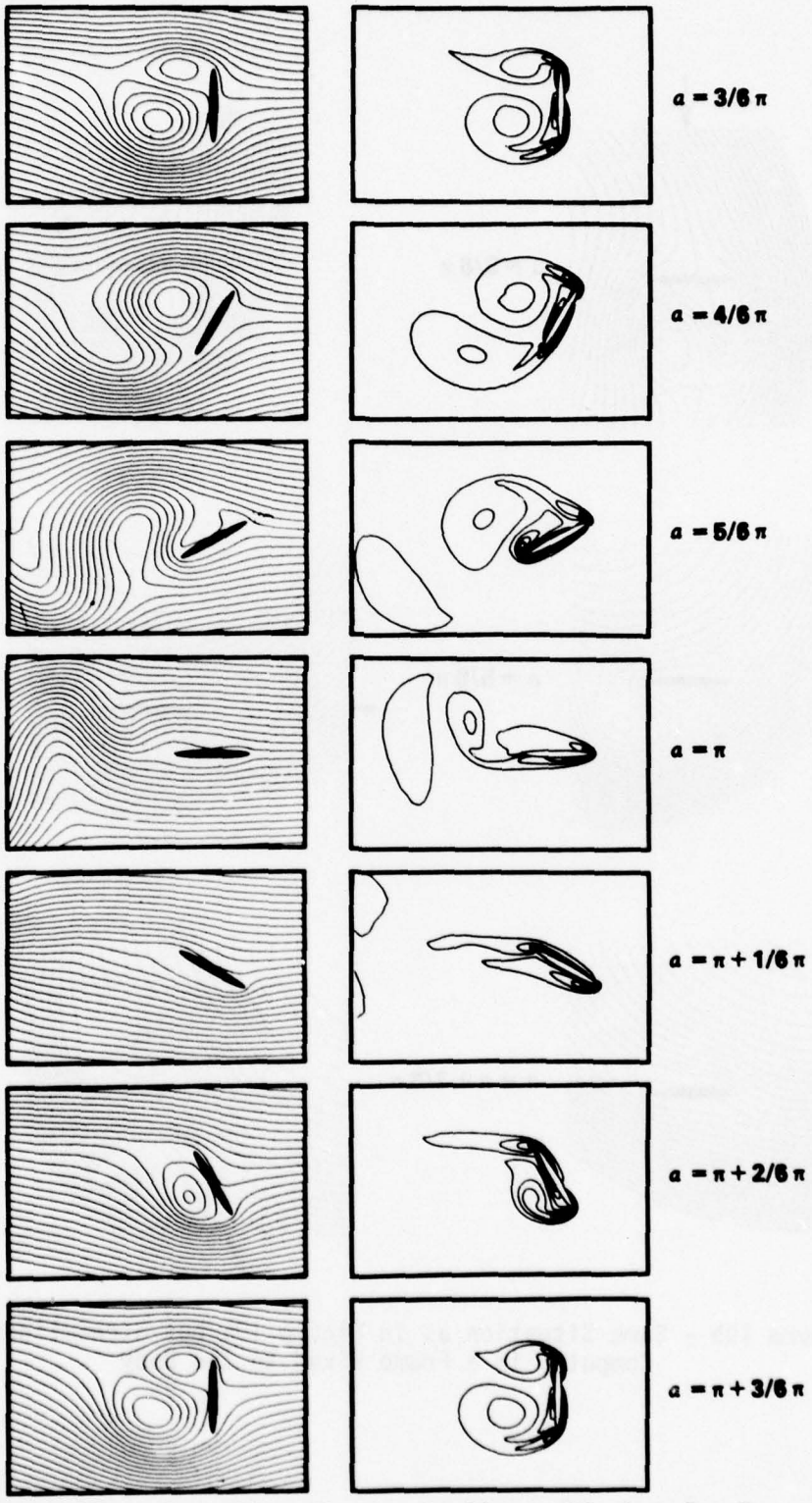

Figure 19a - Same Situation as in Figure 16a but for Ro = 6

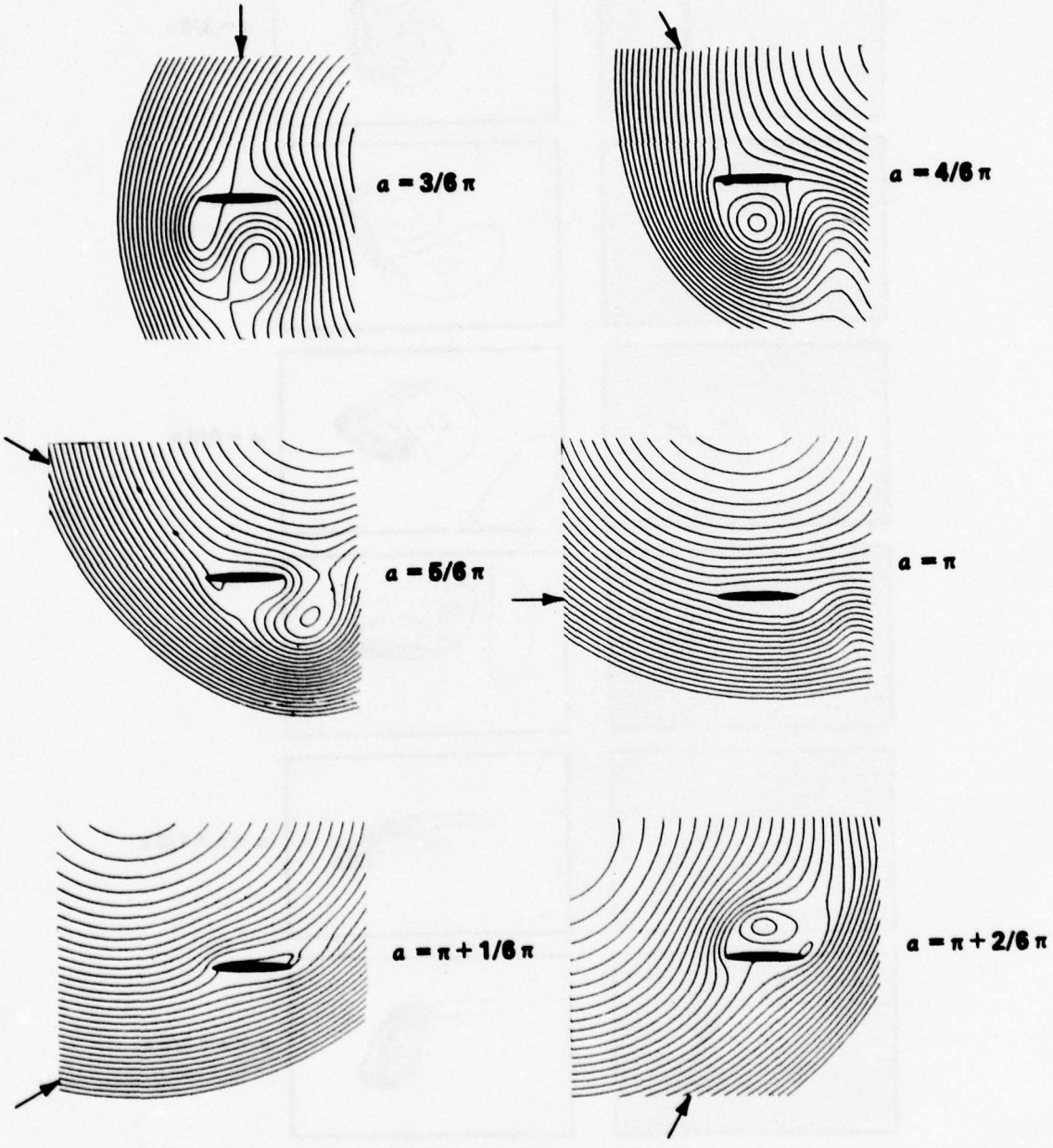

Figure 19b - Same Situation as in Figure 19a but Streamlines are Computed in a Frame Fixed to the Body

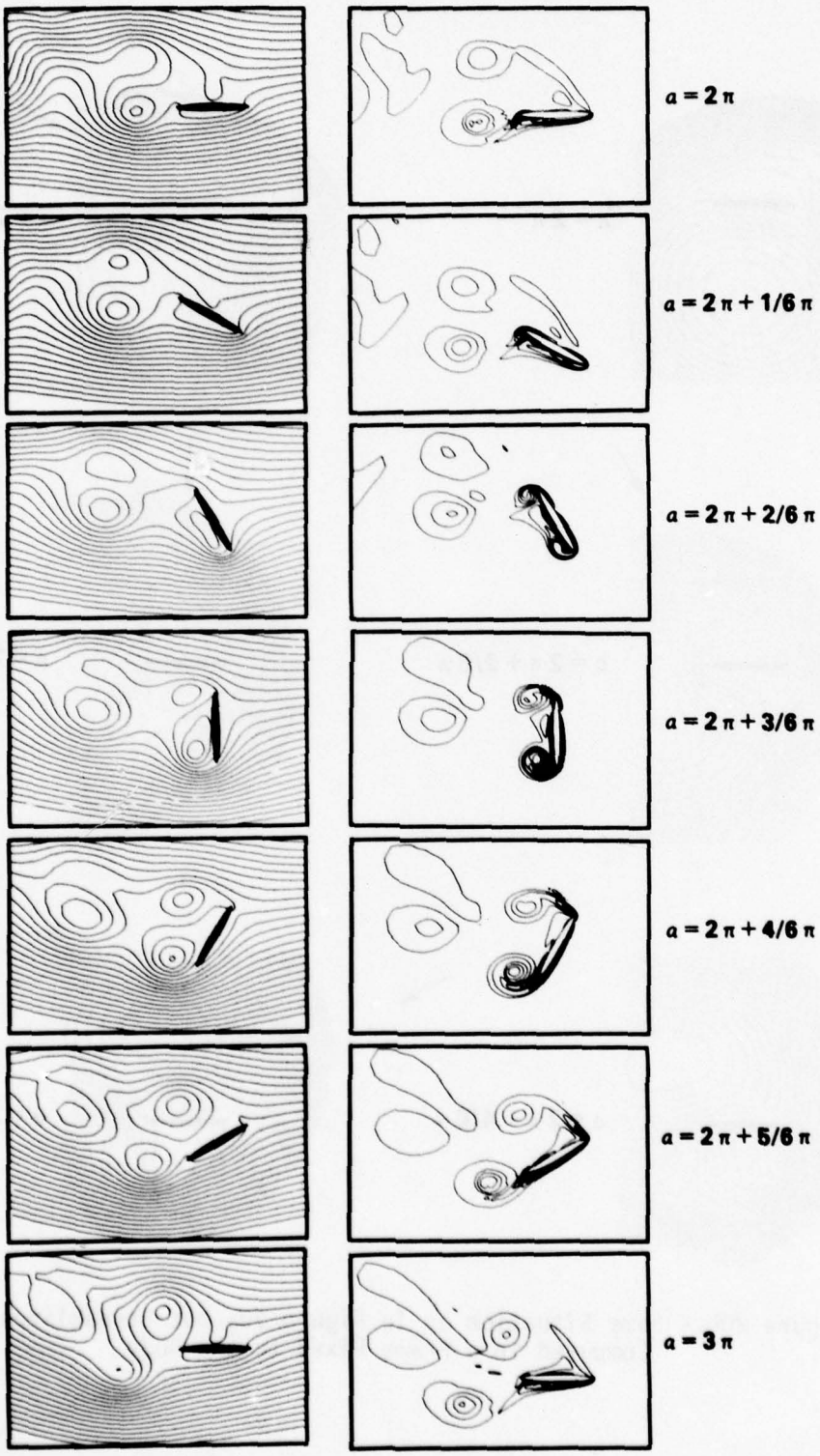

Figure 20a - Same Situation as in Figure 16a but for Ro = 2, Re = 400

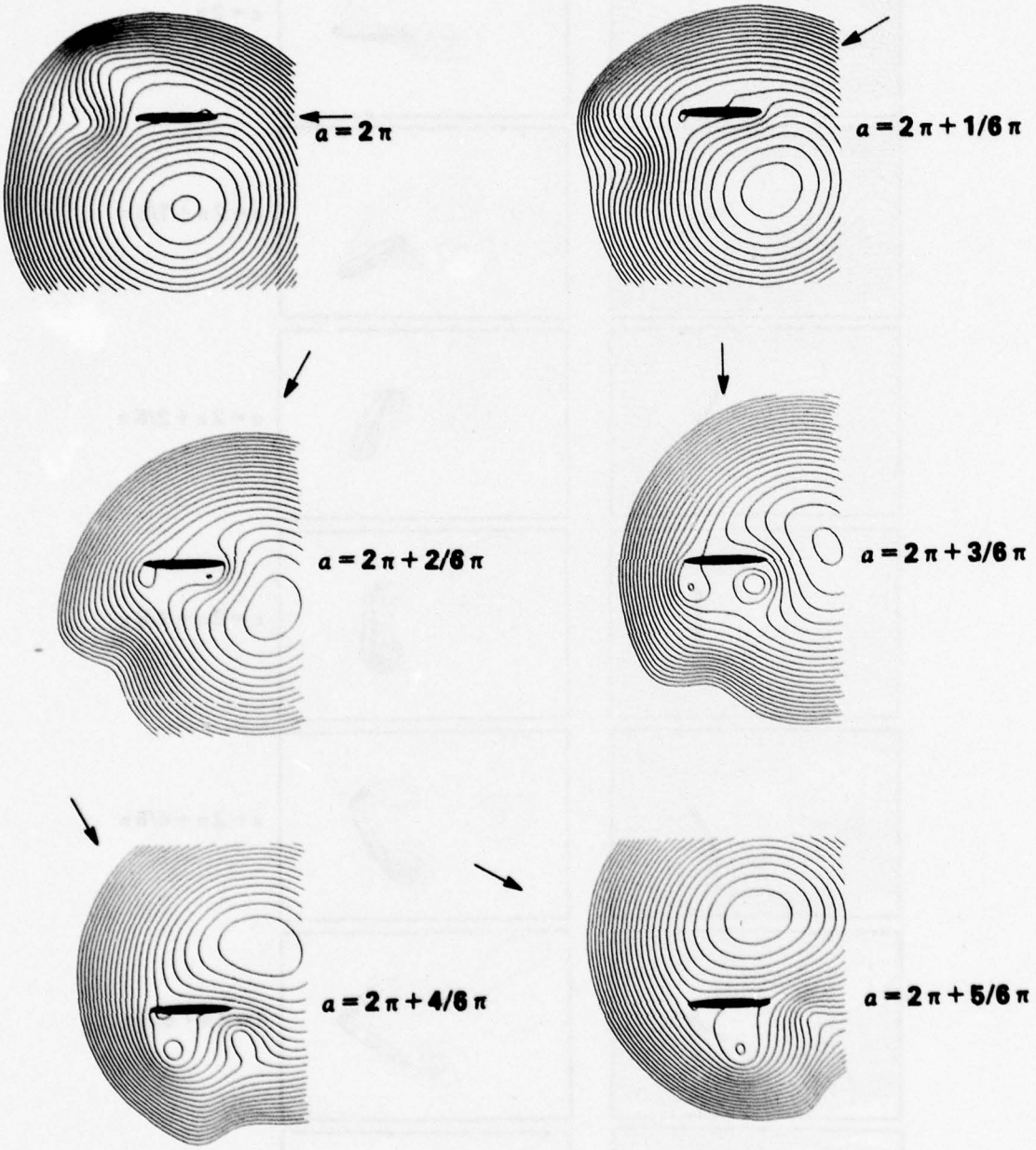

Figure 20b - Same Situation as in Figure 20a but Streamlines are Computed in a Frame Fixed to the Body

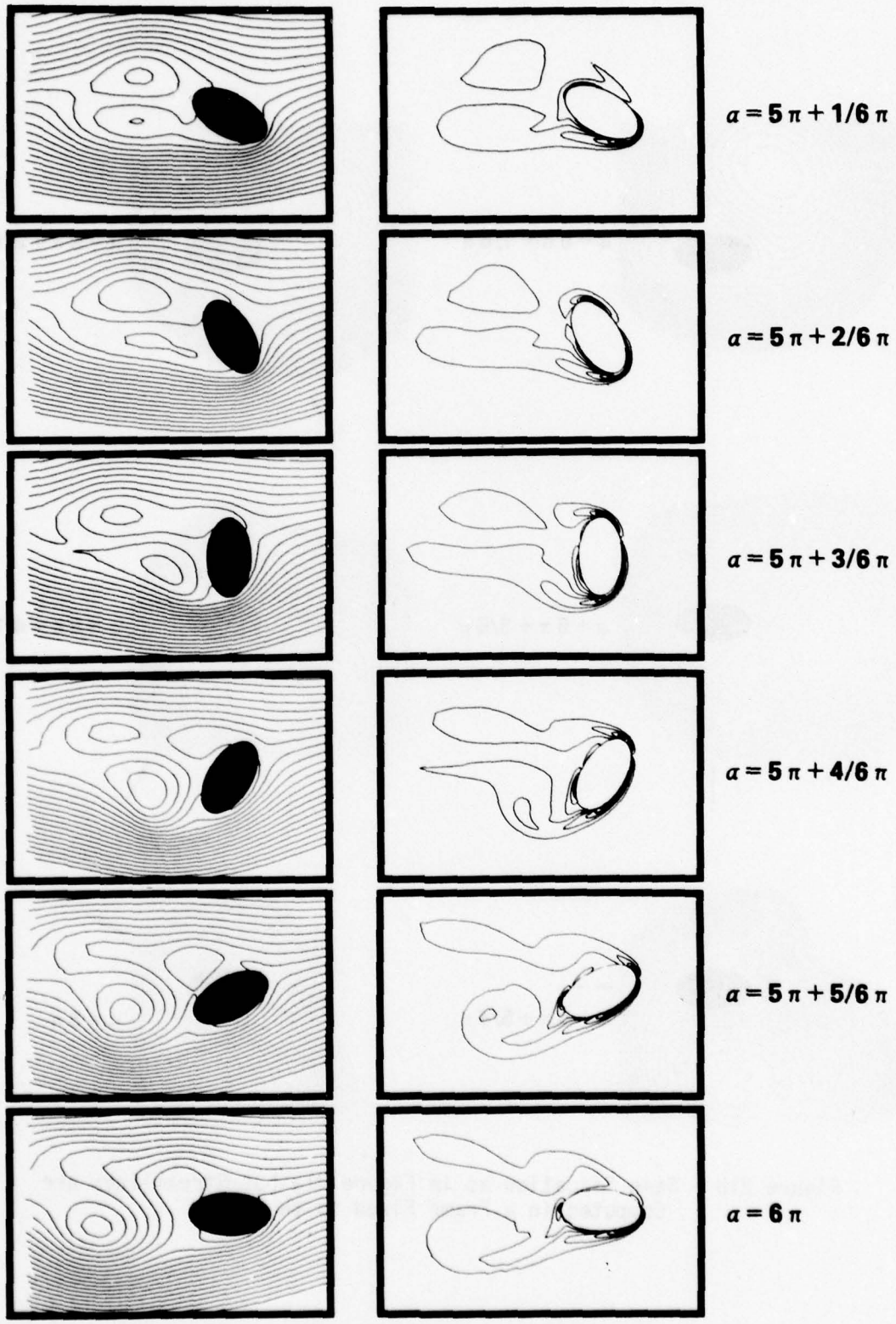

Figure 21a - Same Situation as in Figure 16a but for $Ro_{d/2} = 2$, $Re_d = 200$, $\eta_1 = 0.6$

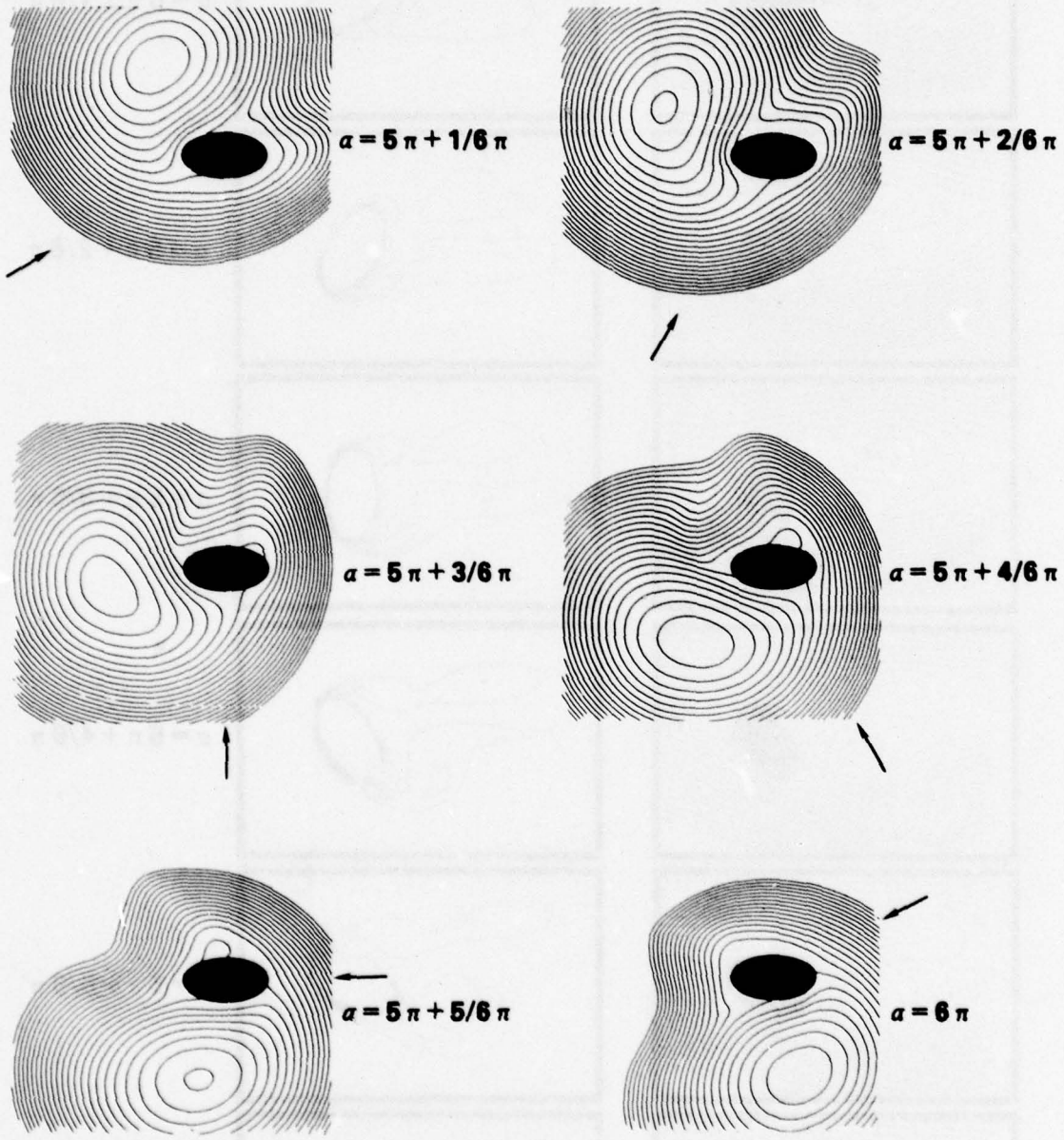

Figure 21b - Same Situation as in Figure 21a but Streamlines are Computed in a Frame Fixed to the Body

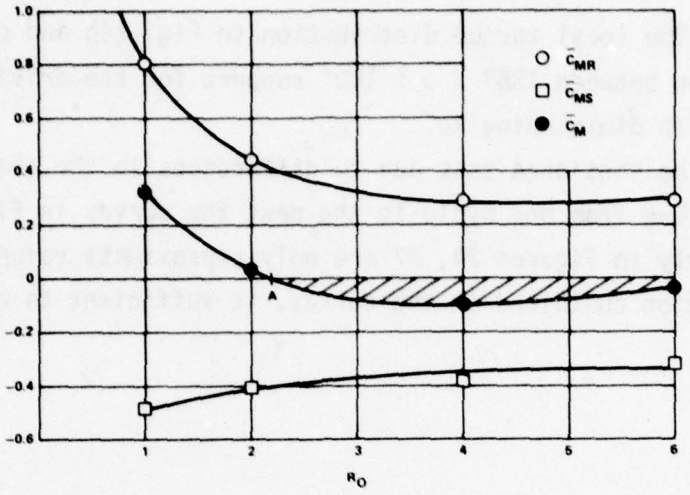

Figure 22 - $\bar{C}_{MR}$, $\bar{C}_{MS}$, and $\bar{C}_{M}$ versus Ro for Re = 200, η_1 = 0.1. In the Shaded Area the Body Autorotates but Increases its Rotation Until the Point A is Reached. This is the Condition for Stable, Steady-State Autorotation

Rotation enhances $|C_M|$ when compared with the nonrotating case (Fig. 14). Behind a fixed plate C_M oscillates according to the frequency f_N of the Kármán-vortex street between $0.38 \leq |C_M| \leq 0.95$ for Re = 200, η_1 = 0.1, $\alpha = 45°$.[60] However, in the case of the rotating plate Ro = 2, Re = 200, η_1 = 0.1, $\alpha = 45°$: $C_M = -1.5$. The difference may be explained with the aid of Figures 17 through 20 and Figures 23 and 24. Behind the leading (retreating) edge a vorticity tongue is visible which owes its existence to the boundary layer in front of the edge. Its strength and location determine the local torque contribution. The faster the rotation, the more closely the tongue clings to the rear of the edge since the vorticity has not enough time to be convected downstream. This clinging causes a higher suction effect behind the edge (see curves of the surface pressure in Fig. 23b and c). This may also be explained in the following way: with faster rotation vortex separation (stall), which is defined by the first occurrence of a vorticity extremum inside the fluid, is delayed. This hysteresis effect is due to the acceleration of fluid with growing α causing a reduction of the adverse pressure gradient. For instance, for Ro = 2, Re = 200, the vortex at the leading edge separates between 60° and 75°

(Fig. 17). The local torque distribution in Fig. 24b and c shows that in the region between $135° \leq \theta \leq 180°$ support for the driving torque increases with diminishing Ro.

It may be mentioned that due to differences in the absolute values of the pressure from one cycle to the next the curves in Figures 23, 26 and especially in Figures 24, 27 are only approximate values. However, the information contained in the curves, is sufficient to draw physical conclusions.

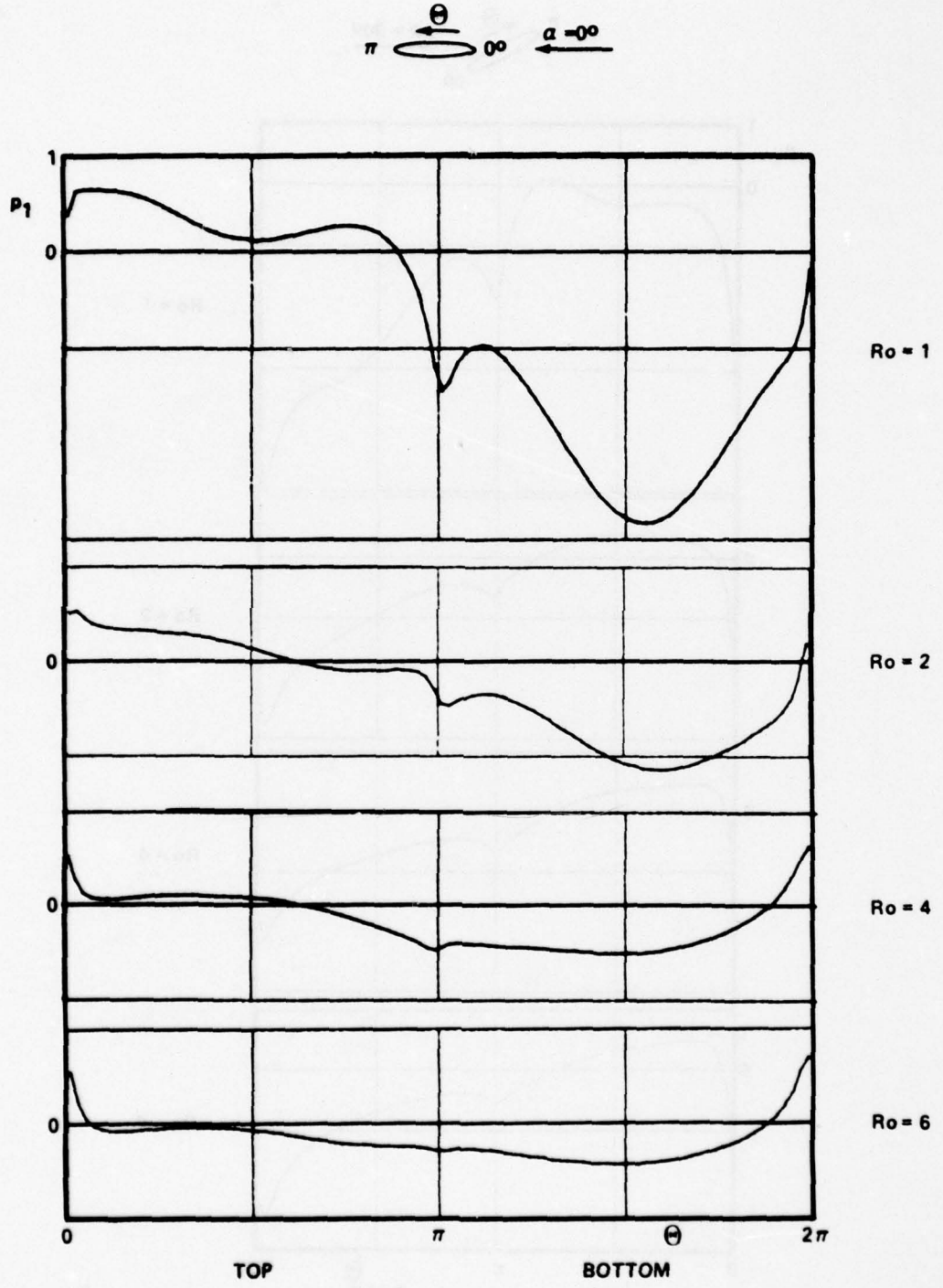

Figure 23a - Surface Pressure versus θ for Various Ro and Angles of Attack at Re = 200

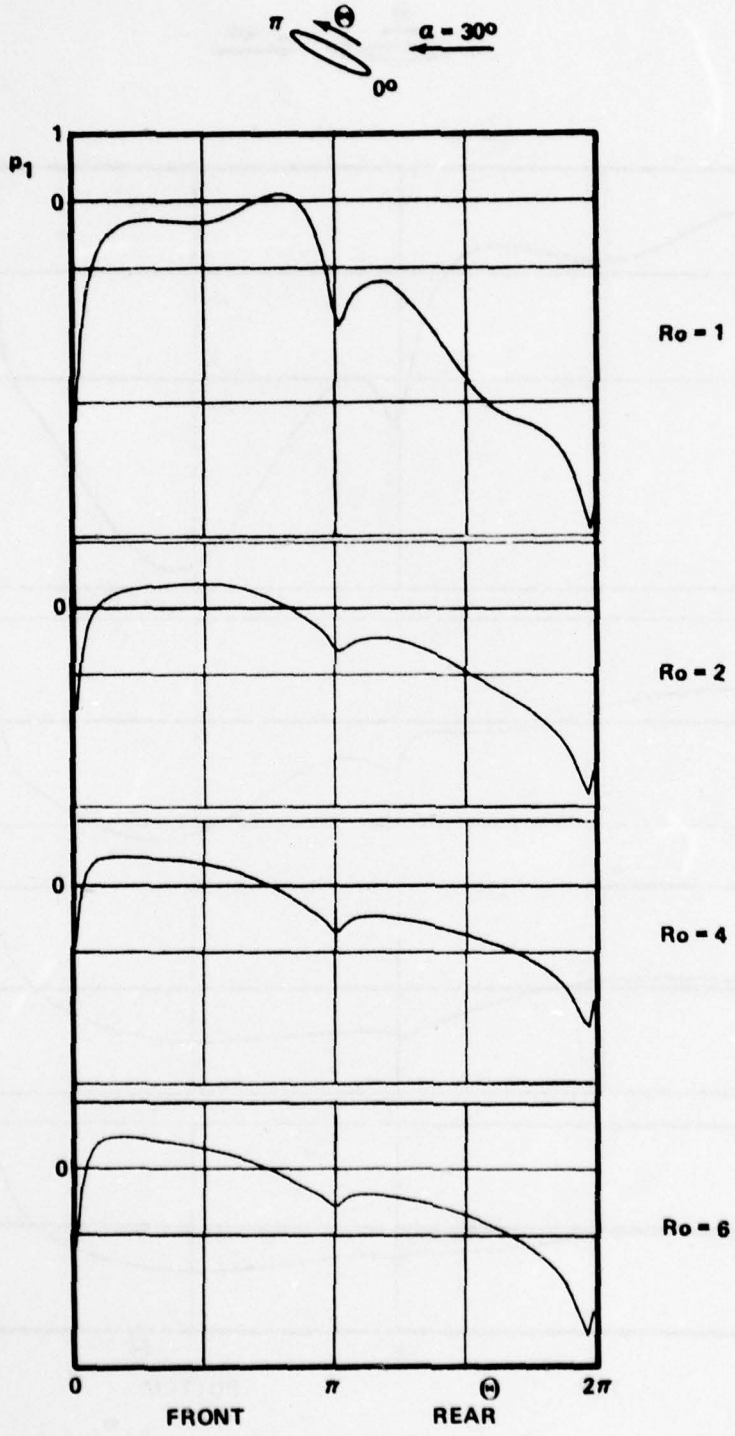

Figure 23b

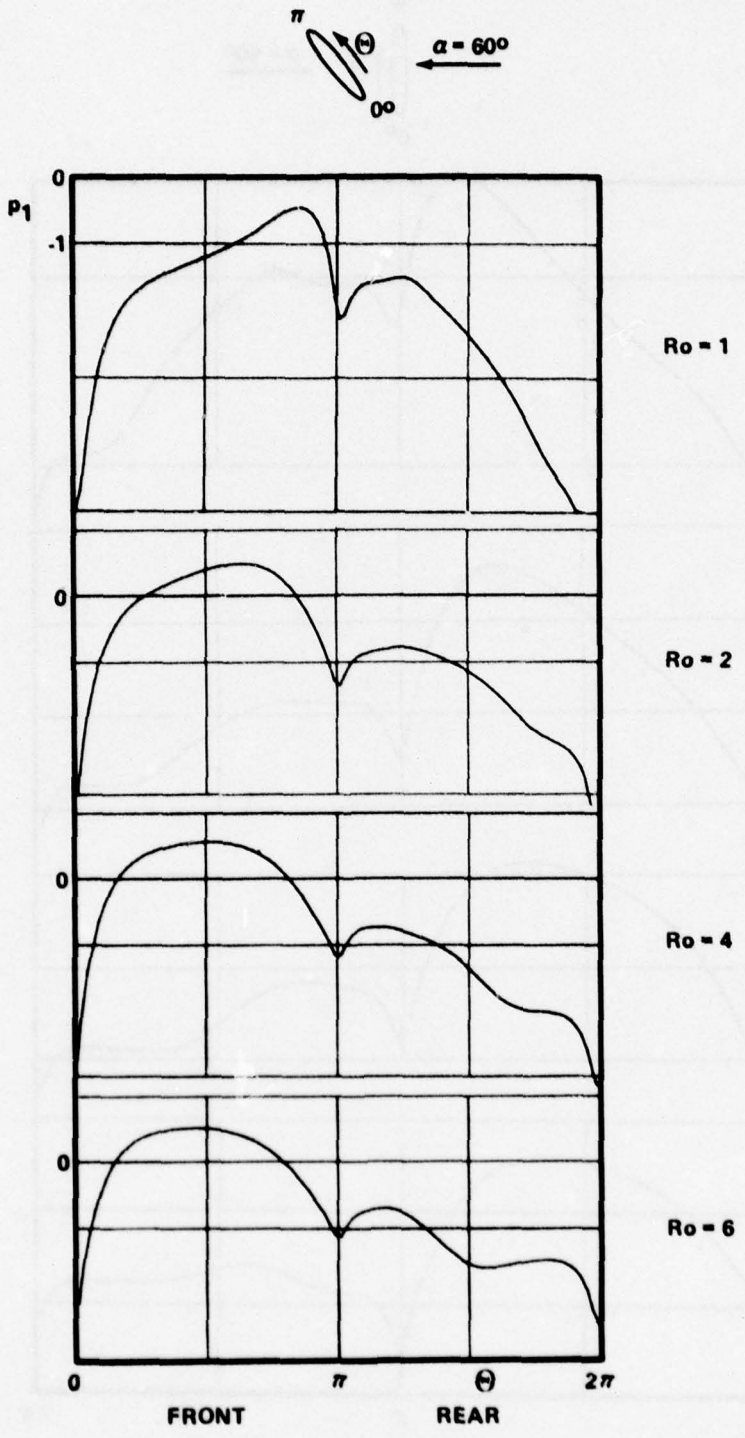

Figure 23c

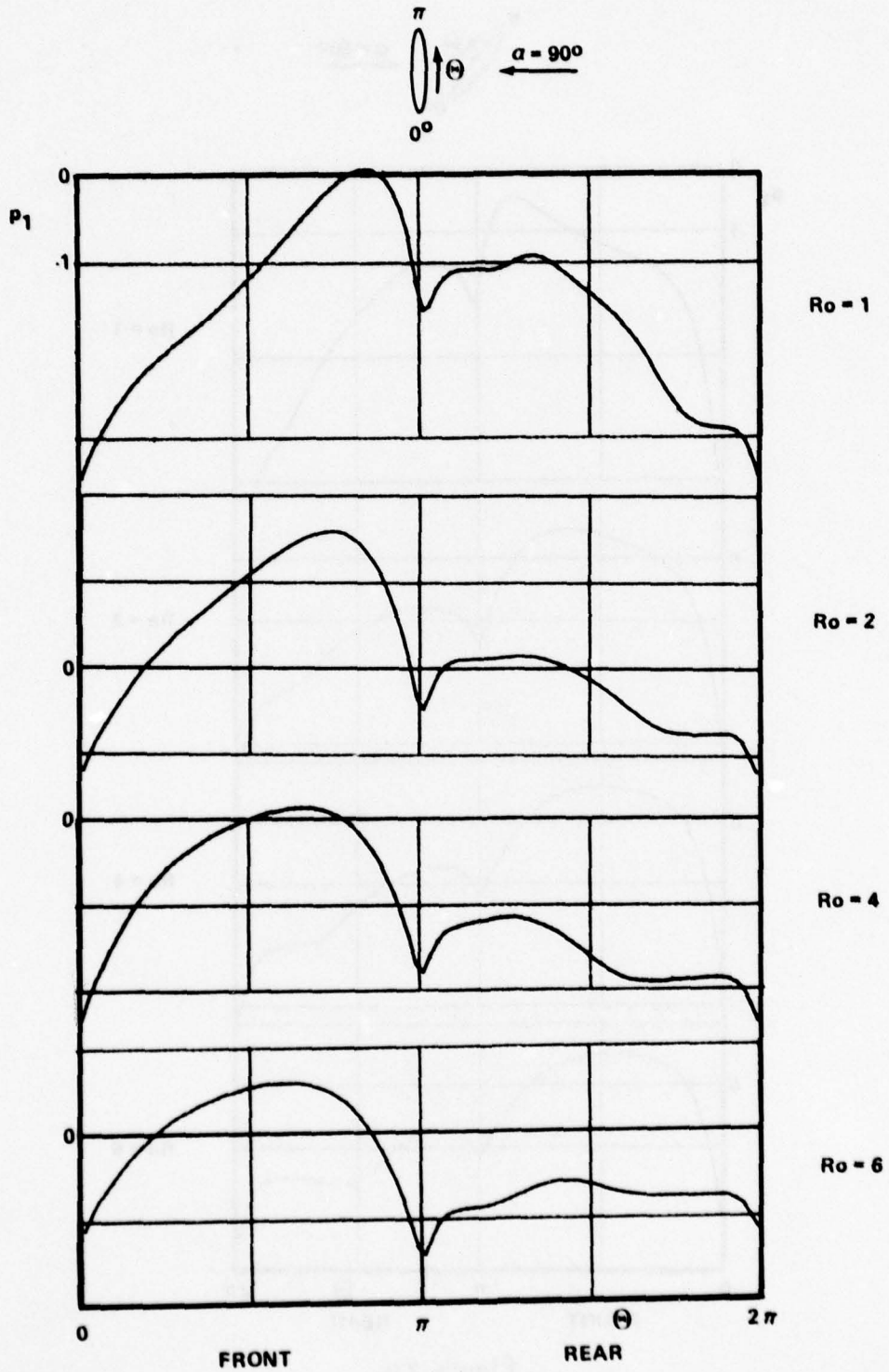

Figure 23d

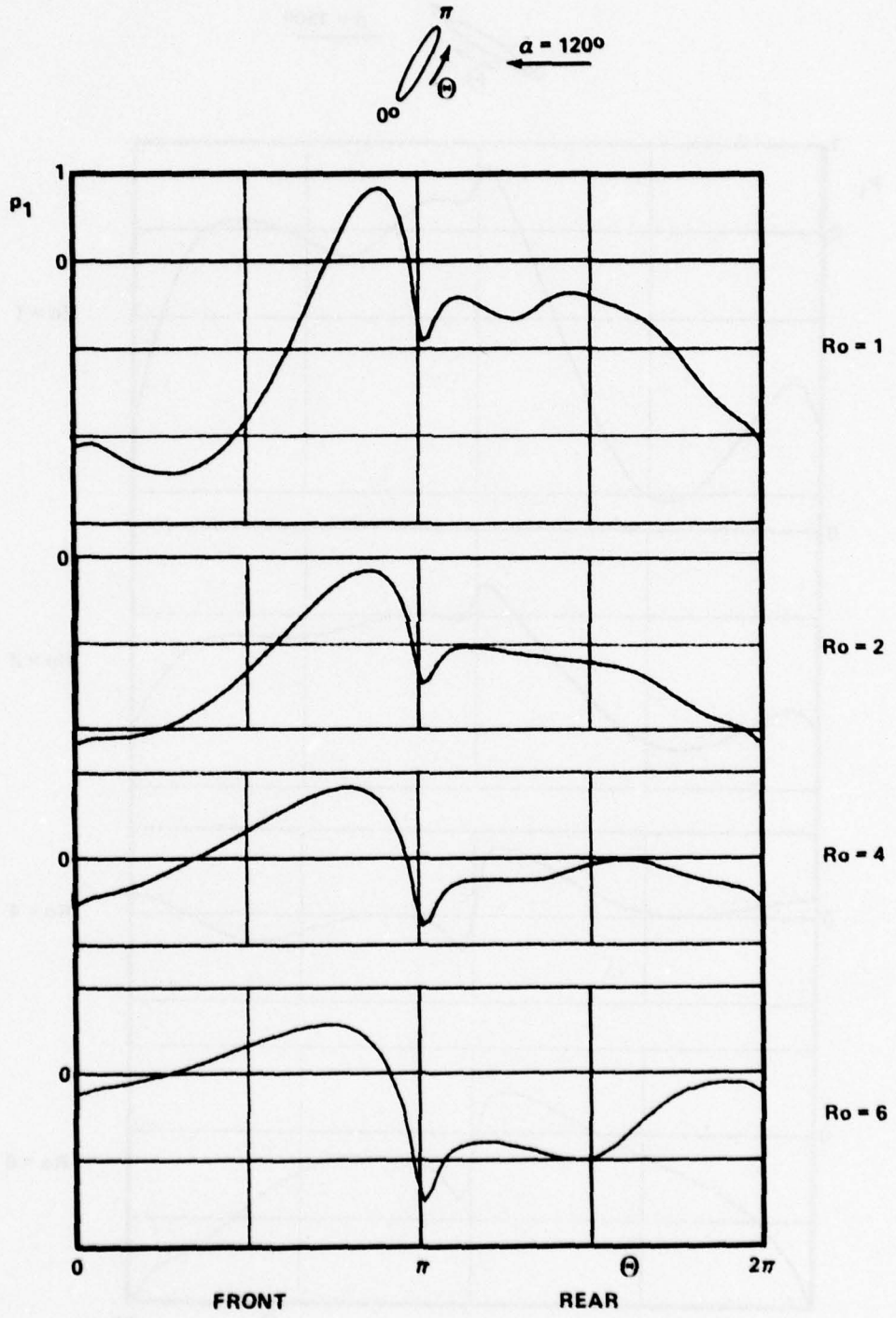

Figure 23e

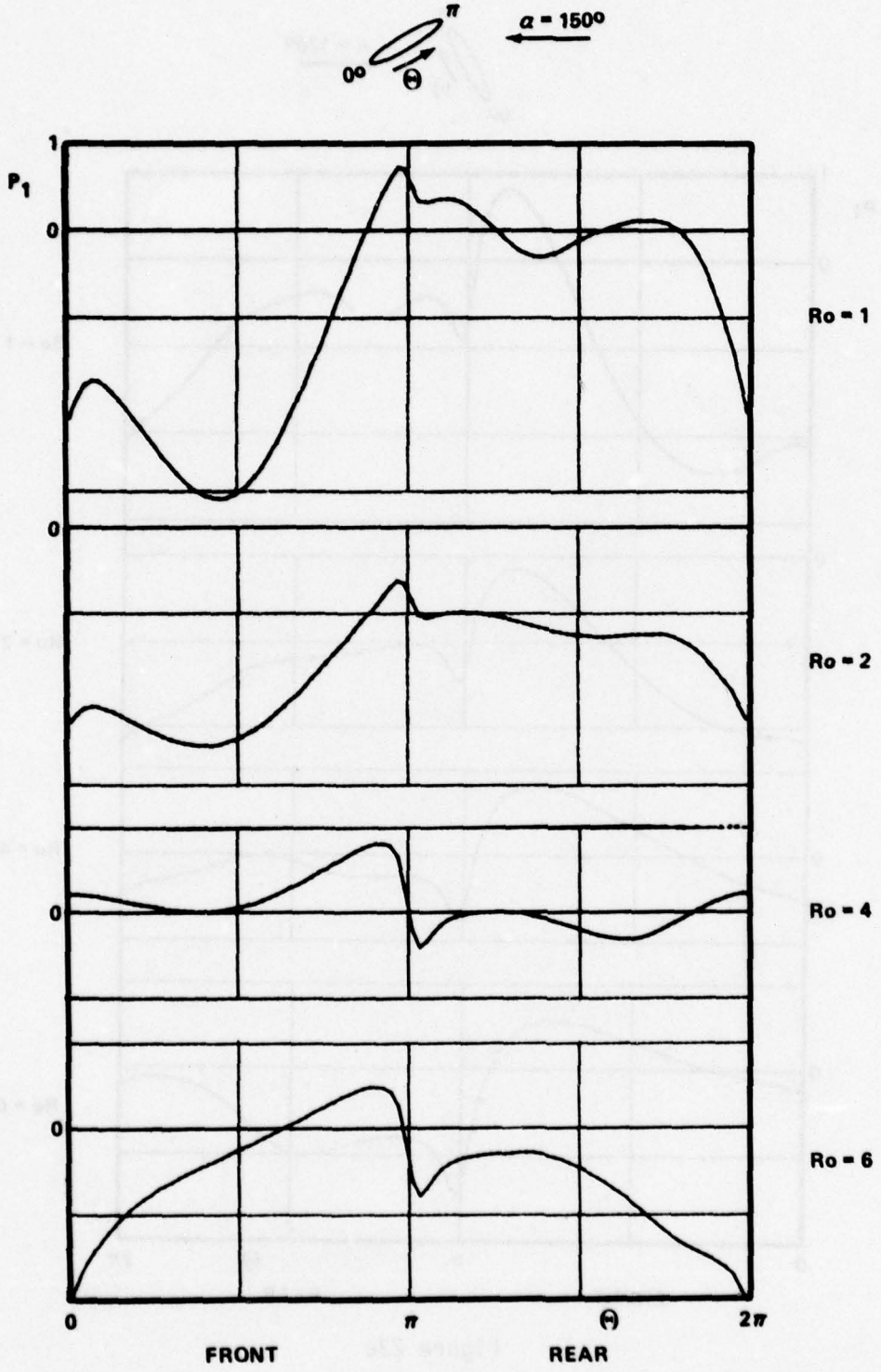

Figure 23f

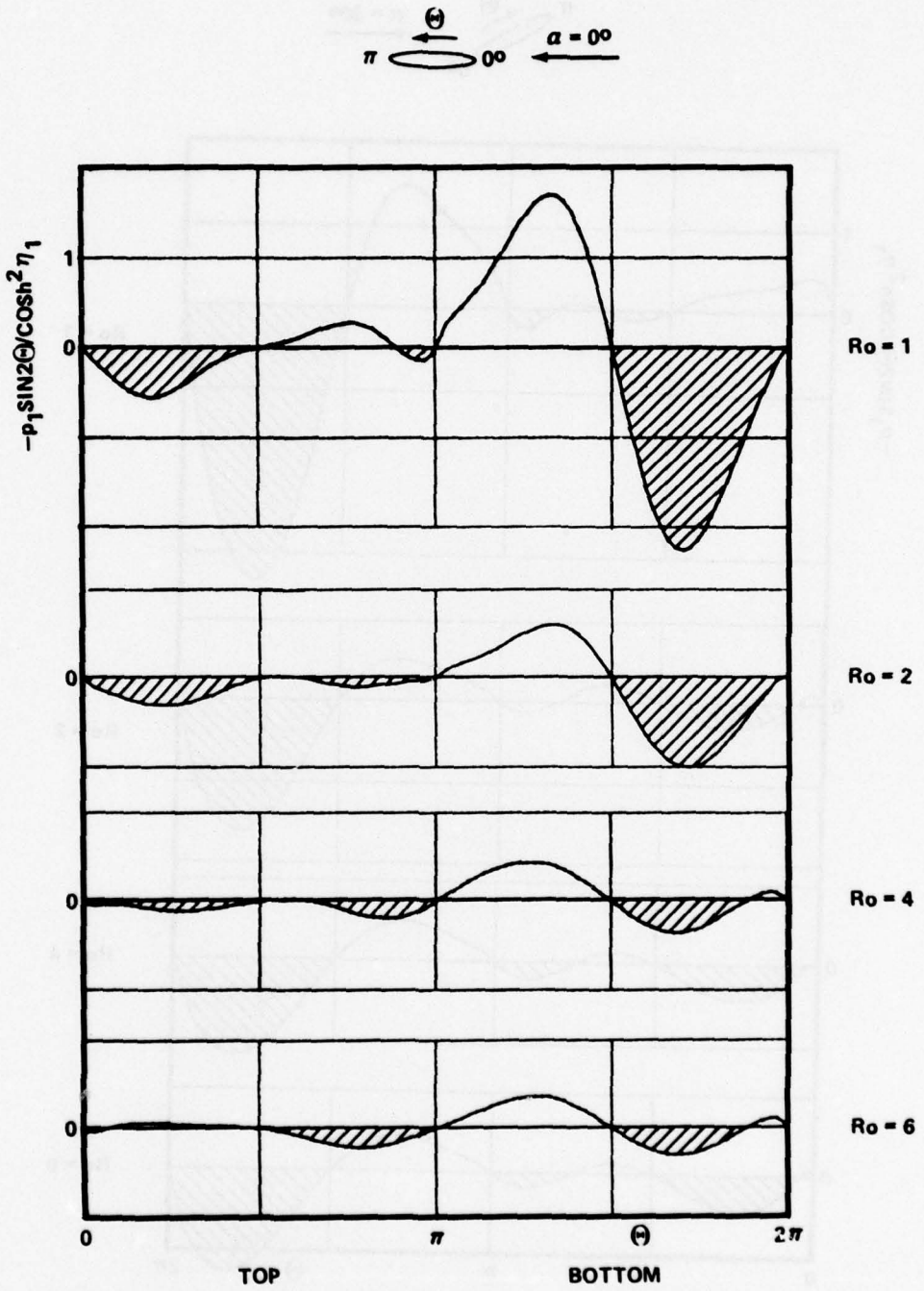

Figure 24a - Local Torque Contribution - $p_1 \sin 2\theta/\cosh^2 \eta_1$ versus θ for Various Ro and Angles of Attack at Re = 200

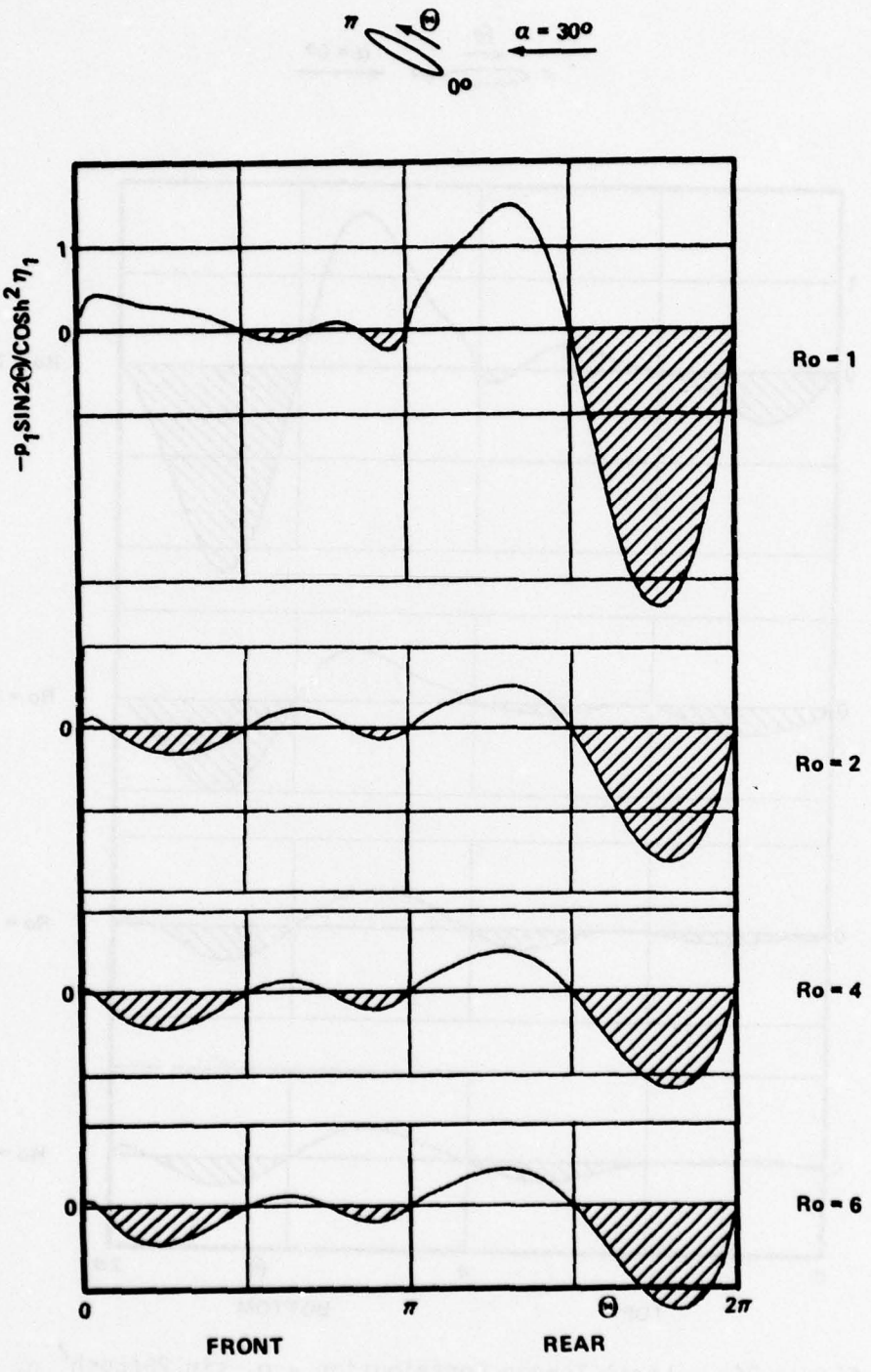
π
Θ
0°
α = 30°
$-p_1 \sin 2\Theta / \cosh^2 \eta_1$
1
0
Ro = 1
0
Ro = 2
0
Ro = 4
0
Ro = 6
0
π
Θ
2π
FRONT
REAR

Figure 24b

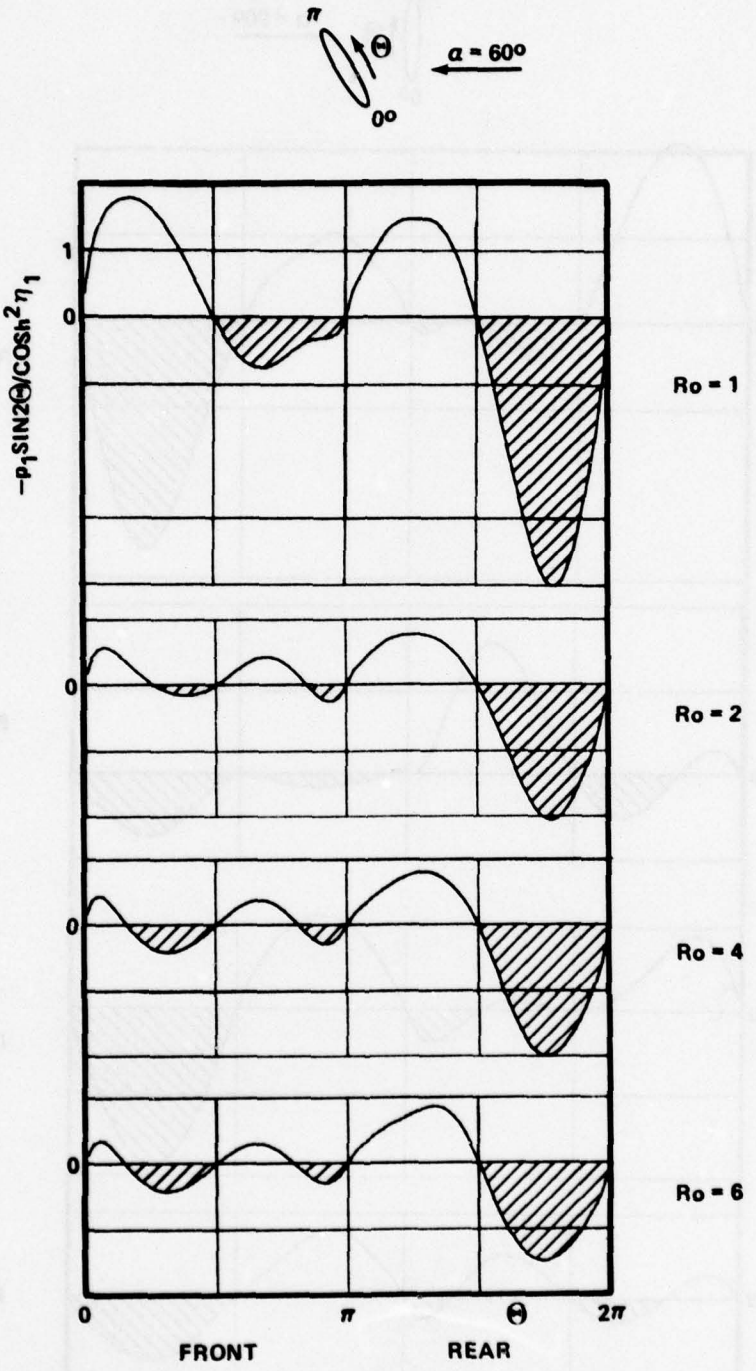
π
Θ
α = 60°
0°
$-p_1 SIN2\Theta/COSh^2\eta_1$
1
0
Ro = 1
0
Ro = 2
0
Ro = 4
0
Ro = 6
0
π
Θ
2π
FRONT
REAR

Figure 24c

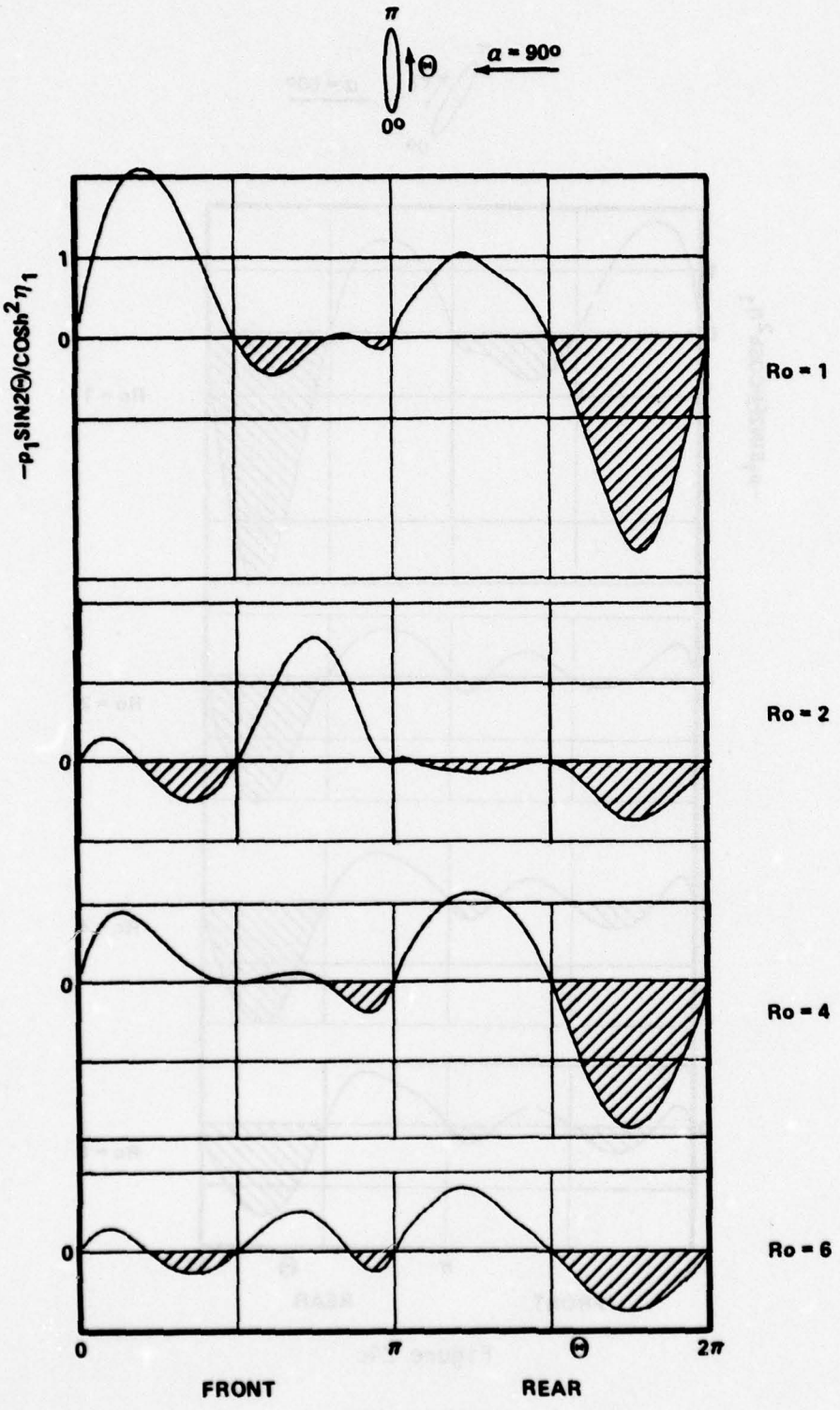
π
Θ
α = 90°
0°
$-p_1 SIN2\Theta/COSh^2\eta_1$
1
0
Ro = 1
Ro = 2
Ro = 4
Ro = 6
0
π
Θ
2π
FRONT
REAR

Figure 24d

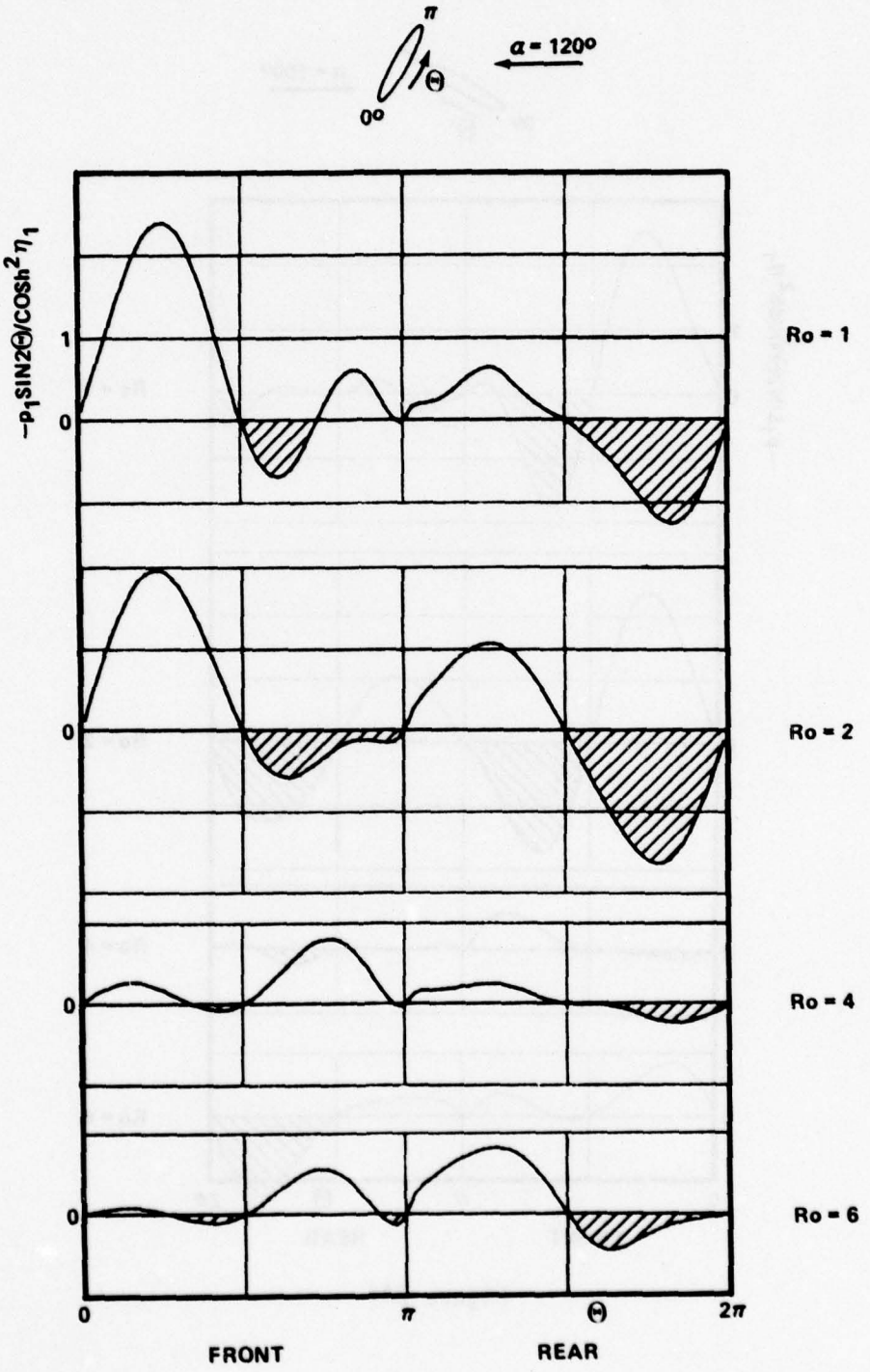
π
α = 120°
Θ
0°
$-p_1 SIN2\Theta/COSh^2\eta_1$
1
0
Ro = 1
0
Ro = 2
0
Ro = 4
0
Ro = 6
0
π
Θ
2π
FRONT
REAR

Figure 24e

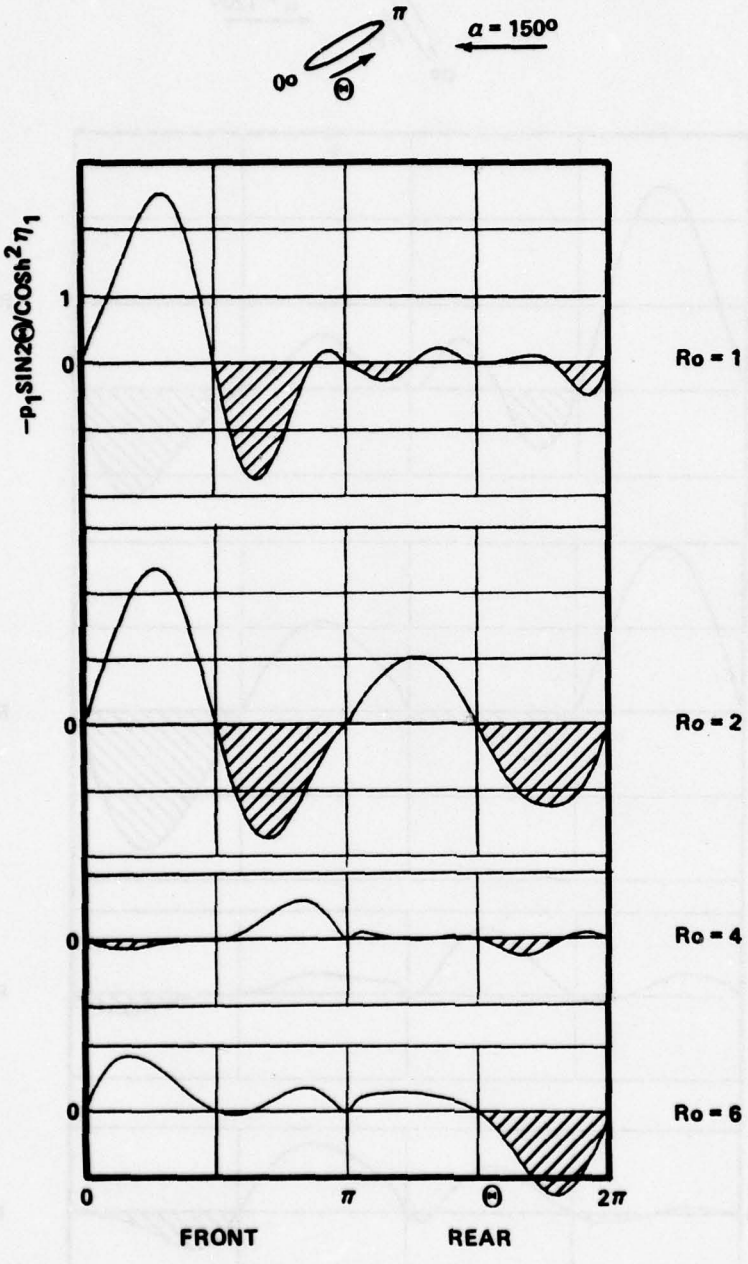
π
α = 150°
0°
Θ
$-p_1 \sin 2\Theta / \cosh^2 \eta_1$
1
0
Ro = 1
0
Ro = 2
0
Ro = 4
0
Ro = 6
0
π
Θ
2π
FRONT
REAR

Figure 24f

Around the trailing (advancing) edge differences in the local torque due to the various shapes of the vorticity tongue are negligible except for Ro ≤ 1. Here, the vortices from the preceding cycle cause a shift in the stagnation points (Fig. 23b and c) in such a way that the shift has an adverse effect on the local torque. To a certain extent this effect counteracts for Ro = 1 the advantage described before. As a result, $\overline{C}_{MS}$ decreases only slightly with smaller Ro (Fig. 22). The main contributor to this comes from the vortex behind the retreating (leading) edge.

Retarding Period

The major differences among the various Ro-cases occur in the retarding period. It is here, where viscous effects decide the balance between $\overline{C}_{MS}$ and $\overline{C}_{MR}$ and, thus, can cause the situation $\overline{C}_{MS} > \overline{C}_{MR}$, that is, autorotation. Again, the flow behavior around the retreating edge (which is now the trailing edge) becomes crucial.

From potential-flow theory it is known (and this is valid for viscous flows also) that the front stagnation point migrates during the supporting period over most of the front side of the plate (Fig. 25a). In contrast, in the retarding period, the front stagnation point remains close to the leading edge (Fig. 25b). This has the following consequence: for Ro = 1 the surface pressure drops sharply over the prolonged boundary layer in front of the plate from the stagnation point toward the center where the lowest pressure due to rotation occurs. A relative maximum exists near the trailing edge at $\theta \approx 12°$ (Fig. 23e and f). This maximum is due to

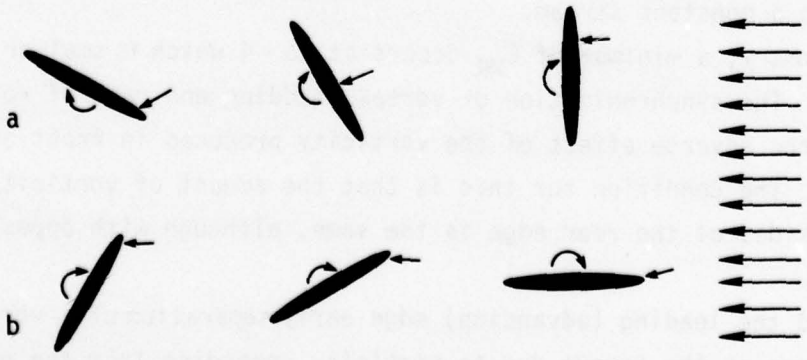

Figure 25 - The Location of the Front Stagnation Point in the Supporting Period (a) and in the Retarding Period (b)

the existence of another stagnation point which has formed because of the presence of a newly generated vorticity tongue while the older vortex has not yet been convected sufficiently far away (Fig. 15c). The sharp pressure drop causes a large adverse torque as can be seen from Fig. 24e and f. With increasing Ro the absolute value of p_1 rises, and the pressure drop diminishes. The rear stagnation point near the trailing edge as well as the stagnation point in front of the trailing edge migrate toward this edge, diminishing the asymmetry of the vorticity tongue. This causes the surface pressure to level off at Ro $\approx$ 4, resulting in $\overline{C}_{MS} > \overline{C}_{MR}$. This peculiar situation does not occur in the supporting period, where always an asymmetric vorticity tongue appears and where due to the behavior of the front stagnation point (Fig. 25a) the surface pressure in front of the plate is high and quite evenly distributed (Fig. 23b). For Ro = 6 a vorticity tongue of opposite sign develops at the rear edge due to the slowness of the rotation (Fig. 15e). The older vortex has already left the vicinity of the plate. The surface pressure drops (Fig. 23f) causing an adverse local torque. The change in the direction of the vorticity tongue at the rear edge in the retarding period can again be explained by the hysteresis effect: with decreasing α the fluid is decelerated, causing an adverse pressure gradient. This effect is high for small Ro, the separation point is on the front side of the plate. For high Ro, the flow behaves like that past a fixed plate, that is, the flow separates behind the edge. Between the two cases the situation of autorotation occurs where the flow separates at the rear edge like a flow past the trailing edge of a flat plate parallel to a constant stream.

In summary, a minimum of $\overline{C}_{MR}$ occurs at Ro = 4 which is smaller than $\overline{C}_{MS}$ (Fig. 22). The synchronization of vortex shedding and rate of rotation minimizes the adverse effect of the vorticity produced in front of the rear edge. The condition for this is that the amount of vorticity shed from both sides of the rear edge is the same, although with opposite signs (Fig. 15d).

Around the leading (advancing) edge early separation of a vortex weakens the influence on the torque due to vorticity spreading from the edge to the extent that it is favorable for autorotation. This effect can be seen when the vorticity field in the initial phase is compared with that

at a later time (Fig. 17a), $\alpha = \frac{\pi}{2} + \frac{2\pi}{6}$ and $\pi + \frac{5\pi}{6}$. In the first case the vortex is much stronger than at the later time. The strong vortex has a larger adverse effect on the torque. This adverse effect is smallest for Ro = 4 (Fig. 24e and f).

Although the occurrence of a minimum in $\bar{C}_{MR}$ is a necessary condition for autorotation, it is not sufficient. It is well known that plates with sharp edges autorotate better than those with blunt edges[4,47] and that blunt bodies do not necessarily autorotate. In order to study this effect, flows around a thick elliptical cylinder were investigated.

In the limit $\eta_1 \to \infty$ the elliptic cylinder becomes a circular one. The distinction between retarding and supporting periods disappears, and the torque is always positive, at least for the Oseen-type flow[59] and the special cases studied by Thoman and Szewczyk.[65] The fat ellipse $\eta_1 = 0.6$ has been selected as a typical example of conditions between the extremes $\eta_1 = 0$ and $\eta_1 = \infty$. From simple geometrical considerations one expects that tip effects are no longer pronounced and that the larger surface area (when d is kept constant) has an adverse effect on autorotation. Dynamically, one expects for $\eta_1 = 0.6$ less concentration of vorticity around the blunt tips and larger frictional effects.

Table 3 shows that indeed the average moment coefficient $\bar{C}_M$ is positive for $\eta_1 = 0.6$, and that this body does not autorotate. However, Table 3 also indicates that the difference between $\bar{C}_{MR}$ and $\bar{C}_{MS}$ is not as dramatic as one might expect. This means that the curvature effects (when comparing the results for $\eta_1 = 0.1$ and $\eta_1 = 0.6$) are rather subtle, and this is confirmed in Figures 26 and 27. It appears that for $\alpha = 60°$ (Fig. 27) the vortex behind the retreating tip of the body is weaker, and that this is the major cause for the small value of $\bar{C}_{MS}$. The fact that the thick ellipse does not autorotate for Ro = 2, Re = 200, does not mean that it cannot autorotate at all. It is still possible that it could autorotate for higher Ro and for $\Omega \neq$ constant. The autorotation of blunt

---

[65] Thoman, D.C. and A.A. Szewczyk, Numerical solutions of time dependent two dimensional flow of a viscous, incompressible fluid over stationary and rotating cylinders. Univ. Notre Dame, Dept. Mech. Engineering, Tech. Rep. 66-14, 1966.

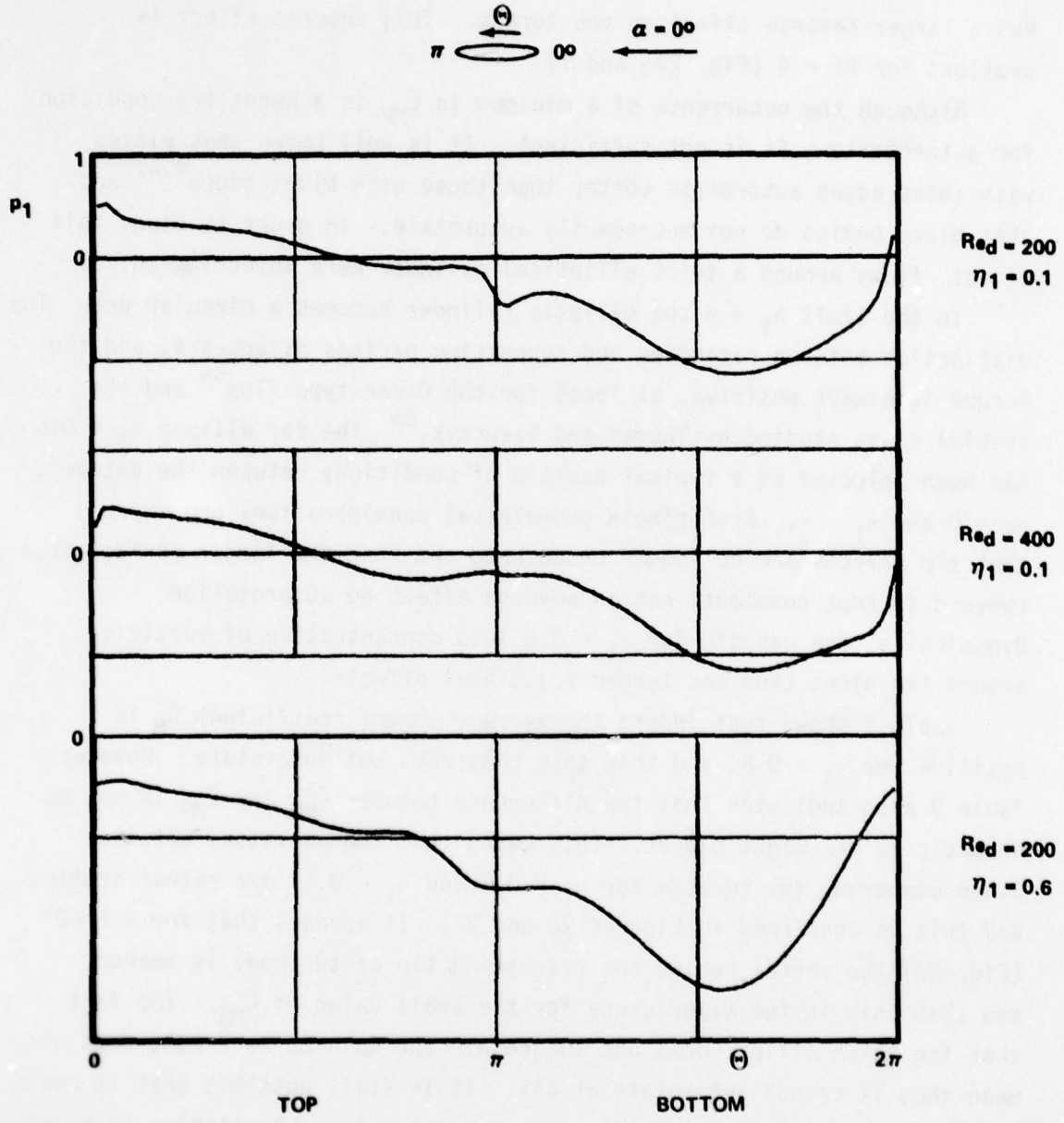

Figure 26a - Surface Pressure versus θ for $Ro_{d/2} = 2$, $Re_d = 200$, $\eta_1 = 0.1$ and 0.6, and for $Ro_{d/2} = 2$, $Re_d = 400$, $\eta_1 = 0.1$ at Various Angles of Attack

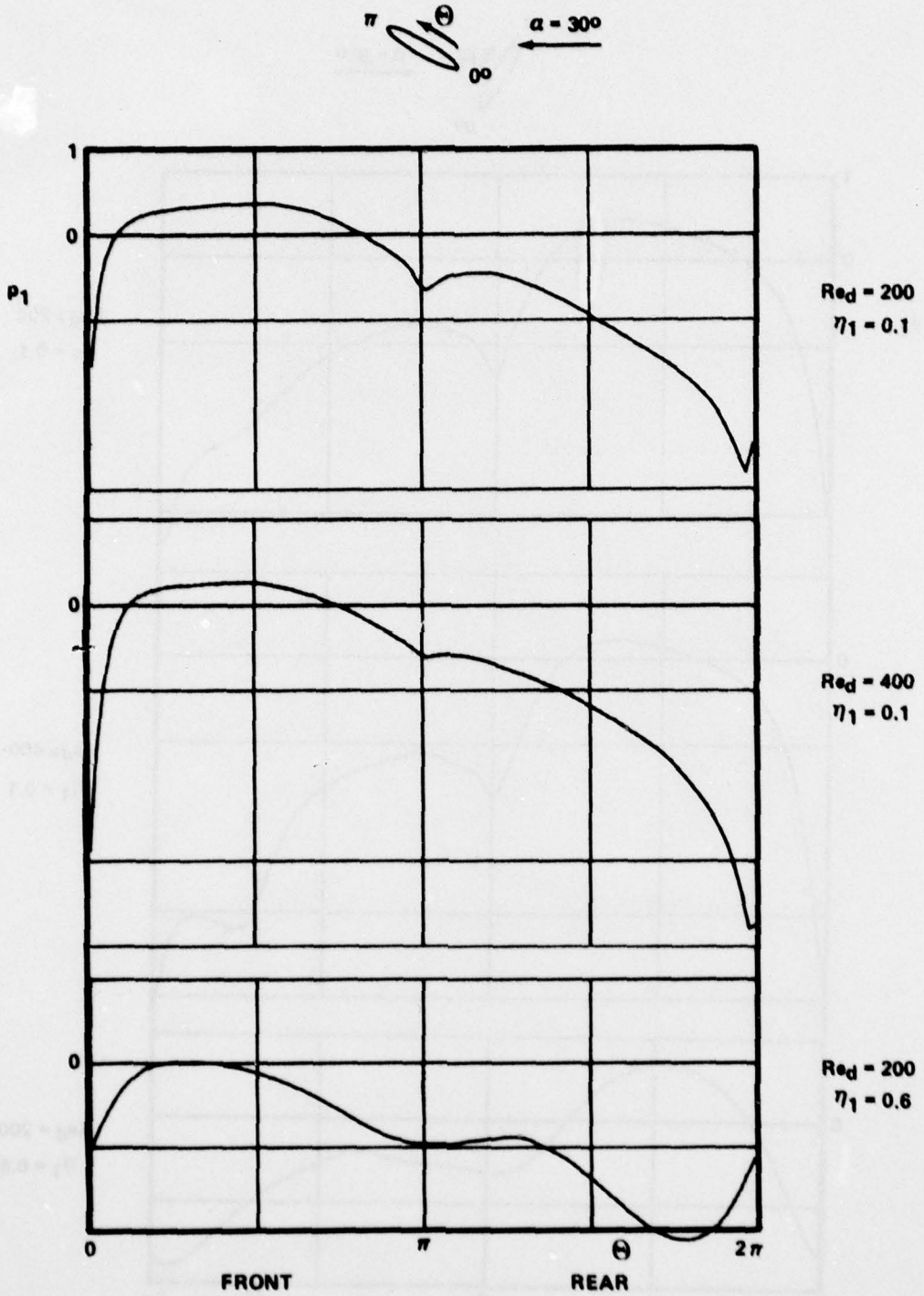
π
Θ
α = 30°
0°
1
0
p_1
Re_d = 200
η_1 = 0.1
0
Re_d = 400
η_1 = 0.1
0
Re_d = 200
η_1 = 0.6
0
π
Θ
2π
FRONT
REAR

Figure 26b

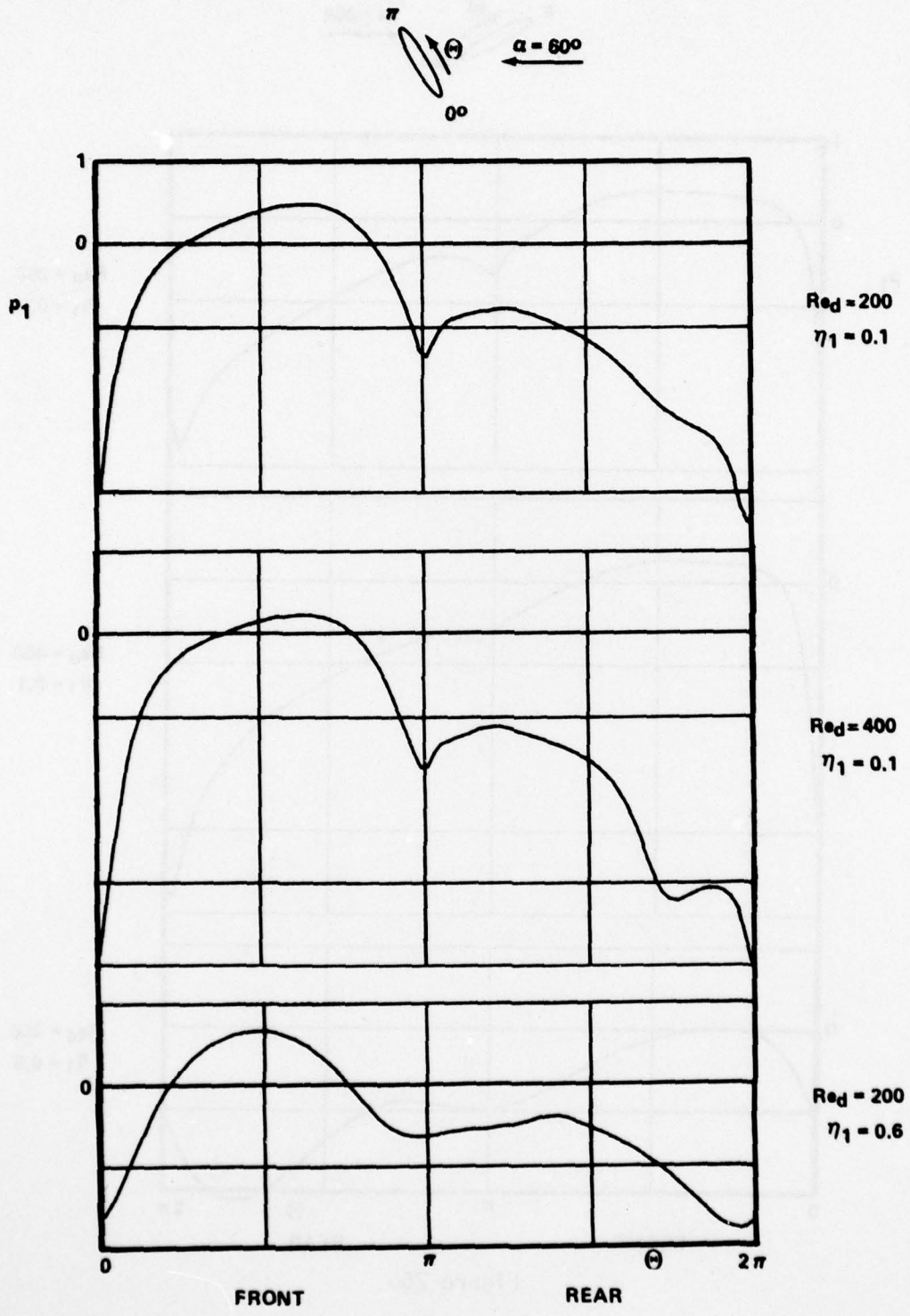
π
Θ
α = 60°
0°
1
0
p_1
Re_d = 200
η_1 = 0.1
0
Re_d = 400
η_1 = 0.1
0
Re_d = 200
η_1 = 0.6
0
π
Θ
2π
FRONT
REAR

Figure 26c

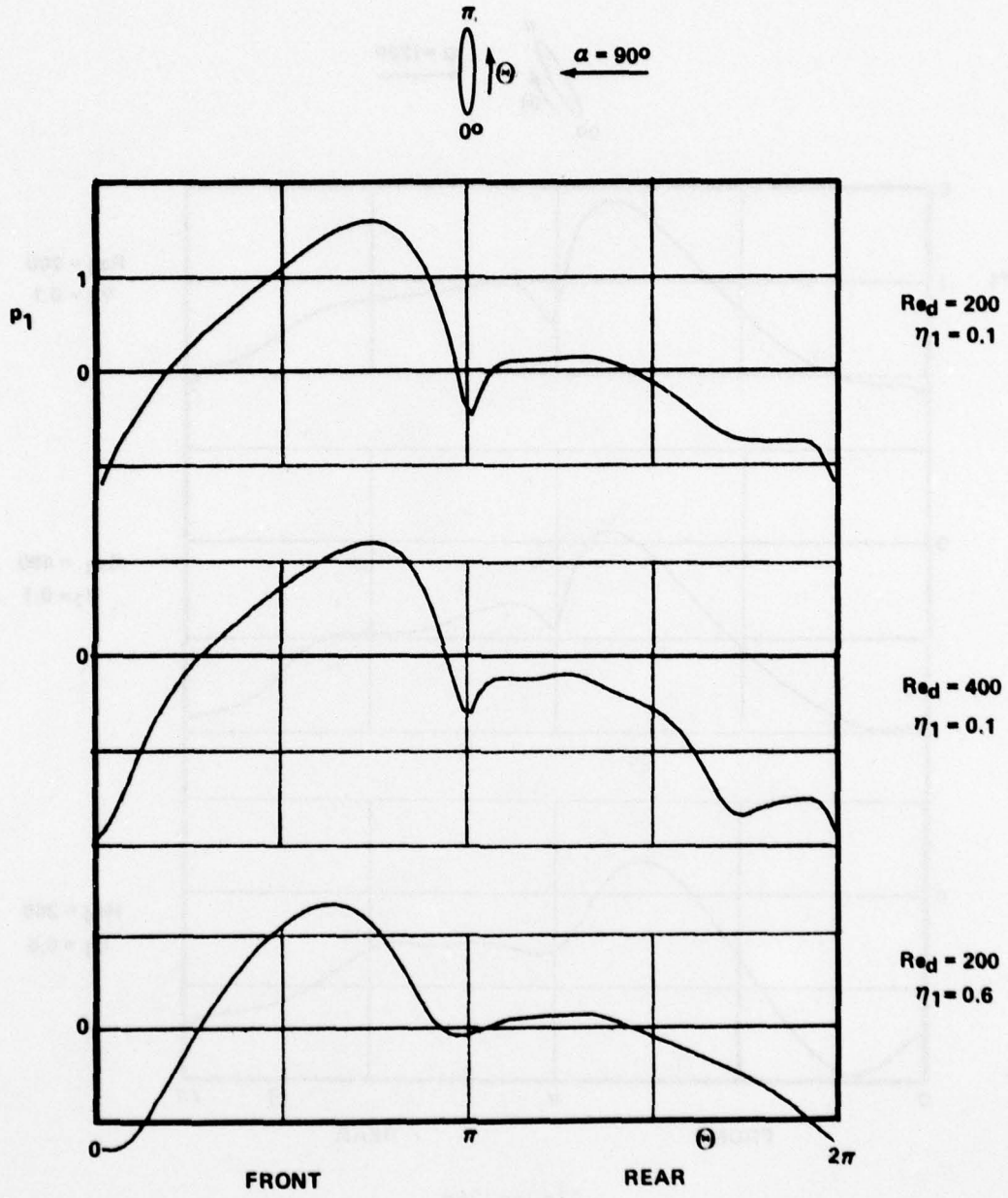
π
Θ
α = 90°
0°
p1
1
0
Red = 200
η1 = 0.1
0
Red = 400
η1 = 0.1
0
Red = 200
η1 = 0.6
0
π
Θ
2π
FRONT
REAR

Figure 26d

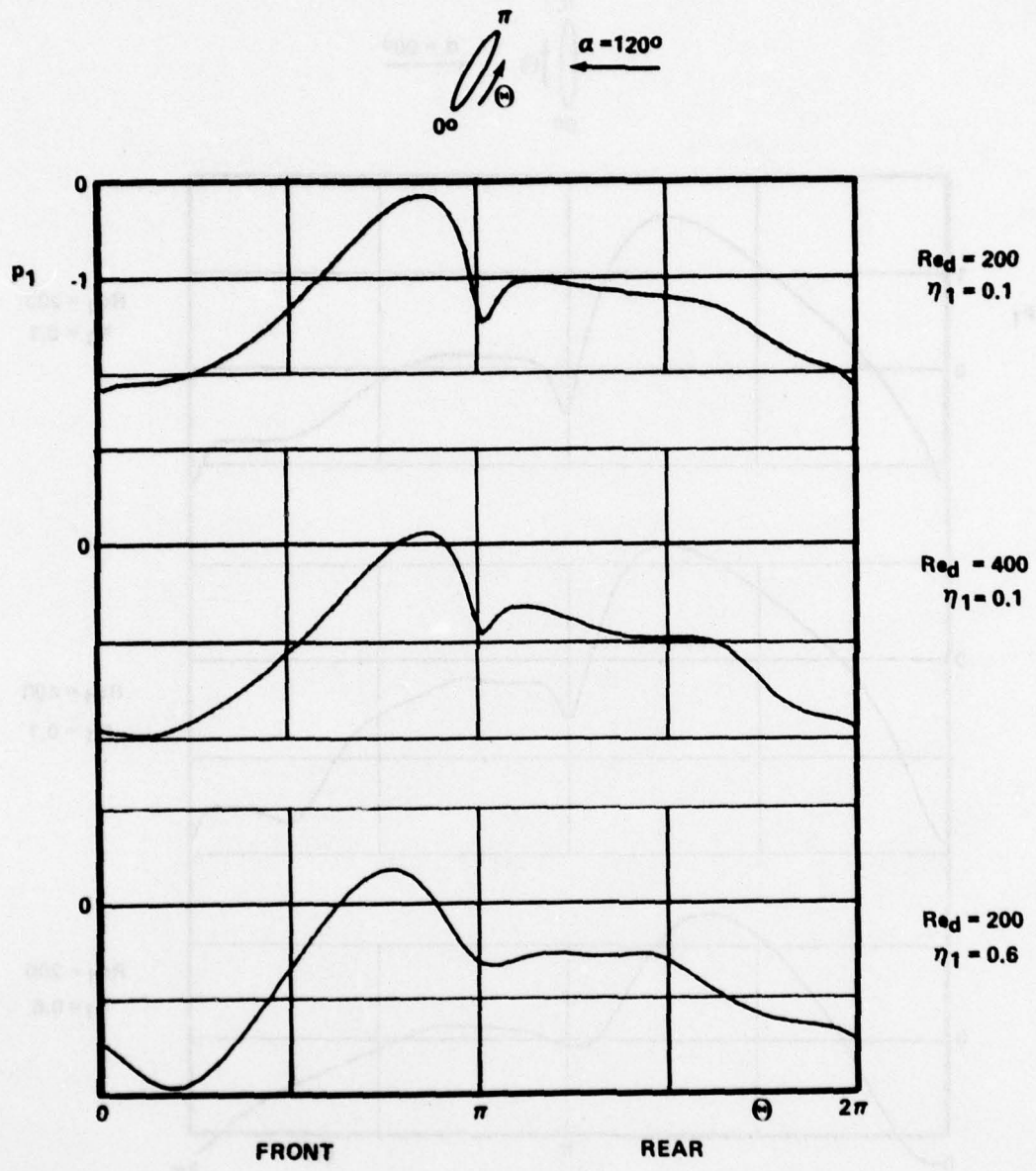
π
α =120°
Θ
0°
0
P1
-1
Red = 200
η1 = 0.1
0
Red = 400
η1 = 0.1
0
Red = 200
η1 = 0.6
0
π
Θ
2π
FRONT
REAR

Figure 26e

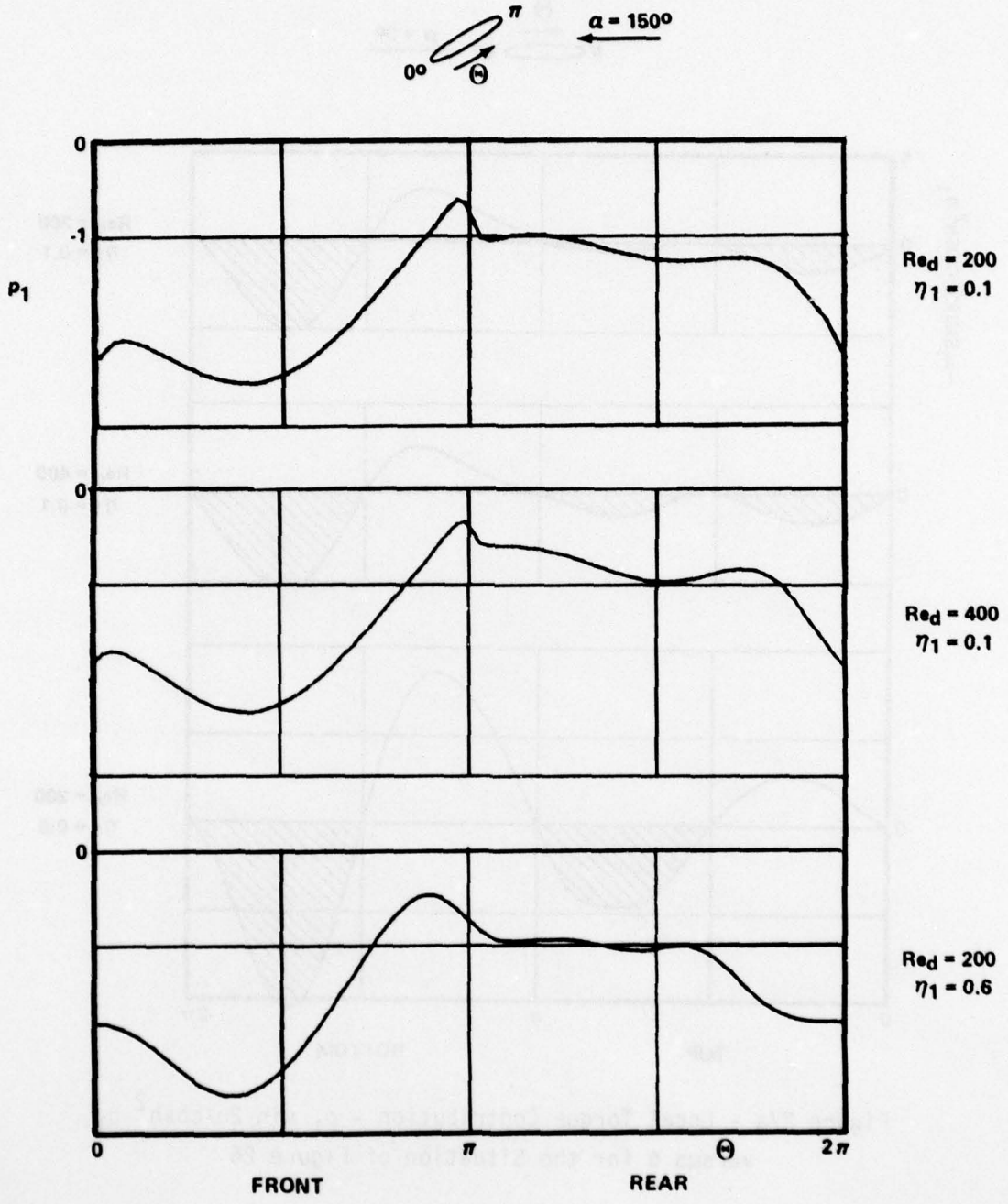
α = 150°
π
0°
Θ
0
-1
p_1
Re_d = 200
η_1 = 0.1
0
Re_d = 400
η_1 = 0.1
0
Re_d = 200
η_1 = 0.6
0
π
Θ
2π
FRONT
REAR

Figure 26f

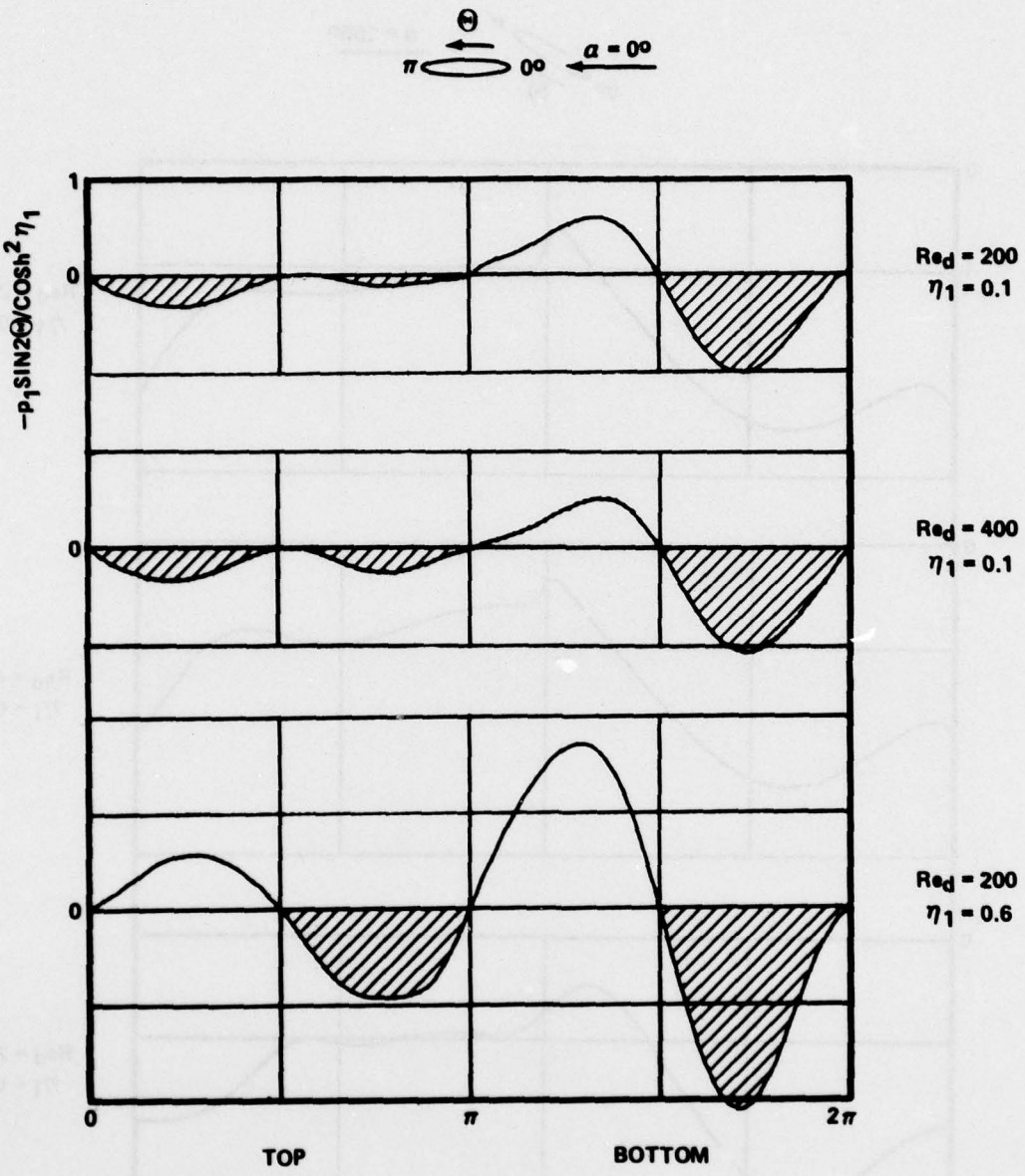

Figure 27a - Local Torque Contribution - $p_1 \sin 2\theta/\cosh^2 \eta_1$ versus θ for the Situation of Figure 26

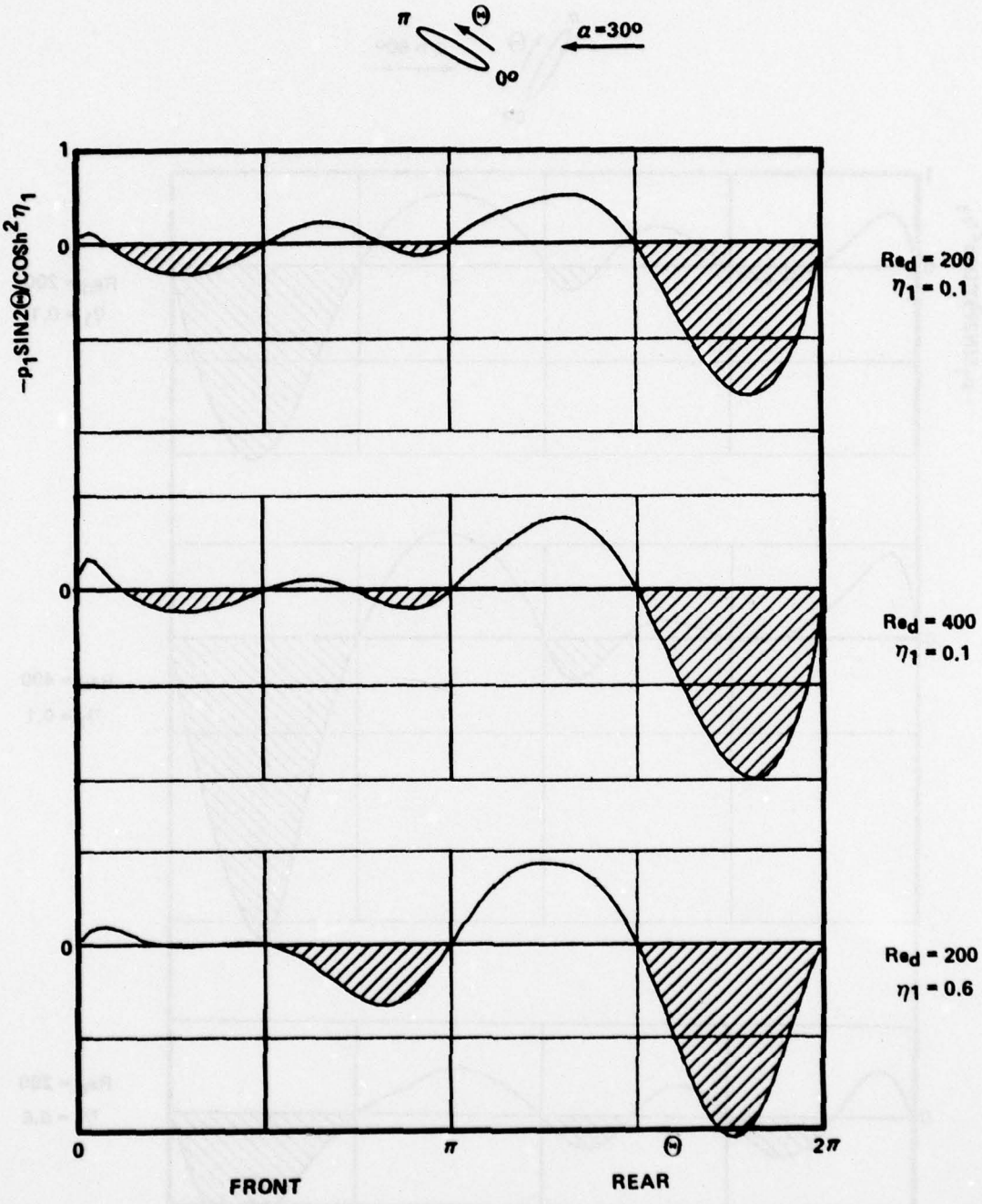
π
Θ
0°
α=30°
1
0
$-p_1 SIN2\Theta/COSh^2\eta_1$
$Re_d = 200$
$\eta_1 = 0.1$
$Re_d = 400$
$\eta_1 = 0.1$
$Re_d = 200$
$\eta_1 = 0.6$
0
π
Θ
2π
FRONT
REAR

Figure 27b

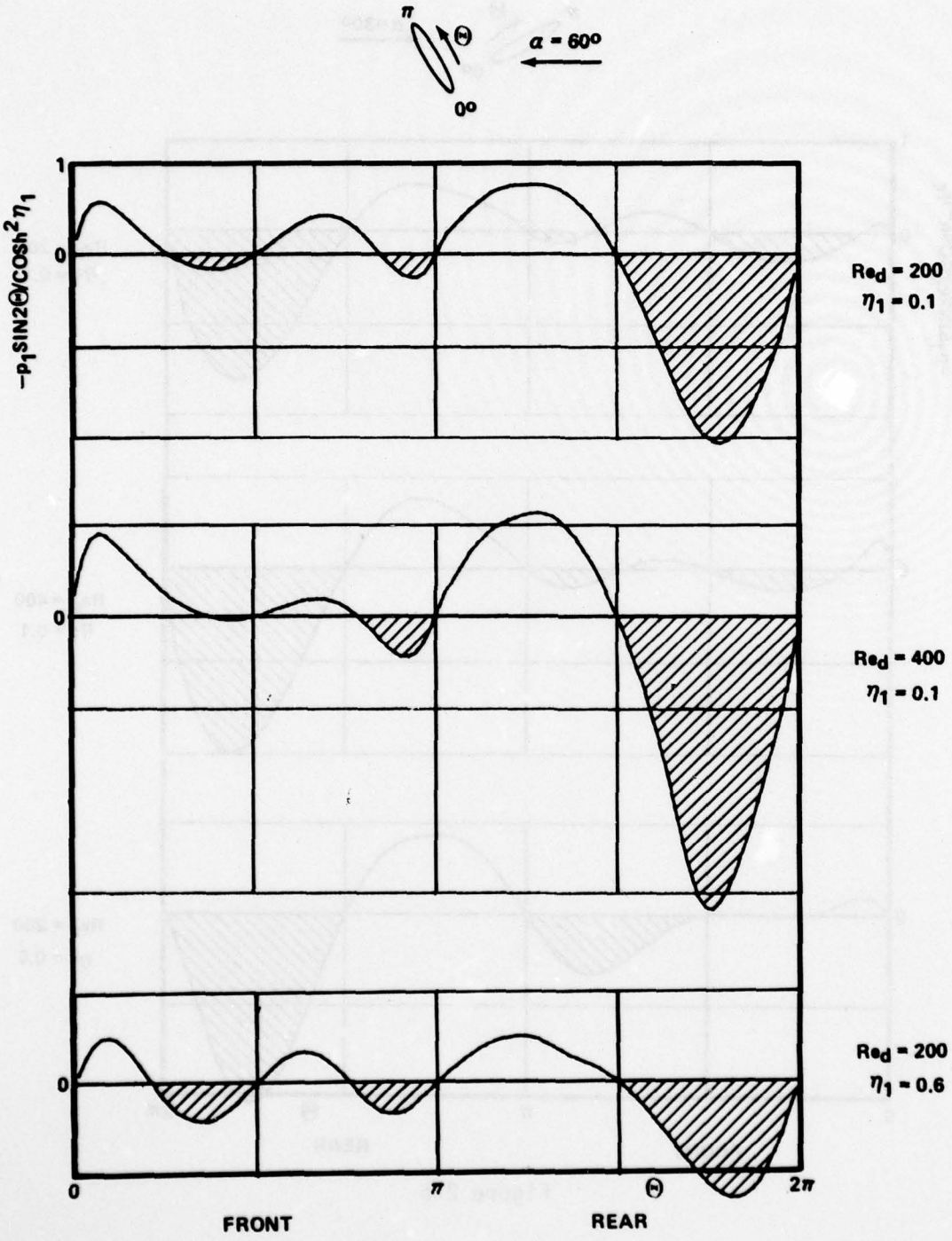
π
Θ
α = 60°
0°
1
0
$-p_1 SIN2\Theta/COSh^2\eta_1$
Re_d = 200
η_1 = 0.1
0
Re_d = 400
η_1 = 0.1
0
Re_d = 200
η_1 = 0.6
0
π
Θ
2π
FRONT
REAR

Figure 27c

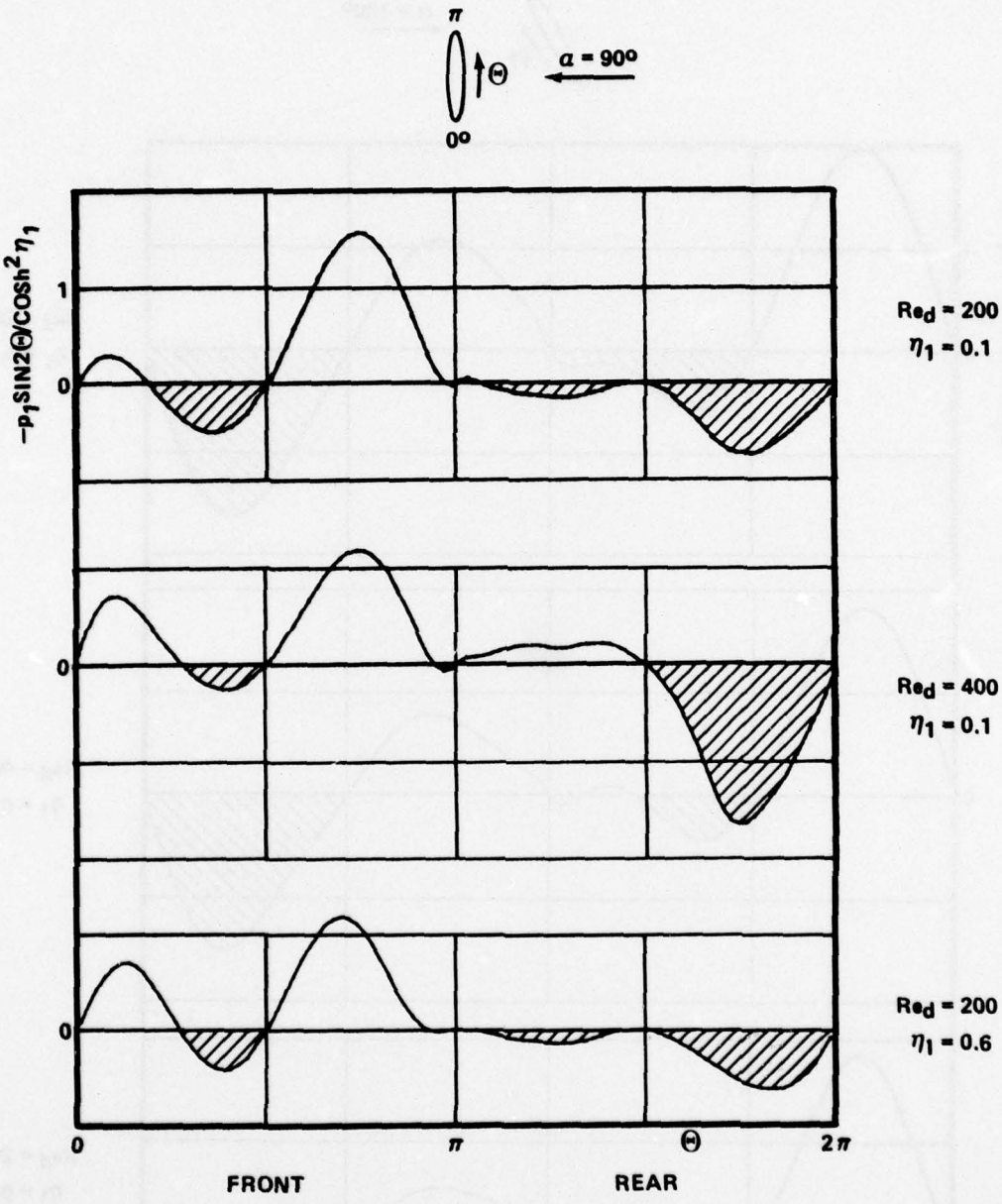
π
Θ
α = 90°
0°
$-p_1 SIN2\Theta/COSh^2\eta_1$
1
0
0
0
0
π
Θ
2π
FRONT
REAR
Re_d = 200
η_1 = 0.1
Re_d = 400
η_1 = 0.1
Re_d = 200
η_1 = 0.6

Figure 27d

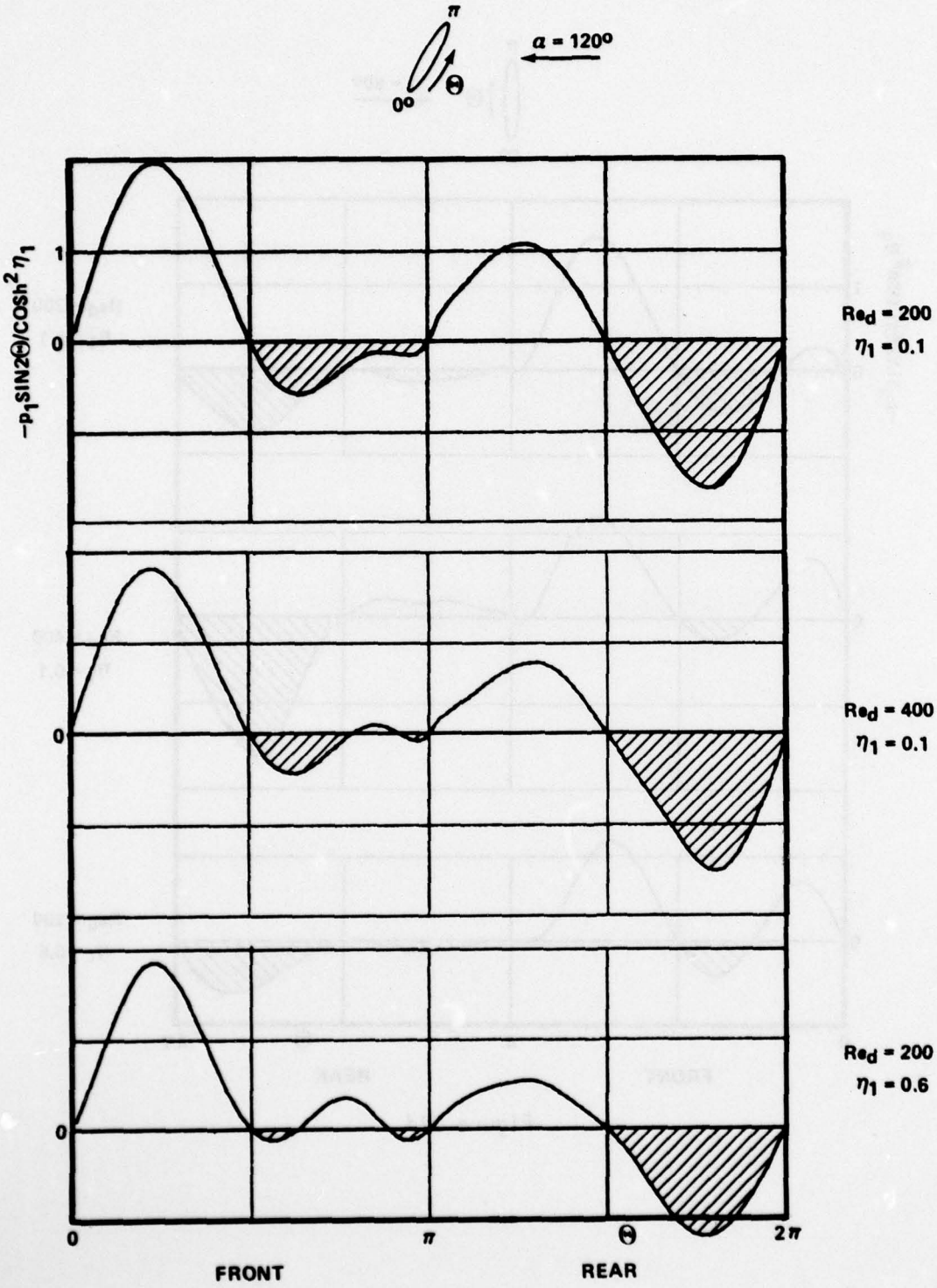
π
α = 120°
0°
Θ
$-p_1 SIN2\Theta/COSh^2\eta_1$
1
0
Re_d = 200
η_1 = 0.1
0
Re_d = 400
η_1 = 0.1
0
Re_d = 200
η_1 = 0.6
0
π
Θ
2π
FRONT
REAR

Figure 27e

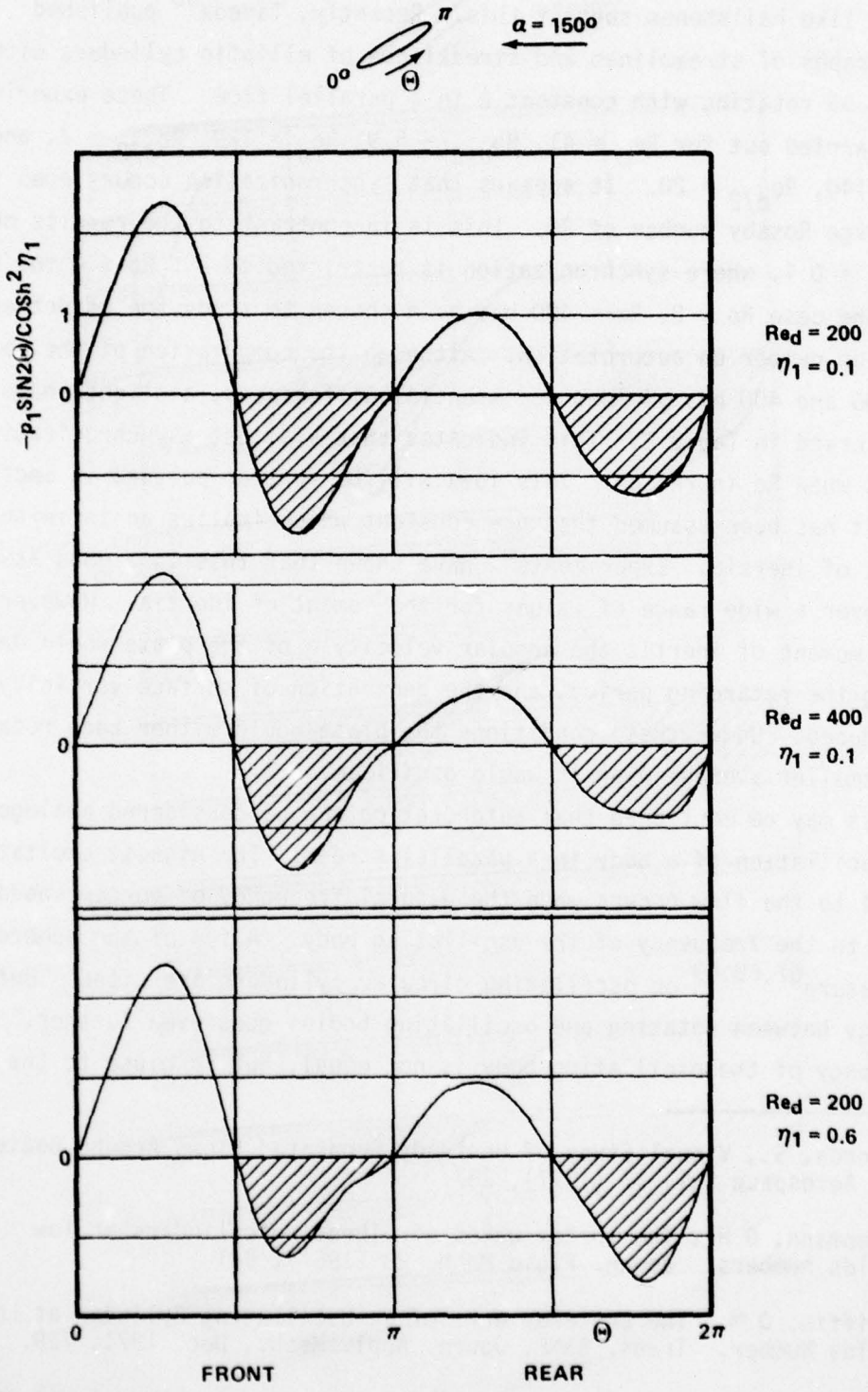
α = 150°
π
0°
Θ
$-p_1 SIN2(\Theta)/COSh^2\eta_1$
1
0
Re_d = 200
η_1 = 0.1
0
Re_d = 400
η_1 = 0.1
0
Re_d = 200
η_1 = 0.6
0
π
Θ
2π
FRONT
REAR

Figure 27f

bodies like hailstones suggest this. Recently, Taneda[66] published photographs of streamlines and streaklines of elliptic cylinders with $\eta_1 = 0.55$ rotating with constant Ω in a parallel flow. These experiments were carried out for $Re_d = 41$, $Ro_{d/2} = 5.9$; $Re_d = 129$, $Ro_{d/2} = 2$; and $Re_d = 140$, $Ro_{d/2} = 20$. It appears that synchronization occurs even for the large Rossby number of 20. This is in contrast to the results obtained for $\eta_1 = 0.1$, where synchronization is restricted to $2 \leq Ro \leq 4$ for $Re = 200$.

The case Ro = 2, Re = 400 has been chosen to study the effect of Reynolds number on autorotation. Although the computation of the cases Re = 200 and 400 has yielded no essential differences, a slight phase shift is observed in Table 2. This indicates that a slight asynchronization occurs when Re increases. This idea will be further pursued in Section 4.2.

It has been assumed that Ω = constant which implies an infinite moment of inertia. Experiments[55] have shown that this is a good assumption over a wide range of values for the moment of inertia. However, for small moment of inertia the angular velocity Ω of the plate would decrease during the retarding period, and the generation of surface vorticity would be reduced. Under these conditions the plate would either keep rotating at a smaller average Ω or it would oscillate.

It may be mentioned that autorotation can be considered analogous to the oscillation of a body in a parallel stream. The highest excitation normal to the flow occurs when the natural frequency of vortex shedding is equal to the frequency of the oscillating body. A few of the numerous literature[67,68,69] on oscillating circular cylinders are cited. But the analogy between rotating and oscillating bodies goes even further. If the frequency of the oscillating body is not equal, but is close to the

---

[66] Taneda, S., Visual Study of Unsteady Separated Flows Around Bodies. Prog. Aerospace Sci. 17 (1977), 287.

[67] Koopmann, G.H., The vortex wakes of vibrating cylinders at low Reynolds numbers. Journ. Fluid Mech. 28 (1967), 501

[68] Griffin, O.M., The Unsteady Wake of an Oscillating Cylinder at Low Reynolds Number. Trans. ASME, Journ. Appl. Mech., Dec. 1971, 729.

[69] Griffin, O.M. and S.E. Ramberg, The vortex-street wakes of vibrating cylinders. Journ. Fluid Mech. 66 (1974), 553.

natural frequency of vortex shedding, the natural frequency will adjust to the oscillating frequency. This phenomenon is called "lock-in". In the case of the rotating plate lock-in occurs in the region $2 \leq Ro \leq 4$ for Re = 200, $\eta_1 = 0.1$. Deviation from this condition causes aerodynamic damping. This effect has been clearly demonstrated at least for $Ro \leq 1$.

Conclusion

Autorotation of plates normal to a parallel flow occurs under the following conditions:

(1) A necessary but not sufficient condition for autorotation is the synchronization of vortex shedding and rate of rotation. A lock-in effect is observed over a certain Ro-range, in which the frequency of vortex shedding adjusts to the rate of rotation. This Ro-range roughly coincides with the shaded area in Fig. 22.

(2) Under condition (1) the difference in the average surface pressure between front and rear side of the plate has a minimum during the retarding period. This corresponds to the condition that the amount of vorticity shed from both sides at the rear edge is about the same (with opposite signs, of course). $\overline{C}_{MR}$ reaches a minimum at $Ro \approx 4$ which is smaller than $\overline{C}_{MS}$. In the supporting period the presence of the vortex at the retreating edge also favors autorotation although not as strongly as in the retarding period. Thus, the characteristics of the vortex at the retreating edge over the entire cycle of rotation is essential for autorotation.

(3) Sufficient surface vorticity around the edges must be produced to meet condition (2). A sharp edge is most favorable for autorotation. The fat elliptical cylinder $\eta_1 = 0.6$ does not autorotate for Ro = 2, Re = 200 (Ω = constant).

(4) The dimensionless moment of inertia must be sufficiently large.

(5) Autorotation requires the fulfillment of all conditions (1) through (4). The exact rate of autorotation is determined by an intricate interplay of (1) through (4). For Re = 200, $\eta_1 = 0.1$, Ω = constant, stable autorotation occurs at $Ro \approx 2$.

AD-A058 338 DAVID W TAYLOR NAVAL SHIP RESEARCH AND DEVELOPMENT CE--ETC F/G 20/4
AUTOROTATION OF PLATES.(U)
AUG 78 H J LUGT
UNCLASSIFIED DTNSRDC-78/058 NL

2 OF 2
AD
A058 338

END
DATE
FILMED
10-78
DDC

4.2 EXTRAPOLATION TO HIGH REYNOLDS-NUMBER FLOW

Except for some instances in biofluid-dynamics, autorotation of technical interest occurs in the high Reynolds-number range. With presently available computers and numerical techniques it is very expensive in computer time to obtain solutions of the Navier-Stokes equations for the problem of autorotation beyond Re = 1000, let alone problems which involve turbulent motions. Experiments have shown that autorotation occurs up to Re = $5 \cdot 10^5$ and probably higher. Is the explanation for autorotation at these high Reynolds numbers different from that for the low values given in Section 4.1? This question will be answered by analyzing available experimental data and a smoke tunnel movie from the University of Notre Dame.

In flows at higher Reynolds number convection of vorticity dominates over diffusion of vorticity. The boundary layers become thinner, producing more vorticity and causing stronger vortices at the retreating edge. Shear layers behind the advancing edge become thinner and eventually become unstable and turbulent. (See Figure 28.)

$Re \approx 200$	$Re \approx 1000$	$Re \approx 10^5$
low Re	intermediate Re	high Re

Figure 28 - Sketch of Flow Patterns Around an Autorotating Plate for Various Reynolds Numbers

The conditions for the occurrence of autorotation summarized on page 85 also hold for high Reynolds-number flow:

(1) Synchronization has been observed in all experiments.

(2) The hysteresis effect can be observed in the smoke tunnel movie in which the delay of vortex separation behind the retreating edge in the supporting period is clearly visible.

(3) The influence on autorotation of surface vorticity around the edges

is demonstrated in Riabouchinsky's experiments from 1909, Figure 29. Although no Reynolds number is given by Riabouchinsky, the value is not in the low Re range. Similar results with the shape of Figure 5 were obtained by Flatau.[47] The Rossby number is about 1.2 for Re $\approx 3 \cdot 10^4$ (Ro = 0.7 for bodies with endplates).

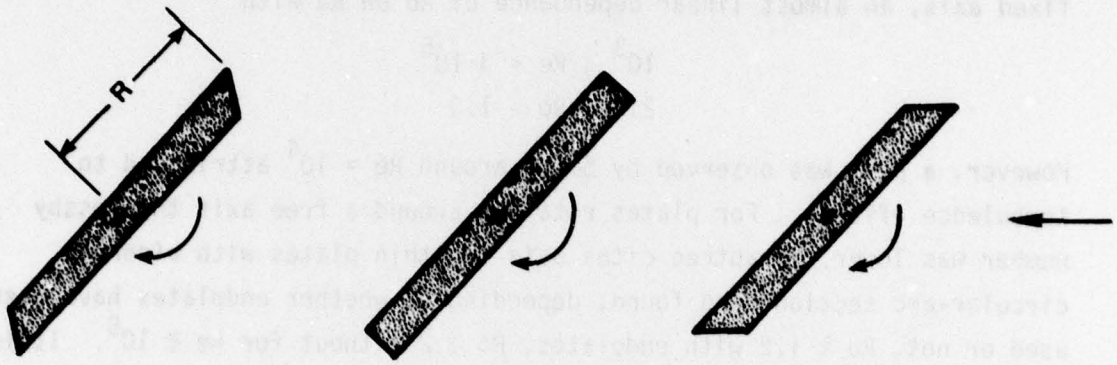

$\Omega R/U$	= 0.627	0.522	0.429
Ro	= 1.60	1.92	2.33

Figure 29 - The Influence of The Edge on Autorotation According to Riabouchinsky[4]

(4) The dimensionless moment of inertia must be sufficiently large at high Reynolds numbers also.[4,55]

(5) The interplay of conditions (1) through (4) is also obvious.

It remains now to compare computer output for low Reynolds numbers with available experimental data at intermediate and high Reynolds numbers. In order to avoid three-dimensional effects on the data during the experiments, in this section only data for aspect ratios larger than 5 are used.[17,22,55] In addition, the comparison is restricted to thin plates and to almost constant rotation so that the Rossby number is a function of the Reynolds number only.

Although potential-flow theory (without considering discontinuity sheets) cannot predict a restricted Ro-range for autorotation, a theoretical limit can be given at which the two stagnation points on the plate migrate into the fluid. This happens at Ro = 0.5. Below this

value, closed streamlines around the body occur. Riabouchinsky[4] noticed that Ro > 1 for autorotation. More detailed data were given by Dupleich,[17] Crabtree,[22] Bustamante and Stone,[48] and E.H. Smith.[55] For the intermediate Re range (Re ~ 2000) Dupleich measured Ro ≈ 1.3, Bustamante and Stone Ro ≈ 1 for high Reynolds numbers. E.H. Smith found, for various airfoils (flat plate, thin elliptic cylinder, wedge airfoil) autorotating around a fixed axis, an almost linear dependence of Ro on Re with

$$10^3 < Re < 3 \cdot 10^5$$
$$2.4 > Ro > 1.0$$

However, a peak was observed by Smith around $Re = 10^4$ attributed to turbulence effects. For plates rotating around a free axis the Rossby number was lower. Crabtree cites data for thin plates with biconvex circular-arc sections and found, depending on whether endplates have been used or not, Ro ≈ 1.2 with endplates, Ro ≈ 2 without for $Re \approx 10^5$. It is also worth noting that thick bodies with biconvex circular-arc sections have higher Ro, despite the fact that the edges are sharp. This observation is in agreement with the argument that a larger surface area causes more friction, and that the difference in surface pressure distribution between the front and rear sides of the plate decreases.

The experimental results on Ro = f(Re) are summarized in the statement that with increasing Re the Rossby number decreases, and that Ro is smaller for plates autorotating around a freely moving axis than for those with a fixed axis.

Force coefficients over one revolution were measured by Smith.[55] Figure 30 shows a comparison of the computed value for Re = 200 with experimental data for Re = 90000. The qualitative agreement is surprisingly good. Quantitatively, one expects from Smith's results smaller values of C_D and C_L for Re = 200. The reason for the discrepancy is not clear. It may be mentioned, however, and this is valid for all experimental data, that the influence of the ball bearings on the measurements is difficult to avoid. The closeness of data for laminar and turbulent flows may be explained by recent studies on organized structures in

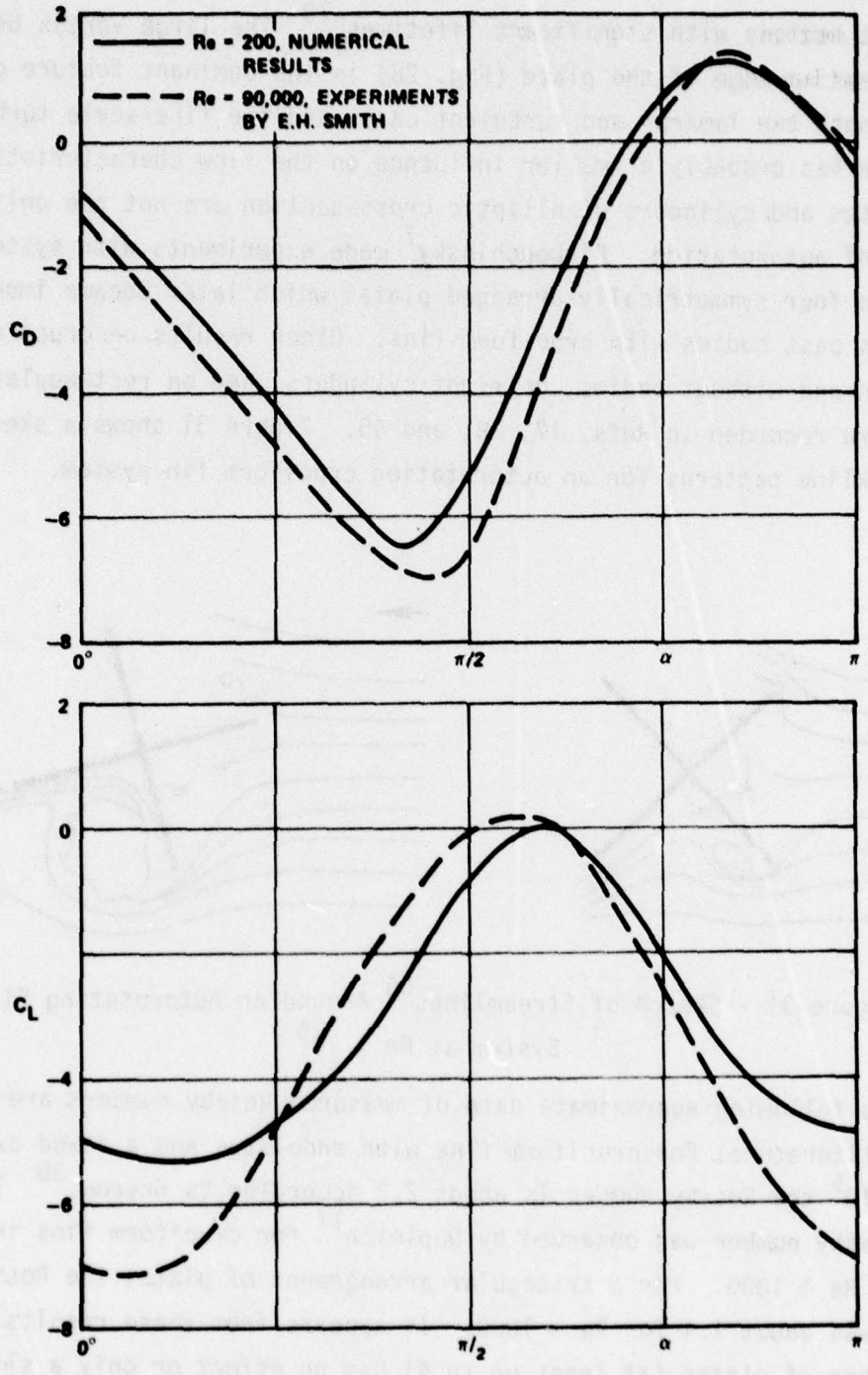

Figure 30 - Drag and Lift Coefficient for One Cycle (half a revolution). Comparison of Numerical Results with Experimental Data for Autorotating Plates. Remember that Negative Drag is Real Drag and Negative Lift is Magnus Lift in the Notation of this Paper

turbulent motions with significant lifetimes.[70] The large vortex behind the retreating edge of the plate (Fig. 28) is the cominant feature of the flow in both the laminar and turbulent case, and the fine-scale turbulent structure has probably a smaller influence on the flow characteristics.

Plates and cylinders of elliptic cross-section are not the only bodies capable of autorotation. Riabouchinsky[7] made experiments with systems of three and four symmetrically arranged plates which later became important for flows past bodies with cruciform fins. Other results on cruciform fins with and without bodies, on right cylinders, and on rectangular prisms are recorded in Refs. 17, 38, and 45. Figure 31 shows a sketch of streakline patterns for an autorotating cruciform fin system.

Figure 31 - Sketch of Streamlines[56] Around an Autorotating Fin System at Re $\approx 10^5$

The following approximate data of measured Rossby numbers are given in the literature: For cruciform fins with endplates and a fixed axis at Re $\approx 5 \cdot 10^5$ the Rossby number is about 2.2 according to Greene.[38] The same Rossby number was observed by Dupleich[17] for cruciform fins in free fall at Re $\approx$ 1000. For a triangular arrangement of plates the Rossby number was about 1.4 for Re $\approx$ 1000. It appears from these results that the number of plates (at least up to 4) has no effect or only a slight influence on the Rossby number.

---

[70] Roshko, A., Structure of Turbulent Shear Flows: A New Look, AIAA Journal 14 (1976), 1349.

4.3 COMMENTS ON 3D-FLOW

The discussions in the previous pages were restricted to two-dimensional flows, that is, the span of the plate or elliptic cylinder was considered to be infinitely long. This is not the case in reality, and the influence of a finite span on the flow characteristics must be evaluated. In addition, the axis of rotation need not be perpendicular to the flow, a situation which makes the problem extremely complicated. At present, three-dimensional flows of such complexity can be studied only experimentally. To begin with, the axis of rotation is considered to be normal to the flow.

A measure for the finiteness of the span is the aspect ratio: span to chord. All experiments agree that the rate of autorotation and the lift-to-drag ratio diminish with decreasing aspect ratio. Quantitative data were given by Bustamante and Stone[48] who summarized them in the formula

$$1/Ro = 1 - e^{-0.2\,AR} \qquad (18)$$

where AR is the aspect ratio. Endplates preserve, to a certain extent, the two-dimensionality. Thus, when a high rate of autorotation is desired or when three-dimensional effects in wind tunnels are to be reduced, endplates are advantageous.[22,38,47]

To aid in understanding the influence of a finite span on autorotation, the flow field may be idealized as a potential flow with vortex lines or tubes (for curved vortex fields). Clearly, in two-dimensional flows all vortex lines are straight, infinitely long, and perpendicular to the plane. A body with finite span, however, will be surrounded by a flow in which the vortex lines are either closed or must end on the body. They are bent at the ends of the wing, thus giving rise to a secondary flow. This flow interferes with the primary (two-dimensional) flow by weakening it in two ways: decreasing the strength of the primary flow, and speeding up the process of instability since curved vortex tubes are highly unstable in general.[71]

---

[71] Taneda, S., Studies on Wake Vortices (I), An Experimental Study on the Structure of the Vortex Street Behind a Circular Cylinder of Finite Length. Reports of Research Institute for Applied Mechanics, Vol. I, No. 4, Dec. 1952.

The location and arrangement of the vortex tubes can only be conjectured without photographic evidence. The following discussion may be guided by simpler, confirmed cases. Taneda[71] presented the following model. For a Kármán-vortex street behind a fixed circular cylinder of finite length, based on the evaluation of photographs:

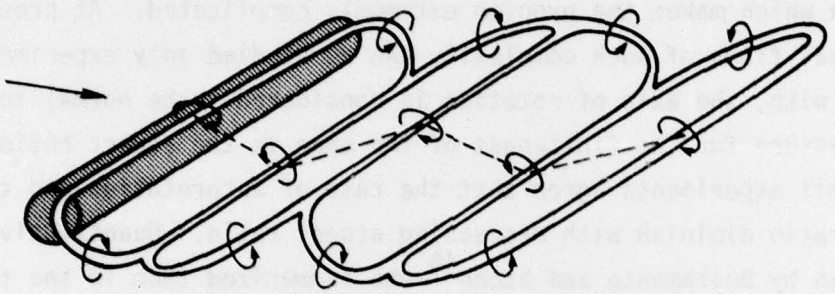

Figure 32 - Taneda's Vortex-Tube Model of 1952 for the Periodic Vortex Shedding Past a Circular Cylinder

If the cylindrical body is nonsymmetric, as in the case of a wing at high angle of attack, the vortex tubes are still closed and linked together but will be stretched where the vortex strength is large. Thus, Helmholtz (or Kelvin's) laws are not violated.

If the aspect ratio decreases so that a sphere, or cube type body results, the vortex tubes will simplify to the double-helix model developed by Pao and Kao.[72]

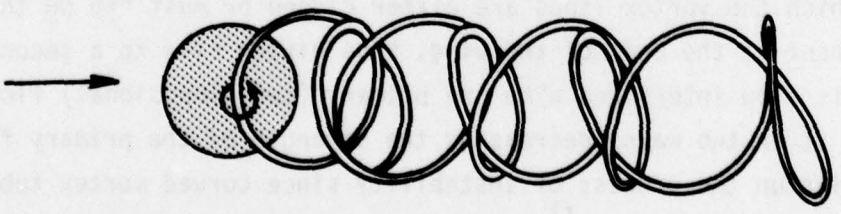

Figure 33 - The Double-Helix Model by Pao and Kao of 1975 for the Periodic Vortex Shedding Past a Sphere

---

[72] Pao, H. and Kao, T.W., On Vortex Shedding in the Wake of a Sphere. Catholic University of America, Tech. Rep. No. HY-75-001, May 1975.

The axis of a rotating body is always a vortex line or tube. The reader may be reminded of the well-known vortex model for a propeller. The vortex tubes around an autorotating plate are then imagined in the following way: the two-dimensional model (Figure 34a) consists of two starting vortices whose circulations balance the circulation of the rotating plate (see Fig. 17a). After each half cycle vortices of unequal strengths are shed, but they also balance so that the total circulation remains zero. Figure 34b shows a proposed three-dimensional model in which the vortex tubes are linked together. This configuration, of course, is very unstable down stream.

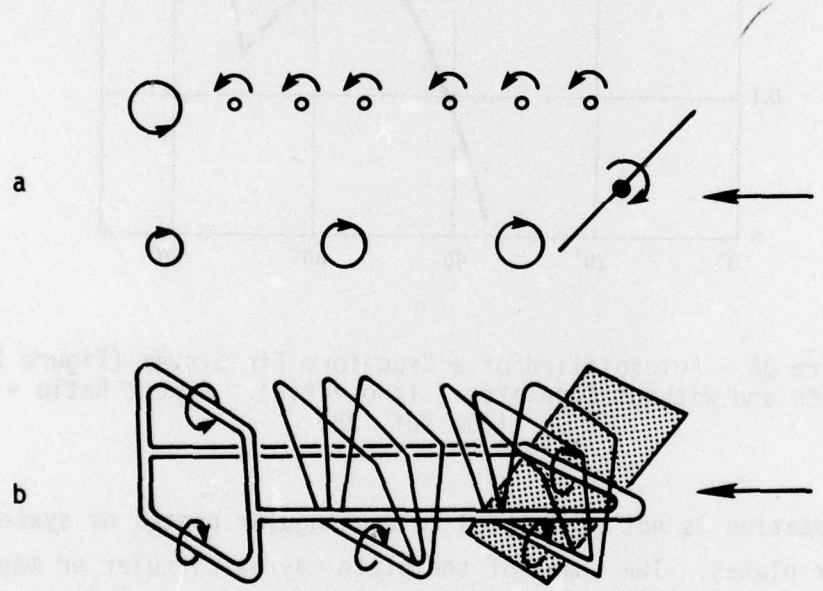

Figure 34 - Proposed Vortex-Tube Model for an Autorotating Plate of (a) Infinite Span, (b) Finite Span

The situation becomes even more complicated if the axis of rotation is not perpendicular to the flow but forms an angle β with the flow direction in the range $0° < \beta < 90°$. The axis may even gyrate (Ref. 45, p. 529). Some experimental data[38] are available for a cruciform fin configuration. These data are presented in Figure 35.

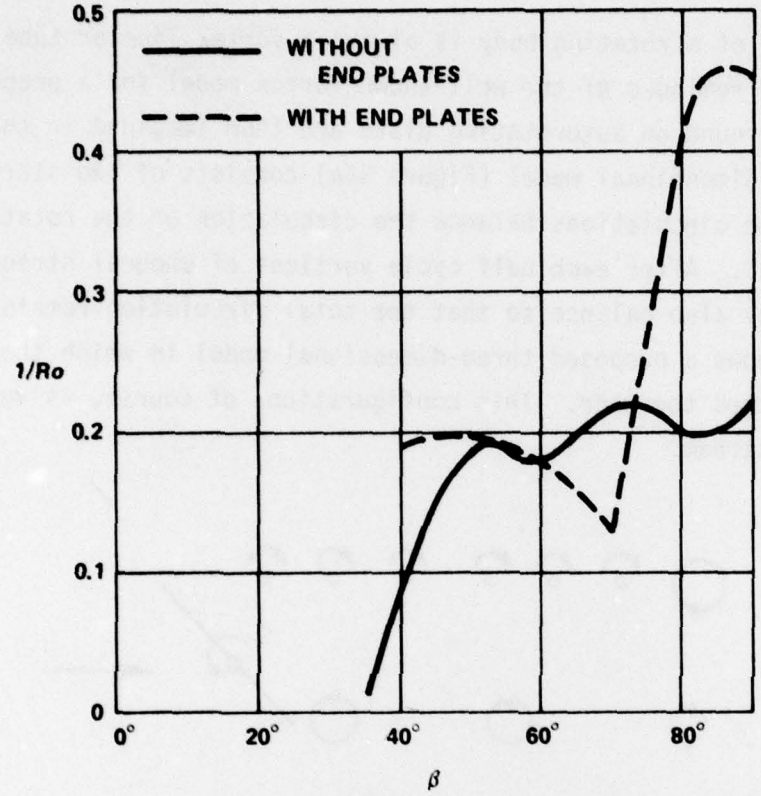

Figure 35 - Autorotation of a Cruciform Fin System (Figure 2e) With and Without Endplates. $1/Ro = f(\beta)$. Aspect Ratio = 3 (from Ref. 38)

Autorotation is not restricted to rectangular plates or systems of rectangular plates. The shape of the plate may be circular or may have a delta form. Experiments have been performed by Bustamante and Stone.[48] The Rossby number at high Re-flow is for circular disks about twice as large as for long rectangular plates. For delta-shaped plates the Ro-number is even higher. The rate of autorotation can be optimized for different purposes. If autorotation is desired, the rate of spin can be enhanced by a proper, propeller-like shape of the body with endplates.[45,47] However, such a devise then assumes a gyro-type configuration and is not strictly autorotating in the sense of the definition on page 5.

Autorotation can be suppressed by the use of slots,[39,40,41] fences,[55] and probably by shrouded fins. Slots were proposed by the

author,[39] and the results of subsequent experiments have been reported in Refs. 40 and 41. It is still not clear which slot position would be most effective. Slots slanted with respect to the edges of the plate would be very effective since they would disturb the two-dimensionality of the vortex tubes (which are parallel to the wedges).

The influence of fences on autorotation was investigated by E.H. Smith.[55] The interpretation of the results is consistent with the present theory: fences at the axis of rotation disturb the development of the boundary layer along the entire front of the plate in the retarding period. As was pointed out on page 68, the prolonged development of this boundary layer is the main cause of autorotation. Smith's experiments with Re = 78000 show that the Rossby number can be increased by a factor of 4 through the use of fences at the midsection of the plate. Fences at the tips act similarly as Riabouchinsky-type bodies (Figs. 5 and 29).

ACKNOWLEDGMENTS

I owe thanks to a number of people in Code 184. With Dr. H. J. Haussling and Mr. S. Ohring I enjoyed fruitful discussions. Mr. J. Telste prepared the computer runs, and Mrs. S. Wybraniec did the bulk of computer plotting of the curves.

REFERENCES

1. McCormick, B.W., Aerodynamics of V/STOL flight. Academic Press. New York, 1967.

2. Norberg, R.A., Autorotation, Self-Stability, and Structure of Single-Winged Fruits and Seeds (Samaras) with Comparative Remarks on Animal Flight. Biol. Rev. 48 (1973), 561.

3. Poe, G.G. and Acrivos, A., Closed-streamline flows past rotating single cylinders and spheres: inertia effects. Journ. Fluid Mech. 72 (1975), 605.

4. Riabouchinsky, D.P., Thirty years of theoretical and experimental research in fluid mechanics. Journ. Royal Aeron. Soc. 39 (1935), 282.

5. Durand, W.F. (editor), Aerodynamic Theory. Dover Publications 1963. Vol. V, 208.

6. Bairstow, L., Applied Aerodynamics. 2nd ed. Longmans, Green and Co., New York, 1939. Chapter V, 212.

7. Smith, A.M.O., On the Motion of a Tumbling Body. Journ. Aeron. Sciences 20 (1953), 73.

8. Maxwell, J.C., On a particular case of the descent of a heavy body in a resisting medium. Scientific Papers. Cambridge University Press (1890), 115.

9. Barkla, H.M. and Auchterlonie, L.J., The Magnus or Robins effect on rotating spheres. Journ. Fluid Mech. 47 (1971), 437.

10. Lamb, H., Hydrodynamics. Sixth edition. Dover Publication, 1945.

11. Mouillard, M., Théorie de l'Aéroplane. L'empire de l'air, 1881, 210.

12. Gerlach, E., Zeitschr. für Luftsch. 5 (1886), 65.

13. Ahlborn, F., Der Schwebflug und die Fallbewegung ebener Tafeln in der Luft. Abh. d. Naturw. Ver. Hamburg XV, 1897.

14. Köppen, W., Illustr. aër. Mitteil. 5 (1901), 158.

15. Joukowsky, N., De la chute dans l'air de corps légers de forme allongée, animés d'un mouvement rotatoire. Bulletin de l'Inst. aérodynamique de Koutchino, fasc. 1 (1912), 51.

16. Ahlborn, F., The Magnus Effect in Theory and in Reality. Translation in NACA TM 567, May 1930.

17. Dupleich, P., Rotation par Chute Libre des Ailettes Rectangulaires de Forme Allongée. Publications Scientifiques et Techniques du Secretariat d'Etat a l'Aviation, 1941, No. 176. Translated into English in NACA TM 1201, April 1949.

18. von Holst, E., Der rotierende Flügel als Mittel zur Hochauftriebserzeugung. Jahrbuch 1941 d. deutschen Luftfahrtforschung I, 372.

19. Küchemann, D., Auftrieb und Widerstand eines rotierenden Flügels. Deutsche Luftfahrt forschung, Forschungsbericht 1651, 1942.

20. Wiese, H. Drehleistungsmessungen an rotierenden Flügeln. AVA Göttingen, Bericht 42/A/14. 1942.

21. Küchemann, D., Dreikomponentenmessungen an einem Flügel mit rotierendem Hilfsflügel. Deutsche Luftfahrtforschung, Forschungsbericht 1513, 1941.

22. Crabtree, L.F., The rotating flap as a high-lift device. Royal Aircraft Est. Farnborough Tech. Note, Aero 2492, 1957.

23. Schneller, E., The lunar motion of fin stabilized projectiles. Report from the Technische Hochschule Darmstadt 1940/1941. Translated by CADO, Wright-Patterson Air Force Base, Dayton, Ohio, ATI 3271.

24. Fuchs, R. and Hopf, L., Aerodynamik. R.C. Schmidt & Co., Berlin, 1922, 424.

25. Bryant, L.W. and Gates, S.B., The Spinning of aeroplanes. Journ. Royal Aeron, Soc. 31 (1927), 619.

26. Knight, M., Wind tunnel tests on autorotation and the "Flat Spin." NACA Rep. 273, 1927.

27. Neihouse, A.I., Klinar, W.J., and Scher, S.H., Status of spin research for recent airplane designs. NASA TR 57, 1960.

28. Spangler, S.B. and Dillenius, M.F.E., Investigation of Aerodynamic Loads at Spin Entry. Report ONR-CR212-225-2, May 1976.

29. Paturi, F., Nature, Mother of Invention. Harper & Row, New York, 1976.

30. McCutchen, C.W., The Spinning Rotation of Ash and Tulip Tree Samaras. Science 197 (1977), 691.

31. Results of the Second U.S. Manned Orbital Space Flight May 24, 1962. NASA SP-6, 1962.

32. Campbell, J.P., Low-Speed Aerodynamic Research Related to the Landing of Space Vehicles.

33. Moore, F.K., Lift Hysteresis at Stall as an Unsteady Boundary-layer Phenomenon. NACA Rep. 1291, 1956.

34. Nicolaides, J.D. and Griffin, T.F., On a Fluid Mechanism for Roll Lock-in and Rolling Speed-up Due to Angle of Attack of Cruciform Configurations. Bu Ord Tech. Note No. 16, Sept. 1955.

35. Nicolaides, J.D., On the Rolling Motion of Missiles. Bu Ord Tech. Note No. 33, March 1957.

36. Nicolaides, J.D., Final Technical Note. Bu Ord 1961.

37. Brown, F.N.M., Summary report on Cruciform fin study. University of Notre Dame, Indiana, Dept. of Aeronautical Engineering, Contract NORD 17702, May 1958.

38. Greene, J.E., An Investigation of the Rolling Motion of Cruciform-fin Configurations. NAVORD Rep. 6262, March 1960.

39. Lugt, H.J., Self-sustained Spinning of a Cruciform Fin System. Proc. Fifth U.S. Navy Symposium on Aeroballistics. Naval Ordnance Lab., White Oak, Md., 1961.

40. Daniels, P., Fin Slots vs Roll Lock-In and Roll Speed-Up. Journ. Spacecraft and Rockets 4 (1967), 410.

41. Daniels, P. and Clare, T.A., Aerodynamic Characteristics of the Slotted Fin. Journ. Aircraft 9 (1972), 603.

42. Cohen, C.J., Clare, T.A., and Stevens, F.L., Analysis of the Nonlinear Rolling Motion of Finned Missiles. AIAA 12 (1974), 303.

43. Daniels, P., A Study of the Nonlinear Rolling Motion of a Four-Finned Missile. Journ. Spacecraft and Rockets 7 (1970), 510.

44. Fiechter, M., Kegelpendelung, Autorotation und Wirbelsysteme schlanker Flugkörper. Zeitschr. Flugwissenschaften 20 (1972), 281.

45. Burgess, F.F. (ed.), Proceedings of Conference on Dynamics and Aerodynamics of Bomblets. Vol. I. Tech. Rep. AFATL-TR-67-195, Oct. 1967.

46. Zaroodney, S.J., On the Mechanism of Dispersion and Short Ranges of Mortar Fire. Ballistic Research Lab. No. 668, 1948.

47. Flatau, A., An Investigation of the Rotational and Aerodynamic Characteristics of High Aspect Ratio Rotors. U.S. Army Edgewood Arsenal CRDL TM 1-4, 1964.

48. Bustamante, A.C. and Stone, G.W., The Autorotation Characteristics of Various Shapes for Subsonic and Hypersonic Flows. Journ. AIAA 69-132, 1969.

49. Kry, P.R. and List, R., Angular motions of freely falling spheroidal hailstone models. Physics of Fluids 17 (1974), 1093.

50. Kry, P.R. and List, R., Aerodynamic torques on rotating oblate spheroids. Physics of Fluids 17 (1974), 1087.

51. List, R., Rentsch, U.W., Byram, A.C., and Lozowski, E.P., Journ. Atmos. Sci. 30 (1973), 653.

52. Soong, T.C., The Dynamics of Discus Throw. Trans. ASME, Journ. Appl. Mech., Dec. 1976, 531.

53. Stilley, G.D., Aerodynamic Analysis of the Self Sustained Flare. AD-740117, Naval Ammunition Depot, Crane, Ind., Oct. 1972.

54. Willmarth, W.W., Hawk, N.E., Galloway, A.J., and Roos, F.W., Aerodynamics of oscillating disks and a right-circular cylinder. Journ. Fluid Mech. 27 (1967), 177.

55. Smith, E.H., Autorotating wings: an experimental investigation. Journ. Fluid Mech. 50 (1971), 513.

56. Lugt, H.J., On the autorotation of fin systems. U.S. Naval Weapons Lab., Dahlgren, Va., Tech. Memo. No. K-22/65, Jan. 1965.

57. Milne-Thomson, L.M., Theoretical Hydrodynamics, The MacMillan Co., N.Y., 1968, 5th ed.

58. Miller, M.C., Surface Pressure Measurements on a Spinning Wind Tunnel Model. AIAA Journ. 14 (1976), 1669.

59. Lugt, H.J. and Ohring, S., Rotating elliptic cylinders in a viscous fluid at rest or in a parallel stream. Journ. Fluid Mech. 79 (1977), 127.

60. Lugt, H.J. and Haussling, H.J., Laminar flow past an abruptly accelerated elliptic cylinder at 45° incidence. Journ. Fluid Mech. 65 (1974), 711.

61. Lugt, H.J. and Haussling, H.J., The Acceleration of Thin Cylindrical Bodies in a Viscous Fluid. Journal of Applied Mechanics 45 (1978), 1.

62. Lugt, H.J. and Ohring, S., Efficiency of numerical methods in solving the time-dependent two-dimensional Navier-Stokes equations. Proc. Int. Conf. Numerical Methods in Fluid Dyn., Southampton, p. 65. New York: Crane, Russak & Co.

63. Lugt, H.J. and Ohring, S., Rotating thin elliptic cylinder in a parallel viscous fluid flow. Proc. 4th Int. Conf. Numerical Methods in Fluid Dyn., Boulder. Lecture Notes in Phys. Vol. 35, p. 257. Springer.

64. Dawson, C.W. and Marcus, M., DMC - A Computer Code to Simulate Viscous Flow About Arbitrarily Shaped Bodies. Proc. 1970 Heat Transfer and Fluid Mechanics Institute, Stanford University Press, 1970.

65. Thoman, D.C. and Szewczyk, A.A., Numerical solutions of time dependent two dimensional flow of a viscous, incompressible fluid over stationary and rotating cylinders. Univ. Notre Dame, Dept. Mech. Engineering, Tech. Rep. 66-14, 1966.

66. Taneda, S., Visual Study of Unsteady Separated Flows Around Bodies. Prog. Aerospace Sci. 17 (1977), 287.

67. Koopmann, G.H., The vortex wakes of vibrating cylinders at low Reynolds numbers. Journ. Fluid Mech. 28 (1967), 501.

68. Griffin, O.M., The Unsteady Wake of an Oscillating Cylinder at Low Reynolds Number. Trans. ASME, Journ. Appl. Mech., Dec 1971, 729.

69. Griffin, O.M. and Ramberg, S.E., The vortex-street wakes of vibrating cylinders. Journ. Fluid Mech. 66 (1974), 553.

70. Roshko, A., Structure of Turbulent Shear Flows: A New Look. AIAA Journal 14 (1976), 1349.

71. Taneda, S., Studies on Wake Vortices (I), An Experimental Study on the Structure of the Vortex Street Behind a Circular Cylinder of Finite Length. Reports of Research Institute for Applied Mechanics, Vol. I, No. 4, Dec. 1952.

72. Pao, H. and Kao, T.W., On Vortex Structure in the Wake of a Sphere. Catholic University of America, Tech. Rep. No. HY-75-001, May 1975.

INITIAL DISTRIBUTION

Copies	
2	USA ARRADCOM 1 A. Flatau 1 Library
1	USA AIR MOBILITY R&D LAB SAVDL-D/W. McCroskey
3	CHONR 1 Code 102/R. Lundegard 1 Code 438/R. Cooper 1 Code 438/M. Cooper
1	USNA/Library
2	NAVPGSCOL 1 T. Sarpkaya 1 Library
1	NAVWARCOL
1	ROTC, MIT
3	NSWC, Dahlgren 1 C. Cohen 1 P. Daniels 1 Library
1	NSWC, White Oak/Library
2	NAVSEA 1 SEA 03C/J. Huth 1 SEA 0351/T. Peirce
1	NAVAIR/440, W. Volz
1	NAVSHIPYD BREM/Lib
1	NAVSHIPYD CHASN/Lib
1	NAVSHIPYD MARE/Lib
1	NAVSHIPYD NORVA/Lib
1	NAVSHIPYD PEARL/Lib
1	NAVSHIPYD PTSMH/Lib

Copies	
12	DDC
2	AFFDL 1 A. Fiore 1 W. Hankey
3	NASA AMES 1 T. Leonard 1 U. Mehta 1 Library
2	NASA LANGLEY 1 D. Bushnell 1 Library
1	U. of Cincinnati/K. Ghia
1	U. of Michigan/W.W. Willmarth
1	U. of Notre Dame/T. Mueller
1	Johns Hopkins U., APL/ V. O'Brien
1	Nielsen Engineering & Res. Inc. Mountain View, CA 94043 1 S.B. Spangler
1	Xerox Corp., Rochester, N.Y. 1 T.C. Soong

CENTER DISTRIBUTION

Copies	Code	Name
1	012	R. Allen
1	1102.1	B. Nakonechny
1	1500	W. Cummins
1	154	W. Morgan
1	1541	P. Granville
1	1552	J. McCarthy
1	1560	G. Hagen

Copies	Code	Name
1	1564	J. Feldman
1	1600	H. Chaplin
1	1606	S. de los Santos
1	1800	G. Gleissner
1	1802.2	F. Frenkiel
1	1805	E. Cuthill
2	1809.3	D. Harris
30	1840	H. Lugt
5	1843	J. Schot
1	1844	S. Dhir
1	1900	M. Sevik
1	1901	M. Strasberg
1	1960	D. Feit
10	5214.1	Reports Distribution
1	522.1	Unclassified Lib (C)
1	522.2	Unclassified Lib (A)
1	522.3	Aerodynamics Lib

Journal 14 (1976), 1349.